The Design and Manufacturability of Metastasis Mimetic Devices Used for Cancer Research

by

©2012
John Preston White III
B.S. Mechanical Engineering, The University of Kansas, Lawrence, KS, 2009

Submitted to the graduate degree program in Mechanical Engineering and the Graduate Faculty of the University of Kansas in partial fulfillment of the requirements for the degree of Master of Science

Dr. Terry N. Faddis _____
Committee-Chairman

Dr. Ronald L. Dougherty _____
Committee Member

Professor Robert C. Umhultz _____
Committee Member

Date defended: _____

The Thesis Committee for John Preston White III

certifies that this is the approved version of the following thesis:

The Design and Manufacturability of Metastasis Mimetic Devices Used for Cancer Research

_____

Committee-Chairman Dr. Terry Faddis

Date approved: _____

Abstract

Metastatic cancer causes the death in 80% of its patients, due to the failure of detecting the metastatic events early enough and the failure to effectively treat and eliminate the metastatic cancer cells. A limited understanding of the molecular and cellular mechanisms of the metastatic disease inhibits the development of effective therapies and the ability to prematurely diagnose metastatic disease. There have been numerous in-vitro devices and experimental approaches invented in the past to mimic individual stages of the metastatic disease, but not the entire cellular migration.

In this thesis, the development of six distinct metastatic devices will be described to replicate multiple aspects of metastatic cell behavior and mimicking multiple steps of the metastatic process. These new in-vitro devices have been designed to overcome the current challenges of previous devices. All of the designs were constructed with a new and innovative way of incorporating a porous membrane filter into a metastatic device. The first three designs include the use of two chambers that can hold cells or tissue, which are connected by an optically clear channel mounted on top or embedded into the base plate.

All of the designs presented were able to accurately replicate the multiple steps of the progression of metastatic cancer such as cell proliferation, migration, invasion, intravasation, extravasation, and colonization of other tissues. The Type II and Type V devices worked the best, due to the greatest number of cells that migrated to the other side and the most consistent results.

Acknowledgments

I would like to thanks my parents, John White and Helena White, for their encouragement and support throughout my academic career. Also, to the teachers and professors throughout my life who have all contributed to my education and molded me into a young professional.

I would like to express my great appreciation to Dr. Terry N. Faddis, my advisor, for his guidance and support during my research here at the University of Kansas. The knowledge I have gained throughout my academic career and my research under his guidance and advice has been invaluable. I am very grateful; it has been a tremendous learning experience that I will carry throughout my life. I would like to thank Nikki Cheng and Wei Bin Fang for testing the devices and for their input throughout my research. I would also like to thank the graduate director Dr. Bedru Yimer and other members of my thesis committee, Dr. Ronald L. Dougherty, and Professor Robert C. Umhultz for their support and their time to serve on my committee.

Table of Contents

Chapter 1
Introduction and Scope of Work

1.1 Introduction

Throughout the past decades there have been several improvements in breast cancer therapies, but metastatic breast cancer still results in an 80% mortality rate[11]. Metastatic cancer causes the death of most its patients, due in part to limited treatment options and the lack of understanding the mechanisms of the disease process. This lack of understanding of the biology of metastatic disease in humans is the primary obstacle that stands in the way of identifying and developing an effective treatment strategy. It is fueled in part by a dearth of adequate technologies to analyze multiple aspects of metastatic cell behavior[11].

Currently, rodents are being used to investigate the metastasis process, which has been limited to following the dissemination of injected cancer cells. This method imposes several disadvantages that are costly and complex to analyze. The cell culture systems are limited to studying signaling pathways and one cellular process at a time. There are also inherent differences between the biological systems of a mouse and a human, in particular the immune system[10]. These differences make it challenging to understand the molecular and cellular mechanisms of the metastatic process as related to the human disease. This adds to the difficulties of developing a

therapy to target the metastatic disease. So this method of using rodents is not able to fully mimic cellular behavior during metastatic dissemination, which is a multi-stage process[11].

This process involves carcinoma cells from the primary tumor migrating along the lymphatic system or through the circulatory system, to invade the basement membrane and entering into blood vessels in a process known as intravasation. The tumor cells will migrate through the blood vessel channels, where they exits the blood stream towards other tissues in a process known as extravasation, where cancer cells will eventually grow and survive, known as colonization[10].

There are several reasons why metastasis remains the leading cause of death among cancer patients. One of which is the failure to detect the metastatic events early enough, and another is the failure to effectively treat and eliminate the metastatic cancer cells[10]. A limited understanding of the molecular and cellular mechanisms of the metastatic disease inhibits the development of effective therapies and the ability to pre-emptively diagnose metastatic disease[10]. This underlines the importance of understanding the multi-stage interaction between metastatic cancer cells and healthy tissue cells. Therefore, developments of new technologies to study metastatic disease and test potential drugs are necessary in order to fully understand the molecular and cellular mechanisms of the disease.

There have been numerous in-vitro devices and experimental approaches that have been invented to mimic individual stages of the metastatic disease. Some commercially available devices are capable of measuring cellular migration and

invasion in-vitro such as the transwell assay shown in Figure 1.1-1. In this in-vitro device, cancer cells are plated on top of a porous polycarbonate membrane and allowed to migrate from the upper compartment to the underside of the membrane, in response to a stimulus located in the lower compartment. Mouse lung tissue or human lung endothelial cells are be used as stimuli and placed in the lower

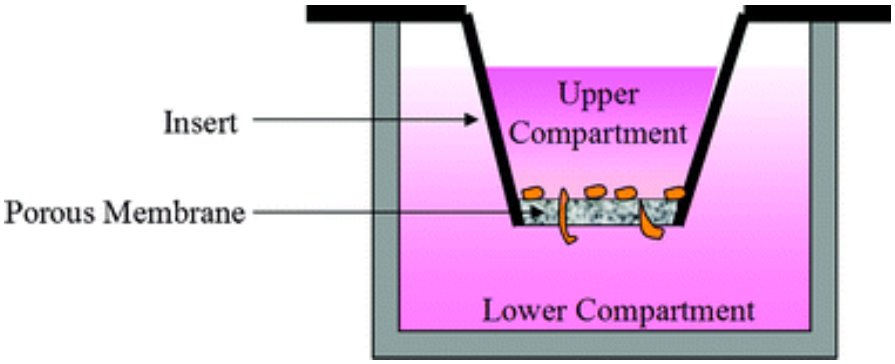

Figure 1.1-1: Transwell Assay[14].

compartment. Fluorescence microscopy can be used to visualize and measure the number of cells that respond to the stimulus and invade through the endothelial cell walls. This process mimics intravasation and extravasation of the metastatic disease. Because the membrane is very thin and the cells migrate from the top to the bottom side, such a device cannot be used to observe cellular migration or measure the migration across a given distance. Also, the migration cannot be analyzed continuously over time by researchers. The experimental approaches that have been performed in the past include culturing cells in 2 or 3 dimensions in order to examine cells proliferation, migration, and survival[10]. However, these approaches do not allow for researchers to study the entire cellular migration, but is limited to analyzing

one cellular process at a time. Therefore, current devices and experimental approaches do not adequately mimic the metastatic process[10].

Microscopic analyses of cells or molecules are traditionally performed on microscope slides, multilayer plates, and Petri dishes or object carriers[8]. Traditionally, microscope slides have been made of glass or silica glass not plastic, due to poor optical clarity as compared to glass. An exception to this is the use of plastic Petri dishes, where there is an opening toward the microscope or the spectrometer, so that the light emitted by the molecule does not have to pass through plastic on the way to the detector[7]. The Petri dish is specifically used for cell microscopy, but it does not have flow system such as a channel or reservoir to apply a defined flow. An object carrier is a flow chamber that is made of plastic, with at least one flow channel in the base plate connecting two liquid reservoirs on the upper side for light-optical microscopic examinations. These culture devices have been used in various biological medical examinations for light-optical microscopy or spectroscopic techniques. Besides using pure light-optical microscopy for examining cells, there is fluorescence, phase contrast or confocal microscopy, as well as the UV spectroscopy[7]. These traditional methods usually have difficulty to achieving precise physical or biochemical control of different types of cells[2]. Additionally, it is difficult to monitor cell migration behavior and to properly mimic the in-vivo microenvironment of the organisms in which the tumor resides.

The device from Ibidi, LLC is a microfluidic perfusion culture system that is currently on the market, which allows for examining cell migration across a given distance and over time. This in-vitro device is the size of a microscope slide and is comprised of a high-class plastic material such as polycarbonate, which does not have a birefringence or auto-fluorescence similar to that of glass. Polycarbonate is desirable for its optical properties which are ideal for high-resolution microscopy. This system was developed for quick and efficient flow of liquids to exchange between two liquid reservoirs connected by a long channel as shown in Figure 1.1-2. While this device is capable of measuring the migration of cells in response to stimuli over a period of time using time lapse micrography, is still lacks certain capabilities to analyze the entire metastatic process. The liquid reservoirs are too small, ranging from 1 to 20 mm in diameter and 3 to 30 mm in height. This does not allow for a large amount of cells to be plated, roughly a maximum of 7,000 cells may be plated in

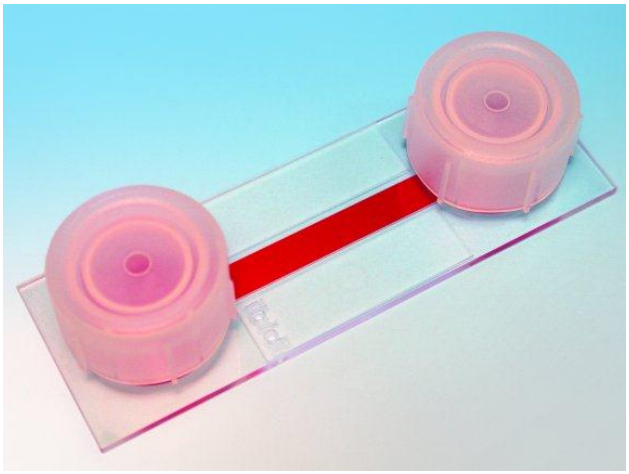

Figure 1.1-2: μ-Slide I from Ibidi LLC is a combination of a cell culture chamber and a coverslip for imaging inside a channel[5].

a 250 µl volume[10]. The reservoirs do not allow for tissue to be place inside the chambers. Only liquids can be examined with this device.

In addition, since the channel is openly connected between the two liquid reservoirs, the liquids flow quickly through the channel due to gravity and capillary action. It is essential for the two liquid reservoirs to remain at different levels for this action to occur. Only one liquid reservoir can be filled at a time, while the other liquid reservoir remains empty or partially filled[7]. Hence, there is no control over the liquid flow, because the channel is continuously open to the two liquid reservoirs. This indicates that fluid placed in one chamber will rapidly move to the other, preventing a long lasting chemical gradient[10]. Because of the openly connected channel, it is not possible to coat the walls of the cells on either end of the channel. This prevents the ability to analyze intravasation process of the disease with this device. The length of the channel in this device also causes limitations for cell survival for any extended period of time. Since the length of the channel is 50 mm, this results in a long extended path for the cells in order to travel to reach the other chamber[10]. In these types of devices, the cells are usually stimulated in a serum free medium, because cells cannot survive for a long period of time without serum protein. So, the distance that is required to travel may affect the survivability rate of the cells; if the researcher has to wait for any extended period of time for the cells to migrate to the other reservoir[10].

1.2 Scope of Work

This new in-vitro device has been designed to overcome the current challenges of previous devices. This novel device presents several unique advantages which will now enable researchers to analyze multiple aspects of metastatic cell behavior and mimicking multiple steps of the metastasis process. There are six distinct designs of metastasis mimetic devices presented in this thesis. The first three designs include the use of two chambers, one as an input and the other as a collection chamber. Both can hold cells or tissue. These two chambers are connected by a channel mounted on top or embedded into the base plate, which is optically clear. The opening on either end of the channel is a porous membrane barrier mounted in between the channel and chamber interface. This porous membrane at each end of the channel enables researchers to measure transendothelial invasion of tumor cells, by controlling the molecular diffusion and also serving as a scaffold for coating endothelial cells. This is especially important for examining cells in the metastasis process, because it will allow researchers to study how tumor cells can migrate through a wall of endothelial cells to enter into the circulation and exit out of the circulation. Being able to examine this process is important for determining how drugs will affect metastatic tumor cells. The last three designs omit the use of a channel completely and uses only one chamber placed in a cell culture dish. The chamber still incorporates the porous membrane into the design, while stimuli will be used inside or outside the chamber to analyze the number of cells that migrate into or out of the chamber. Cells

or tissues are plated in the input chamber and monitored over time for any changes in cell proliferation, migration, invasion, intravasation, extravasation or colonization in response to a chemotactic or haptotactic stimulus in the collection chamber.

Since there are no similar commercially available devices, this device is a significant advancement in technology to model cancer cells during the metastasis process. This device is capable of mimicking multiple steps of the progression of metastatic cancer such as cell proliferation, migration, invasion, intravasation, extravasation, and colonization of other tissues. The use of a porous membrane in this device allows for a coating of endothelial cells, which can mimic part of the blood vessel. This is an important contribution to the effectiveness of chemotherapy drugs in the metastatic disease, by determining the drug's ability to enter and exit the blood stream. The chambers on the device are large enough to accommodate a wide range of cells and tissue. This could be used to study cells in other areas of biomedicine including immunology, development, and physiology, because cell proliferation, migration, invasion, intravasation, and extravasation occur for different biological processes. This device enhances the current 3D cell culture models used to mimic the microenvironment of the primary tumor. Significant research questions will be answered with this device, such as how molecular and cellular differences in different microenvironments can influence the behavior of metastatic cells. This non-invasive device can be used to analyze multiple aspects of cancer cell behavior, and is capable of measuring cell migration through short distances.

Currently, the purpose of this device is to study metastatic breast cancer cells, but ultimately this device would enable researchers in multiple areas of cancer biology to understand the physiology of the metastatic disease. It also could be used to study other biological processes which involve changes in cell morphology, such as cell movements or invasion into the bloodstream. In the future, this device would be a more relevant and cost effective way to provide drug developers a powerful platform to test new therapeutic targets.

Chapter 2
Customer Requirements and Preliminary Design

2.1 Customer Requirements

Primarily, researchers and medical professionals such as doctors will be working with this metastatic device in a laboratory environment. In this research project, the customer requirements were derived from several meetings with Nikki Cheng, assistant professor, and Wei Bin Fang, postdoctoral fellow, from the Department of Pathology and Lab Medicine at Kansas University Medical Center. Customer requirements specified by the manufacturing, assembly and shipping personnel were also taken into consideration throughout the design process. Several requirements were conveyed that needed to be incorporated into this new metastatic device such as having a high optical clarity within the channel in order to allow for high-resolution microscopy. Some features required for the device are that it needs to easily fit a removable porous membrane filter at both ends of the channel. The chambers will need to be removable in order to allow microscopic inspection of the membrane filter between the chamber and channel interface. The two chambers needed to be moved closer together, roughly a half an inch apart or less in order to create the proper chemical gradient. The diameters of the two chambers needs to be

large enough to hold a human tissue samples or approximately 2 million cells. The entire device needs to be constructed out of a material that is biocompatible with human tissue and cells, and with the environment. This materials also needs to be able to withstand standard sterilization techniques such as the autoclave, ethylene oxide and gamma radiation (Table 1). The researchers do not want to use adhesives to assemble the device, because they could interfere with the experiments and with the optical clarity of the device. Other features include a device that should be easy to assemble onsite and in a laboratory environment. Furthermore, the device should not use adhesives to create a hermetic seal. This means the device should not leak to the outside or along the inside, between the two chambers caused by capillary action. This metastatic device should be disposable after one use; so it needs to be inexpensive to manufacture and easy to package and transport.

2.2 Design Considerations

Designing a microfluidic perfusion culture system involves many decisions, including the choice of material, system layout, manufacturing process, packaging, and sterilization techniques[9]. While other design parameters are dictated by the intended application and the customer requirements for the device; biocompatibility and sterilization techniques are a fixed requirement. The goal of understanding any design is to translate the customer requirements into engineering specifications, on how those requirements can be implemented into a sustainable design. With each customer requirement, the available options for the design narrows. Through the construction of several prototype designs, design considerations and specifications of the device were determined to fulfill the needs of the customer.

Through several iterations of construction, the layout of the device was determined, along with the size and thickness of the overall design. The material selection of the device influenced the majority of the other requirements in the design. The material for this device needs to be optically transparent similar to that of glass, resistant to cracks and scratches, and have low a birefringence, which can refract light in a different direction, or auto-fluorescence, which can emit light. This material needs to be biocompatible with human tissue and cells, inexpensive to buy and manufacture, and easy to transport.

The material for the capillary tube also needs to be determined using similar requirements. The capillary's diameter, wall thickness, and length need to be

determined in order to find the correct chemical gradient using capillary action in the cell migration. Similar techniques can be used to determine the proper dimensions of the channel for the other designs. Capillary cutting techniques must be explored in order to have a smooth and even cut since the capillary tube will be significantly close to the thin membrane filter. This can reduce the risk of the membrane being punctured by the small sharp jagged edges leftover from the cleaved end. The capillary and channel length must be reduced to 1-3 cm in order to allow researchers to measure the cell migration from one chamber to the other in a shorter amount of time, approximately 5-48 hours depending on the experimental conditions. This shorter distance traveled can allow experimental results to be obtained quicker, and enhance the probability of the cells surviving longer in serum free conditions for high-throughput screening of cells or drugs.

Experiments must be conducted to determine how the capillary interfaces with the chambers, while also being held against the porous membrane. The use of various material gaskets must be explored to find the best seal to stop a leak from occurring. To stop any leaks in between the two chambers caused from capillary action, inert silicone grease can be used. This silicone grease also helps hold the porous membrane filter in place and reduces the amount of wrinkle in the membrane while it is being inserted into the device.

The orientation, size and shape of the membrane must be investigated in order to reduce the risk of wrinkles and folds in the membrane filter, which can affect the number of cells that adhere to the bottom of the chamber. Techniques on how to

easily insert the membrane filter to diminish this problem must be considered. Also, the removal of the membrane is important to control the chemical gradient and the analysis of the cell-cell interaction. The 8-40 micron porous membrane can be fitted at both ends of the channel, which lengthens the stability of the chemical gradient and allows for a wall of cells to be plated at either end.

The chambers need to be removable in order to allow for microscopic inspection of the membrane filter and easy retrieval. The chambers diameter, thickness and height need to be determined, and are dictated by the type of material used in the device, because it costs less to buy standard sizes. The diameter and height of the chambers should be large enough to accommodate human tissue samples or a maximum of approximately 2 million cells. This requires the diameters of both chambers to be in the range of 1.5 cm to 6 cm. The chambers help to prevent cells from leaking into the channel prematurely by opening and closing the channel ends. This controls the number of cells entering into the channel and also controls the chemical gradient.

Chapter 3
Prototype Design Types

3.1 Material Selection

The material selection for this new metastatic device was based upon several factors. The optical clarity of a material was one of the most important requirements specified by the researchers. This requirement helped to quickly identify potential materials and quickly disqualify candidate materials for the device. This material needs to have a high optical clarity similar to glass, in order to have no obstructions observed due in part by the material itself. This includes having a negligible birefringence or auto-fluorescence, while also being durable and tough. Some of the other material requirements for this device include biocompatible with human tissue and cells, and the ability to withstand standard sterilization techniques. The material should be easy to work with, such as a thermoplastic for ultrasonic bonding or injection molding, while also being inexpensive to manufacture since the device is to be disposable.

Manually constructed prototypes were developed, which was dependent on the use of standard sizes from vendors in order to keep the cost of the prototype low. The cost of each prototype would significantly increase if standard sizes and

dimensions were not used in the construction of these devices. The sizes of the chambers were specified to be in the range of 1.5 cm to 6 cm by the researchers, but also were dependent on the standard sizes provided by the vendors. The inside diameter of the external chamber and the outside diameter of the internal chamber were dependent on the vendors supply. Due to the tight clearance between the internal and external chambers, both the external and internal chambers needed to be purchased from the same vendor in order to eliminate variances between manufacturers. The material selection for this metastatic device was determined by fulfilling all of the requirements of the researchers and by using available standard sizes from vendors.

A number of microfluidic perfusion devices are produced using a variety of materials including glass, silicone and polymers (Table 2). The device should be constructed using the same material, so that consistent assembly and manufacturing techniques can be implemented, in order to reduce the cost of the device. A spreadsheet of several types of materials was created in order to organize the varying sizes and dimensions of capillary tubes and chambers from the different vendors (Appendix A).

Initially, glass was the first material considered since a majority of microscope slides are made from it. But for this application, glass would be too brittle and would be prone to scratches and cracking. Determining a functional way of attaching the chambers to a glass slide, without using any bonding agent, would also cause

problems. But, using glass as a material for the capillary tube in connecting the two chambers is a viable option, and is explored more in-depth later on in the chapter.

Polysulfone (PSU) is frequently used in medical and pharmaceutical applications and can be used as an alternative to polycarbonate or acrylic. It is often used as a superior alternative to polycarbonate, due to its ability to resist deformation during load bearing applications over a broad range of temperatures. PSU has great mechanical properties, including that it is gamma radiation resistant and chemically resistant to most acids and solvents. This means PSU can be sterilized multiple times by using standard sterilization techniques such as an autoclave without losing its integrity. Upon further investigation of this material revealed that PSU is not an optically clear plastic. It is semi-translucent, which only comes in a light amber color.

The elastomer polydimethylsiloxane (PDMS) is by far the most commonly used material for the construction of microfluidic perfusion culture systems[9]. PDMS has a number of desirable material properties, especially its biocompatibility and permeability, but it lacks several key mechanical property values. PDMS has several disadvantages as a feasible material for this device due to its silicon-based properties, including its natural flexibility, and it would also increase the cost significantly. In addition, PDMS becomes cloudy when water vapor or ethanol permeates the material. The permeability of the material can cause unwanted evaporation and changes in the osmolality[9], which can affect the results of the experiments.

However, polymers are known to have several desirable mechanical properties, in addition to having excellent biocompatibility and durability capabilities. There are numerous types of polymers, but the crystalline structure of a polymer will determine if the polymer is transparent. As shown in Figure 3.1-1, various samples of polymers were obtained from Zeus Inc., such as fluorinated ethylene propylene (FEP), polytetraflouroethylene (PTFE), ethylene tetrafluoroethylene (ETFE) and perfluoroalkoxy (PFA) that were explored as viable materials due to their excellent biocompatible properties. Unfortunately, all of these polymers were determined to be translucent to be used for the device and the capillary tube. Other polymers such as polymethyl-methacrylate (PMMA), polycarbonate (PC) and polystyrene (PS) were more closely investigated due to the mechanical properties of these materials and

Figure 3.1-1: Sample materials from Zeus Inc. to be considered; **A)** Fluorinated Ethylene Propylene (FEP), **B)** Polytetraflouroethylene (PTFE), **C)** Ethylene Tetrafluoroethylene (ETFE), and **D)** Perfluoroalkoxy (PFA).

their optical clarity similar to glass.

Polymethyl-methacrylate (PMMA) is a highly optically clear plastic that is a versatile, impact and shatter resistant alternative to regular silicon glass, and commonly referred to as acrylic glass. Acrylic glass is a rigid thermoplastic material that has a distortion-free transparent surface, which provides several beneficial mechanical properties. This lightweight, biocompatible and cost-effective material can be easily injection molded and is ideal for the development of a disposable metastatic device. However, hydrogen peroxide gas plasma and ethylene oxide sterilization methods are commonly used rather than other sterilization techniques, such as steam autoclaving, due to the high temperature requirements of 100°C to 135°C (Table 1). Additionally, using gamma radiation sterilization methods on acrylic glass causes a color shift in the material, turning the clear acrylic glass into a yellowish color. Since the continuous service temperature of acrylic glass is 76°C to 88°C (Table 3), in addition to resistance to many chemicals, other methods of sterilization can be used, such as chemical immersion or electron beam. Another disadvantage to using acrylic glass is its proclivity to scratches and surface crazing, even when low stresses are applied for any length of time. This material trait would not work in a device that will be press-fit together when it is assembled.

The use of polycarbonate (PC) was closely examined, because it is a material that is similar to acrylic glass, but is known for its material properties as being stronger and more tolerant of higher temperatures than acrylic glass. Although, polycarbonate is slightly more expensive than acrylic glass, for the additional material

performance, polycarbonate is still a cost-effective material. Unlike acrylic glass, polycarbonate has a higher continuous service temperature (Table 4), which can withstand the harsh environments created from standard sterilization methods, such as the steam autoclave, gamma radiation and ethylene oxide (Table 1). Polycarbonate is widely used in medical devices as a replacement for glass due to its low weight and outstanding clarity of the material. Due to the low levels of monomers and catalysts used in processing polycarbonate, it is generally biocompatible and suited for use in medical applications where the surface of the device may come into contact with blood or other bodily fluids[4]. This thermoplastic polymer can be easily injection molded into a form to produce a smooth and optically clear surface finish. The material properties of polycarbonate will produce a durable and very tough material that has high impact resistance. This means the material will not be prone to cracking or surface crazing during the time a load is applied. These material traits will be suitable for a device that will be press-fit together or eventually be injection molded. Unfortunately, polycarbonate has low scratch-resistance; but this can be easily overcome by applying a hard clear-coat to the outside of the material to improve the performance characteristics. Polycarbonate offers a unique combination of superior clarity and high impact strength[4], which are great characteristics for this type of device. For these reasons, the first three metastatic devices were constructed from polycarbonate.

Polystyrene (PS) is widely used in the medical community as a disposable or reusable material such as Petri dishes, test tubes and other laboratory instruments. It

is a fairly inexpensive thermoplastic, which can be easily injection molded into any light weight and optically clear application. Polystyrene is extensively used in harsh environments where exposure to radiation, chemicals or moisture is a critical factor. That is why sterilization methods used in the post-mold process commonly involve the use of gamma radiation or ethylene oxide. Due to the low melting point of polystyrene, other sterilization methods that involve high temperatures cannot be used, such as steam autoclaving. Additional sterilization methods from Table 1 can be used as long as the sterilization temperatures stay relatively low. Since polystyrene is an inert polymer material, it is often approved by the FDA to manufacture containers for chemicals, solvents and foods. An additional beneficial material property of polystyrene from Table 5 is the water absorption of 0.05% to 0.1%, which is significantly less than acrylic glass or polycarbonate. Polystyrene is a rigid, glossy material, with superior clarity, but is limited by poor impact resistance[4]. As seen in Table 5, polystyrene has lower performance characteristics than acrylic glass and polycarbonate. But the requirement of having high impact resistance can be eliminated, due to the inherent design itself. In the last three designs, the chambers are not required to be press-fitted into place; instead they will be integrated into one device. As a result, from the useful material properties of polystyrene, the last three metastatic devices were constructed from polystyrene.

3.2 Prototype Design

The first design was constructed using a new and innovative way of incorporating a porous membrane filter into a metastatic device. The membrane filter was fitted between two concentric cylinders, with one cylinder having a slightly larger inside diameter than the others outside diameter, so that the two can slide inside one another. The four concentric cylinders form the two chambers on either ends of the slide. Each chamber is made up of two concentric cylinders that slide inside one another as shown in Figure 3.2-1. These concentric cylinders serve several purposes including holding the capillary tube and the porous membrane filter in place, controlling the flow through the channel, while also serving as a biocompatible chamber to hold the human tissue or cells. In the channel connecting the two chambers is a capillary tube that is fitted with a flexible seal at either end made from tygon, silicone or natural latex rubber. These two chambers are press-fit into a circular grooved surface in the slide, while holding the capillary tube in place by rubber gaskets at the ends.

Figure 3.2-1: Internal chamber fitted inside the external chamber.

The use of standard plastic microscope slides were explored, but further research revealed that microscope slides are commonly made from acrylic glass, not polycarbonate. But in order to have a better understanding of a standard microscope slide, a closer examination was required; so a small set of acrylic slides were purchased from Ted Pella, Inc. Inspecting the acrylic slide revealed the standard dimensions used in a microscope slide. The of the length and width of the slide was 3 inches by 1 inch, respectively, which seemed to be suitable dimensions for this new metastatic device. However, the thinness of the plastic slide made it flimsy, and it did not have enough material to support a structure on the surface. The thickness of the slide was 0.043 inch. As seen in Figure 3.2-2, this was too thin to make a deep enough circular groove, in order for the chambers to have a cavity to be press-fit into the slide. The proper depth for the slide was determined by using two slides sandwiched together, in order to double the thickness to approximately 0.086 inch. Additionally, it was observed that all of the microscope slides had a designated area at one end of the slide used for labeling the slide. These characteristics learned from

Figure 3.2-2: Standard acrylic medical slide with circular grooves cut at a depth of 0.016 inch.

inspecting standard plastic microscope slides can be incorporated into the design of this device.

Several different plastics vendors were researched online for polycarbonate material to construct this device. For the design, polycarbonate sheets were bought to machine thicker slides, and the use of polycarbonate tubes to serve as concentric cylinders for the chambers. As shown in Figure 3.2-3, an inexpensive polycarbonate sheet, which was purchased from Home Depot, was fabricated into thicker slides with a thickness of 0.09 inch, the length of 3 inches and a width of 1 inch. Due to additional sheets purchased during the design, the thickness of the sheets varied by ±0.003 inch due to tolerances set by the manufacturer. This caused different polycarbonate sheets to fluctuate in thickness from 0.09± 0.003 inch. It is recommended to purchase enough material at the beginning of the design, so that the varying dimensions caused from the tolerances do not conflict with previous drawings.

Figure 3.2-3: Pre-fabricated 3 inches by 1 inch polycarbonate microscope slide.

The chambers were designed using two separate extruded polycarbonate sizes, purchased from Professional Plastics. The dimensions of the smaller tube had an inside diameter of 0.625 inch and an outside diameter of 0.750 inch, which would function as the internal chamber. The larger tube had the dimensions of 0.750 inch inside diameter and an outside diameter of 0.875 inch, which would function as the external chamber. Both the internal and external chambers have the same wall thickness of 0.0625 inch. These polycarbonate tubes were UL rated, and in addition, made from FDA approved materials, which improves the biocompatibility.

This metastatic device had to be completely press-fit together, which meant the dimensioning of each part would create incredibly tight tolerances. In this design, the external chamber would be press-fit into the circular groove first. Then the internal chamber would be inserted into the external chamber, and press-fit in to place. The deformation of the material itself would allow for a tight press-fit seal. The internal chamber would be exerting an outward force on the external chamber, while at the same time, the external chamber would be exerting an inward force on the internal chamber. These opposing forces will be the mechanism to firmly hold the membrane filter in between the two chambers while the device is in use.

Each part was measured using a set of calipers, to an accuracy of one thousandth of an inch, so that drawings could be prepared. To come up with the dimensions of the machined circular grooves in the slide, and the exact diameters for the polycarbonate chambers, an experiment was carried out. Using a set of calipers, the inside diameter of the internal chamber was measured as 0.625 inch, and the

outside diameter of the external chamber was measured as 0.873 inch. Circular grooves were machined into the surface of a test slide using these measurements as shown in Figure 3.2-4. For the experiment, extreme temperatures were utilized in order to help evaluate how much the machined test slide and the chambers would expand and contract under such conditions. This would help to determine the initial dimensions needed for the drawings in order to create a tight press-fit seal. The test slide and chambers were subjected to the extreme heat of boiling water to 100°C for three minutes and being frozen in ice at 0°C. When the test slide was heated up, the material expanded, causing the outer diameter of the circular groove to loosen by 0.005 inch. While the inner diameter of the circular groove tightened by the same

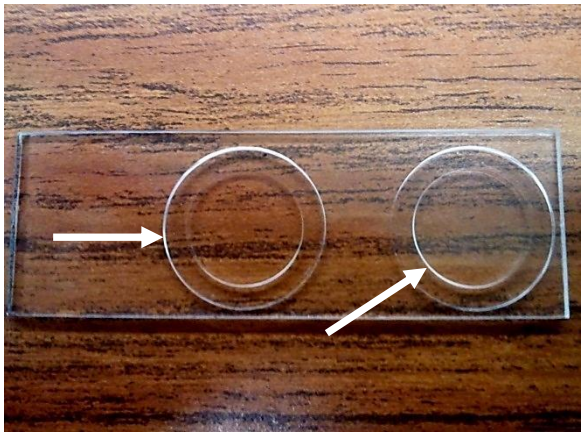

Figure 3.2-4: The white arrows are pointing to the inner and outer diameters of the circular groove cut into the test slide.

rate. This meant that the external chamber needed to be frozen in order for it to contract, and the internal chamber needed to be heated so that it would expand. As the external chamber froze, it contracted causing the chamber to loosen by 0.003 inch. When the internal chamber was heated, it expanded by the same amount. The parts

were then quickly assembled together. As the parts reached room temperature, the assembly began to tighten together creating a water tight seal.

As a result, a 3D AutoCAD model was made of the slide shown in Drawing 3.2-1, using the measurements attained from this experiment. The inner diameter of the circular groove was 0.628 inch and the outer diameter was 0.868 inch. During the construction of the AutoCAD model, a feature was added to the slide. A small channel was cut between the two circular grooves, in order to create a notch for the capillary tube to be held in place. This will keep the small capillary tube from rolling off the slide during the assembly process. Measurements taken from capillary tubes helped to determine the width and depth of the small channel. Furthermore, the depth of the circular grooves was determined by collaborating with the machinist who will manufacture the slides. Using the 3D AutoCAD model, a set of drawings was prepared for the machinist as shown in Drawing 3.2-2. The machinist used the drawings to manufacture a set of prototype slides with and without the small channel.

Once the prototype slides were received back from the machinist, the chambers dimensions could be determined. Using a chop saw, the machinist cut both chambers simultaneously by inserting the stock polycarbonate tubes inside one another. The chambers were cut from the stock tubing in 0.625 inch sections, which left the ends of the chambers rough. The tooling marks in the chambers could cause the device to leak. A variety of sandpaper grits were experimented with, to determine how smooth the ends of the chambers needed to be in order to create a water tight seal. As shown in Figure 3.2-5, the bottoms of the chambers were sanded with 300,

600, and 1200 grit sandpaper on a steel plate to ensure an even surface. It is crucial that the bottom surfaces are sanded evenly, otherwise leaks will occur. A small amount of water was used as lubricant between the sandpaper and the chambers. Not only does the water ensure that a thin layer of material is removed, but it helps dissipate the heat from the part in order to keep it from warping while it is being sanded. The white markings on the sandpaper seen in Figure 3.2-5, are from the

Figure 3.2-5: Sanding the bottom of the chambers on a steel plate.

excess material mixing with the water and grit to create a slurry paste. This helped keep the dust out of the air. When the white slurry fills the sandpaper, a damp towel can be used to easily clean it off, and then the sandpaper can be reused again. Each chamber was sanded using this method until the bottom surface had a smooth and even finish.

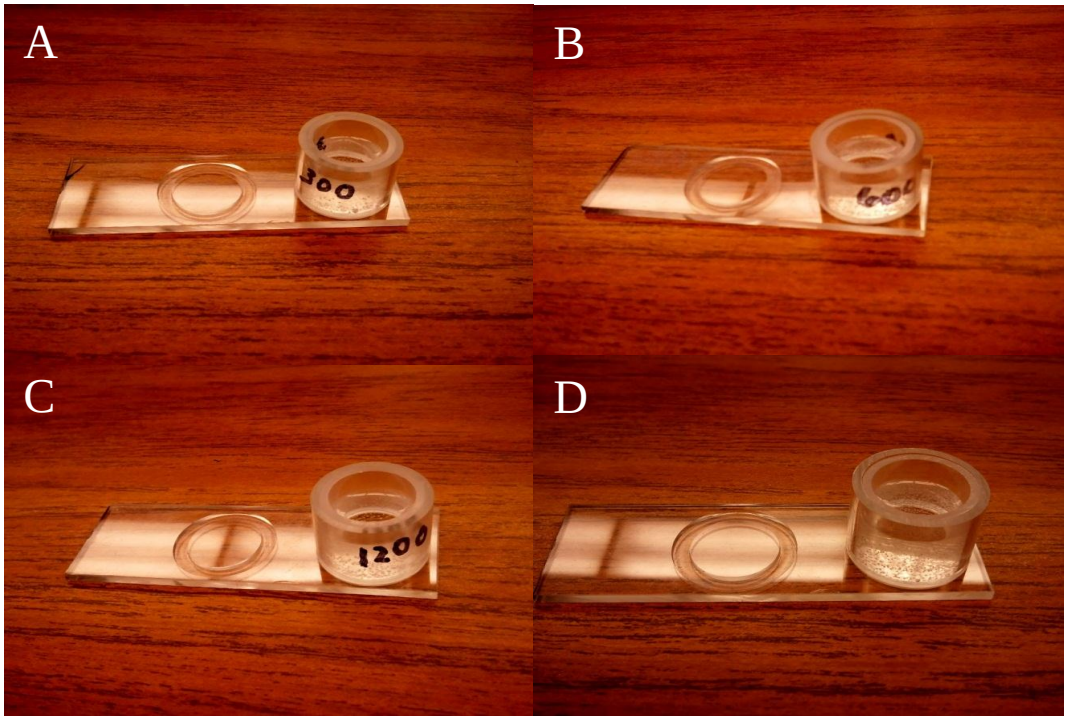

Figure 3.2-6: The chambers are marked with the grit of sandpaper used; **A)** Chamber sanded with 300 grit sandpaper, **B)** Chamber sanded with 600 grit sandpaper, **C)** Chamber sanded with 1200 grit sandpaper, **D)** Chamber not sanded.

As seen from Figure 3.2-6, the chambers are marked with a Sharpie to differentiate the grit of sandpaper used on the chambers. After the chambers were sanded, each set of chambers were press-fit into the slide and filled with water to test for leaks. The chambers were left filled with water for 15 minutes to test for small leaks developing. Sections A through C show that after the allotted time, no leaks occurred in all three types of sanding grits. Accordingly, chambers that were not sanded at all were press-fit into the slide and filled with water for the same amount of time in section D. These chambers as well did not result in a leak.

At the same time, the press-fit was too tight, so it was difficult to press the chambers into the slide. In some cases, the slide cracked at the weakest point due to

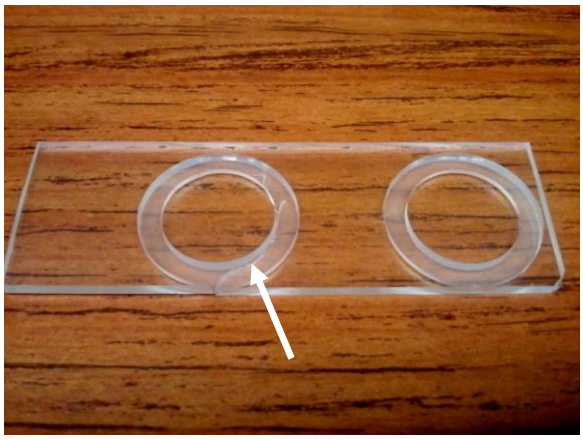

Figure 3.2-7: A stress cracked developed along the inner diameter in thinnest area on the slide.

internal stresses, while the chambers were being press-fitted into place, as shown in Figure 3.2-7. Furthermore, the depths of the circular grooves also contributed to the failure of the slide, because there was not enough material between the bottom of the circular groove and the bottom of the slide. Therefore, modifications to the 3D AutoCAD model and the slide drawings were necessary, shown in Drawing 3.2-3 and Drawing 3.2-4. The modifications decreased the depths of the circular grooves from 0.077 inch to 0.040 inch. This increased the amount of material from 0.016 inch to 0.047 inch between the bottom of the circular groove and the bottom of the slide. Additionally, the inside diameters of both chambers will need to be sanded in order to find the correct dimensions and to add some clearance between the two parts. The chambers should easily press-fit into the slide and not cause the device to leak.

Several experiments were completed in order to determine the correct dimensions of the internal and external chambers. An iterative method was performed, sanding down the inside diameter of the chamber by a thousandth of an

inch at a time, and then testing the chamber for leaks. The bottoms of the chambers were evenly sanded on a steel plate using 300 grit sandpaper, before being press-fit into the slide and filled with water. Initially, the inside diameter of the internal chamber was measured at 0.625 inch, before it was evenly sanded to 0.626 inch. The chambers were press-fit into the slide and filled with water. Once more, the chambers did not leak during the 15 minutes, and still fit too tight to be easily assembled. The inside of the chamber was sanded until an additional thousandth of an inch of material was removed. The inside diameter was 0.627 inch before the testing procedure was repeated. This time, the chamber easily snapped into the circular grooves, creating a snug fit. Section A of Figure 3.2-8 shows that the chambers did not leak when left filled with water for the set time. In section B of Figure 3.2-8, the inside of the internal chamber was sanded to 0.628 inch, which caused the chamber to leak.

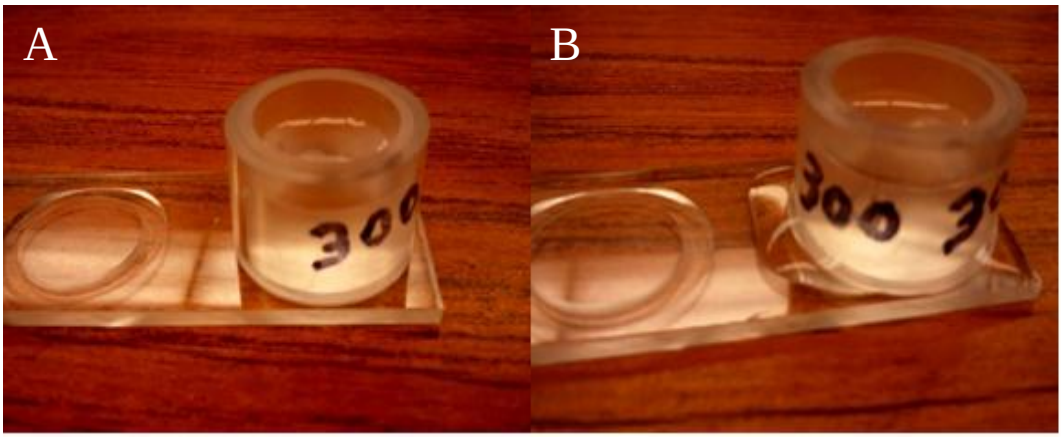

Figure 3.2-8: The inside of the chambers were sanded so it is easier to press-fit the chambers into the slide; **A)** The inside diameter of internal chamber was sanded to 0.627 inch, **B)** The inside diameter was sanded to become 0.628 inch, which resulted in the chamber leaking.

The same experimental procedure was performed with the external chamber in order to determine the correct inside diameter. The inside diameter of the external chamber should be large enough to easily slide the membrane filter and internal chamber in and out, while also constraining the internal chamber. The inside diameter of the external chamber was initially 0.753 inch, before several experimental iterations of the test were completed. The inside diameter of the external chamber was sanded to 0.756 inch until no leaks occurred. Figure 3.2-9 shows the assembly of the device on one completed side using the correct dimensions. The dimensions can easily be replicated on another set of chambers for the other side of the device.

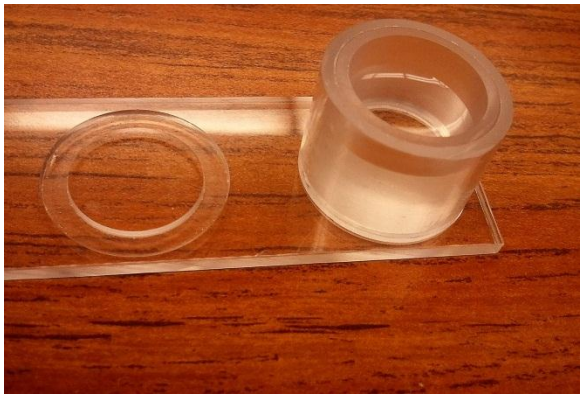

Figure 3.2-9: The assembled device without any leaks using the correct dimensions determined from the experiments.

Once the dimensions of the device were determined, incorporating the membrane filter in between the two chambers, without the device leaking, will be the next experiments. The membrane filters for this metastatic device were delivered from the Department of Pathology and Lab Medicine at Kansas University Medical Center to the Intelligent Systems and Automation Lab in the School of Engineering,

at the University of Kansas. The membrane filters were originally purchased online by Kansas University Medical Center from Whatman, a part of GE Healthcare. Whatman offers a variety of diameters and different pore sizes of the circular Nuclepore™ track-etched polycarbonate membrane filters, which are commonly used in fluorescence microscopy. Two different sets of these membrane filters were purchased from Whatman, with different diameters, but the same 8.0 µm pore size. These types of membrane filters are manufactured from high-quality polycarbonate film and have a smooth flat surface for clear visibility of particles. One set of the polycarbonate membrane filters had a larger diameter of 47 mm, while the other set had a smaller diameter of 25 mm.

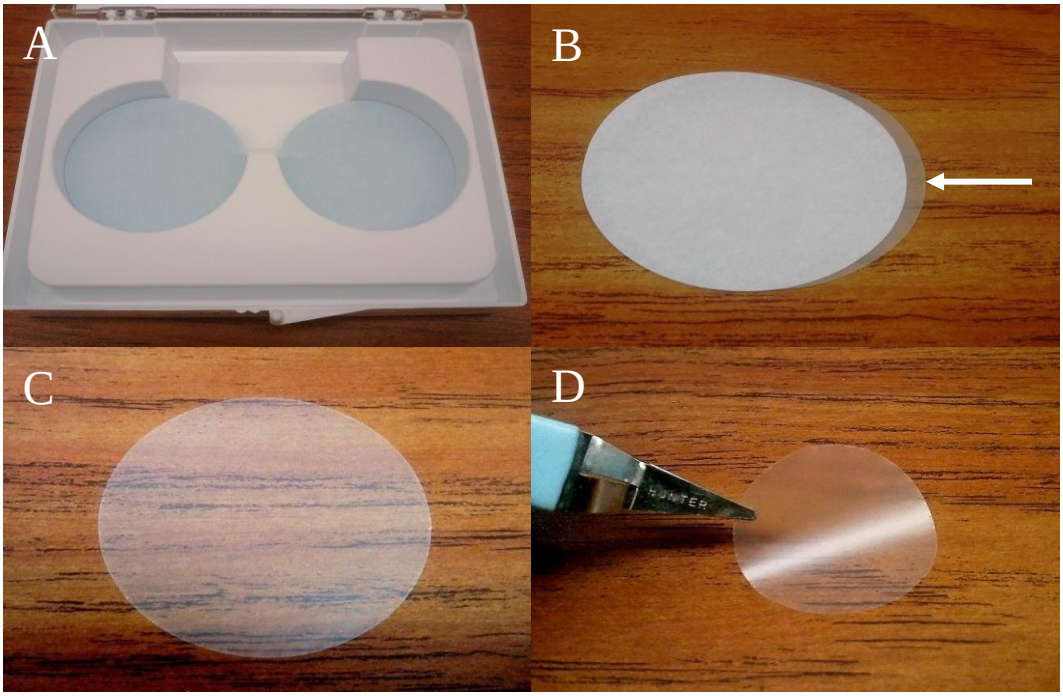

Figure 3.2-10: A) Stacks of membrane filters in the plastic container, **B)** Arrow pointing to the membrane filter underneath the separator, **C)** Showing the 47 mm polycarbonate membrane filter, **D)** Showing the 25 mm polycarbonate membrane filter.

The membrane filters were encased in a plastic container, in order to protect the filters from becoming damaged during transport, as shown in section A of Figure 3.2-10. Between each membrane filter is a blue separator paper, which helps protect each membrane filter and keeps the filters from clinging together due to static electricity, as shown in section B of Figure 3.2-10. The white arrow of section B is pointing to the 47 mm polycarbonate membrane filter beneath the separator paper. Once the membrane filters are removed from the container, the blue separator paper can be discarded. Section C of Figure 3.2-10 shows the larger 47 mm circular membrane filter that is used to investigate how size and shape can affect the number of wrinkles produced in the filter, which can obstruct the cell migration. Section D of Figure 3.2-10 shows the smaller 25 mm circular membrane filter, which is being held by tweezers.

Initially, when the membrane filter was placed in between the chambers, the paper-thin membrane would snag and occasionally tear. This was due to the tight clearance between the two chambers, which is necessary for the device not to leak. However, if the clearance between the two chambers were increased, water would leak in between the two walls of the chambers due to capillary action, but not enough to leak outside of the chambers. In addition, the membrane filter would create several wrinkles, which resembled pleats, when being inserted into the external chamber. The number of wrinkles and creases in the membrane filter can affect the number of cells that adhere to the bottom of the chamber. Several experiments were carried out to investigate how the membrane orientation, size and shape can affect these issues.

Furthermore, techniques for easily inserting the membrane filter in order to diminish these problems were also considered.

The first sets of experiments were conducted in order to stop the membrane filter from tearing while being inserted into the external chamber. The outside diameter of internal chamber needed to be reduced in order to add clearance between the two chamber walls. It was sanded down by 0.010 to 0.015 of an inch, in order to allow enough room for the membrane filter to be inserted without being torn. Additionally, this allowed the internal chamber to move freely, which meant easier removability of the membrane filter, while also providing a means of regulating the flow rate of the device. The internal chamber could be rotated clockwise or counterclockwise to increase or decrease the size of the opening to the channel. This would increase or decrease the flow rate through the channel.

Consequently, this would allow water to easily flow upward between the two chamber walls by capillary action. To resolve this issue, a thin layer of Haynes™ silicone grease was spread around the outside of the internal chamber in order to fill any gaps, to stop the water from entering the narrow space. Haynes™ silicone grease is NSF rated H-1 food-grade grease that is made from ingredients approved by the FDA. It is inert and chemically resistant grease that can be used for food and pharmaceutical applications. This silicone grease can withstand temperatures ranging from -40° F to 400° F, which is ideal for a number of sterilization techniques that can be employed.

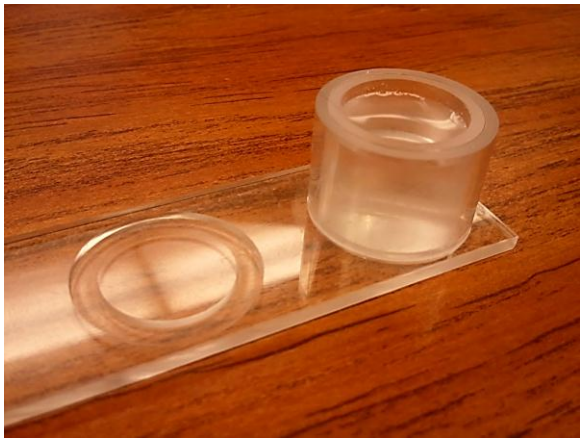

Figure 3.2-11: The silicon grease filled the narrow gap to stop the water from leaking between the chamber walls due to capillary action.

Once the silicone grease was applied, in a thin layer on the bottoms of both chambers and on the outside of the internal chamber, the water stopped leaking between the walls of the chambers; due to capillary action as shown in Figure 3.2-11. The excess silicone grease around the tops and bottoms of the chambers can be easily cleaned off with a damp towel. With the silicone grease incorporated into the design, the chambers needed very little sanding, which meant the dimensions did not need to be as accurate, or the tolerances so tight. The silicone grease will fill all the gaps and imperfections in the press-fit seal, so that the device remains water tight. Furthermore, the silicone grease helped reduced the amount of wrinkles and creases that occurred in the membrane filter while it was being inserted in between the two chambers. The silicone grease allowed for the clearance between the chamber walls to be expanded and gave the chambers a slippery surface to slide across. The silicone grease made it easier for the chambers to slide together, which helped reduce the

amount wrinkles that occurred in the membrane filter when it was being inserted into the external chamber. The silicone grease also helped hold the membrane filter in place while being inserted.

Further experiments were carried out to explore how the membrane's orientation, size and shape can reduce the number of wrinkles and creases in the membrane filter. Both the 47 mm and the 25 mm membrane filters were experimented with, by placing the membrane filters in different orientations inside the chamber. The membrane filter had to completely cover the channel opening, so that the cells could not escape and go around the filter. The orientation of the membrane

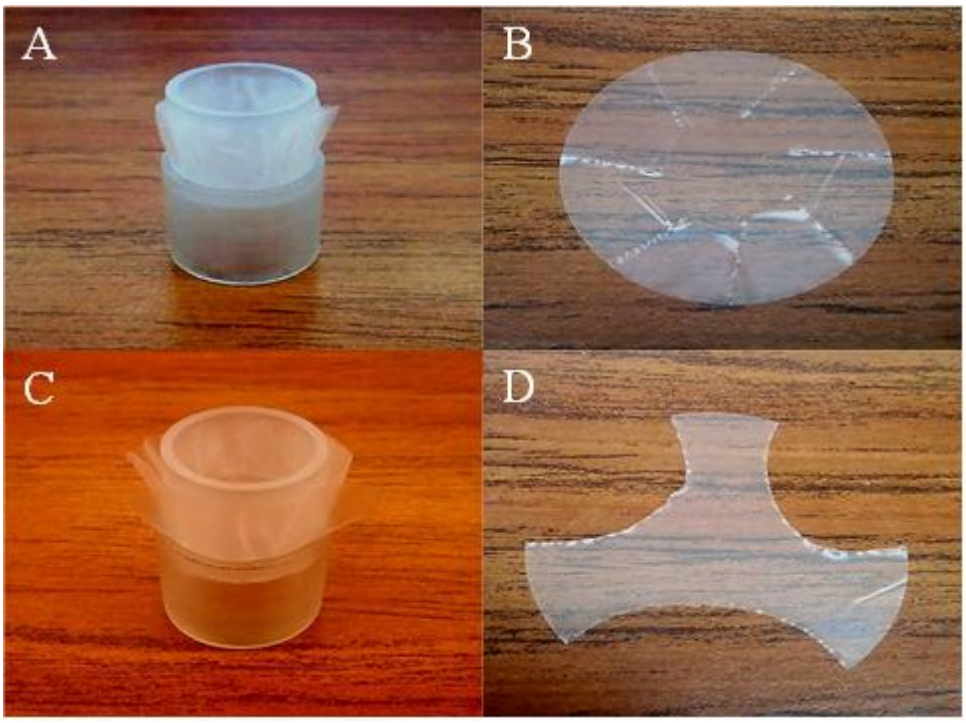

Figure 3.2-12: A) Numerous wrinkles formed in the larger membrane filter while it was being inserted into the external chamber, **B)** Shows how slits were cut into the membrane filter to help the filter fold on itself, **C)** The slits in the membrane filter did reduce the number of creases that formed, **D)** Shows how other geometric shapes were investigated, but also having a continuous cut helped improve the resistance to tearing.

filter needed to reduce or completely remove the number of wrinkles and creases in the membrane filter. Also, the orientation of the membrane filter had to be easy enough for the user to assemble.

Through experimentation with the larger 47 mm membrane filter placement, it was placed around the bottom of the internal chamber. This caused severe wrinkling in the membrane filter when it was being inserted into the external chamber, as shown in section A of Figure 3.2-12. To eliminate the number of creases, the membrane filter was cut into various geometric shapes in order to relieve some of the stresses. Section B of Figure 3.2-12 shows how slits were cut into the membrane filter using an X-Acto® Knife. The slits were cut at an angle to better help the filter fold on itself. This helped reduce the number of creases that formed while the filter was being inserted between the chambers as shown in section C of Figure 3.2-12; but it also increased the chances of the membrane tearing. Since the membrane filter had been

Figure 3.2-13: The white arrow is pointing to the edge of the tear in the membrane filter.

initially torn, cutting slits in the membrane, the formation of new tears would propagate from the ends of the slits and tear the membrane completely while being inserted. The filters that were cut were more likely to tear, than the membrane filters that had not been cut. To help stop the tears from developing at the end of the slit, circular holes were punched at the ends of the cuts. This made a continuous cut with no edges, so the tears would not have a single point from which to propagate. Section D of Figure 3.2-12 shows an example of a continuous cut that was experimentally studied. The membrane filters using this approach did improve their resistance to tearing, but did eventually tear. The white arrow in Figure 3.2-13 is pointing to an edge where the membrane filter tore, but also shows that no wrinkles were formed using this technique.

The smaller 25 mm membrane filter was investigated in the same manner as the larger 47 mm membrane filters; by placing the smaller membrane filter around the bottom of the internal chamber. But the 25 mm membrane filter was too small to

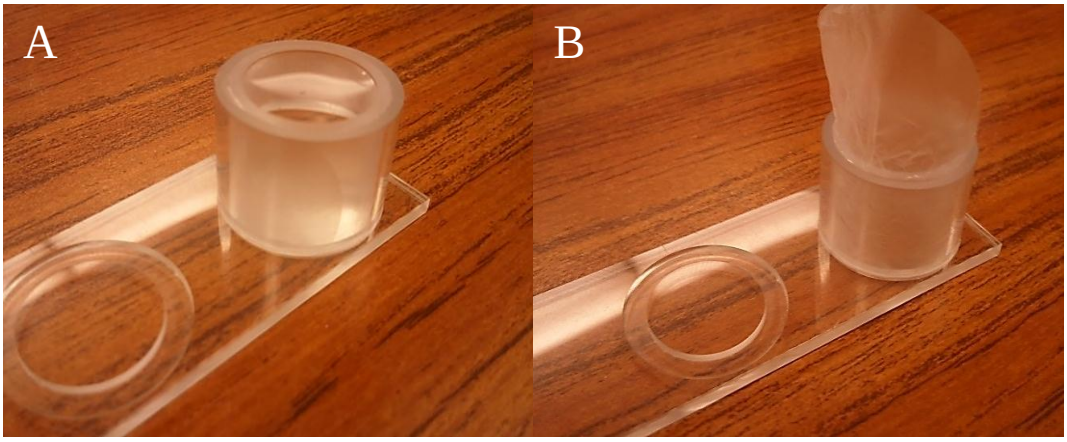

Figure 3.2-14: A) The 25 mm membrane filter wrapped around the side of the internal chamber produced no wrinkles and completely sealed the channel opening; **B)** Same method was applied to the 47 mm membrane filter with similar results.

completely cover the channel opening and caused numerous wrinkles in the filter. The membrane filter was then wrapped along the side of the internal chamber, so that the bottom of the membrane filter folded underneath the bottom lip of the internal chamber as seen in section A of Figure 3.2-14. This method of orientation allowed the membrane filter to completely seal the channel opening as well as completely eliminate any wrinkles or creases in the membrane filter. The silicone grease also helped hold the membrane filter in place, while it was being sandwiched in between the chamber walls. This technique of inserting the membrane filter can be easily applied to the larger 47 mm membrane filter with the same results, as seen in section B of Figure 3.2-14. The excess material of the membrane filter can be cut away or inserted further to cover the bottom of the internal chamber. But it is recommended to not cut the membrane filter and use the smaller 25 mm membrane filter wrapped along the side of the internal chamber using the silicone grease.

The proper technique for inserting the membrane filter into the external chamber using the silicone grease without producing any wrinkles is as follows:

1) Gather the slide and the internal and external chambers, along with one membrane filter and the silicone grease.

2) Cover the bottom end of the external chamber with a thin layer of silicone grease and place it inside the circular grooves on the slide.

3) Hold the internal chamber horizontally by its ends, between the index finger and the thumb, while applying a thin layer of silicone grease around the outside of the internal chamber.

4) Wrap the membrane filter, at its midpoint, around the outside of the same internal chamber with the silicone grease. Be sure to leave ¼ of the membrane filter hanging below the chamber.

5) Be sure to hold the membrane filter and the internal chamber vertically between the index finger and the thumb, when coating the bottom end of the internal chamber with a thin layer of silicone grease. Make sure to not get any silicone grease on the front face of the membrane filter.

6) Insert the sub-assembly into the top of the external chamber on the slide. Be certain that the bottom portion of the filter folds underneath the lip of the internal chamber before completely inserting the sub-assembly.

7) Use a damp towel to wipe away any excess silicone grease from the top and bottom portions of the chambers.

8) The same procedure can be repeated to assemble the other set of chambers on the opposite end of the slide.

The design of the chambers was investigated in order to determine the hole sizes in the chambers. A 3D AutoCAD model of the internal and external chambers was prepared as shown in Drawing 3.2-5, in order to primarily test the proof-of-concept for the rubber gasket. The initial dimensions used for the 3D AutoCAD model were estimated, so that experiments could be conducted to test the rubber gasket for leaks. In Drawing 3.2-6 shows the exact dimensions used to machine the hole sizes in each of the chambers. The rubber gasket was inserted into the

rectangular hole of the external chamber while the chamber was being press-fit into place. Since the device does not have any pressure behind the rubber gasket, the press-fit of the external chamber firmly holds the gasket in place. The circular hole in the internal chamber sets directly center behind the rubber gasket, which is then used as the opening to the capillary tube.

An assortment of rubber tubing was purchased in order to produce the rubber gaskets, because standard O-ring sizes were not small enough to fit around the capillary tube in order to create a hermetic seal. In addition, the shape of the rubber gasket needed to be square for the design and not circular. The rubber tubing provided an easy and relatively inexpensive way of producing a number of gaskets from a variety of materials. In Figure 3.2-15 shows the types of rubber tubing that was used to create the square rubber gaskets. Using an X-Acto® Knife, a square gasket was cut from each type of rubber tubing and placed in the square opening of the external chamber to test for leaks. The gaskets were all cut ten thousandths of an inch larger than the square opening, so the material could deform and compress in order to create a tight seal. Due to the rubber tubing being circular, the square gaskets

Figure 3.2-15: The different types of rubber tubing that was used with to create the rubber gaskets; **A)** Natural Amber Latex Tubing, **B)** White Silicon Tubing, **C)** Clear Tygon S-50-HL Medical Tubing.

all had a curvature, which contoured the shape of the chamber. This helped the rubber gaskets stay abutted against to the chamber wall. The natural amber latex tubing in section A of Figure 3.2-15 performed the best due to the material properties of the latex. The material was soft enough to expand inside the square opening, while the external chamber was press-fit into place. When the chambers were filled with water, the gasket was able to completely seal the opening in the external chamber and stop the device from leaking. The white arrow in Figure 3.2-16 shows how the latex gasket was set into place without the device leaking. The silicone tubing and the clear tygon medical tubing shown in sections B and C of Figure 3.2-15, respectively, were too firm to create a good seal. The material did not deform as much as the latex gasket in order to create a hermetic seal.

Once it was determined that the latex gasket could completely seal the gasket hole, it was necessary to determine the correct dimensions of the hole sizes in both chambers. Using calipers, measurements of the capillary tube were taken in order to help determine the correct dimensions for the hole sizes. These dimensions were

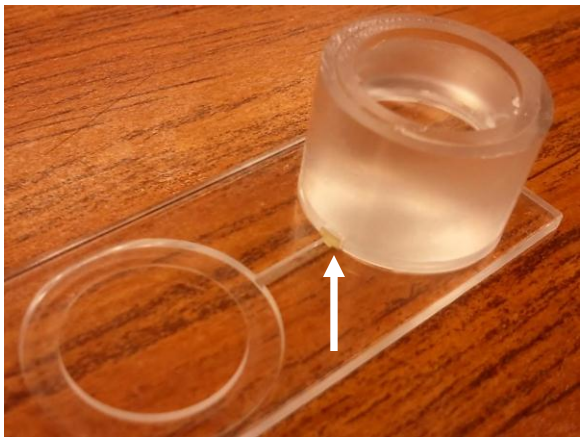

Figure 3.2-16: The white arrow is pointing to the natural amber latex gasket that was able to completely seal the gasket hole.

used to help modify the 3D AutoCAD model shown in Drawing 3.2-7. The dimensions of the square gasket hole in the external chamber were increased from 0.10 square inch to 0.14 square inch. This meant that the dimensions for the rubber latex gasket needed to be 0.15 square inch, so the material can compress to create a tight seal. The diameter of the capillary hole opening in the internal chamber was decreased from 0.050 inch to 0.046875 inch in order to match the opening in the capillary tube. A set of drawings for the chambers were produced for the machinist is shown in Drawing 3.2-8. Figure 3.2-17 shows the final designs of both the internal and external chambers using the correct dimensions.

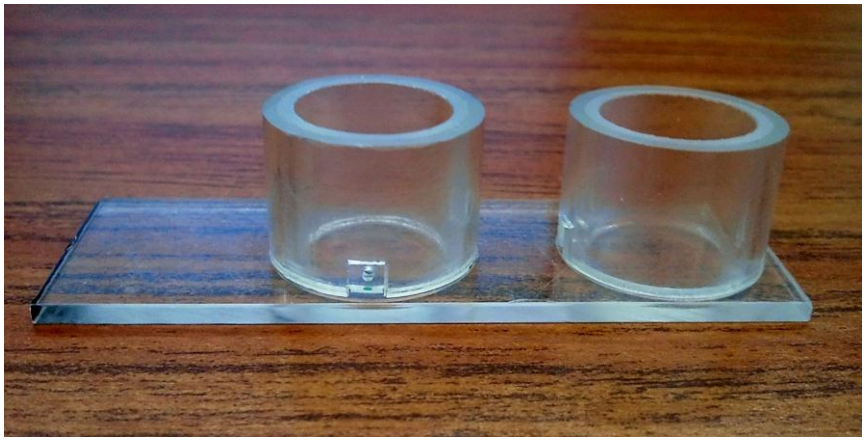

Figure 3.2-17: The front face of the chamber openings using the correct dimensions for both the internal and external chambers.

A variety of different sizes and materials of capillary tubes were investigated in order to determine the best optical clarity and ease of manufacturing. Both glass and plastic capillary tubes were tested in order to find the advantages and disadvantages of both materials. The optical distortion caused by the curvature of the capillary tube was taken in consideration. The plastic capillary tube shown in section

A of Figure 3.2-18 has a comparable optical clarity to that of the glass capillary tube shown in section B of Figure 3.2-18. One obvious advantage of using a plastic capillary tube is that the user does not have to worry about accidently breaking the capillary tube, which could result in someone getting injured. Furthermore, it can be easily cut using an X-Acto® Knife to an accuracy of ten thousandth of an inch. However, for this device, the technique of cutting the capillary tube needs to have an accuracy of one thousandth of an inch. The end-face of the plastic capillary tube

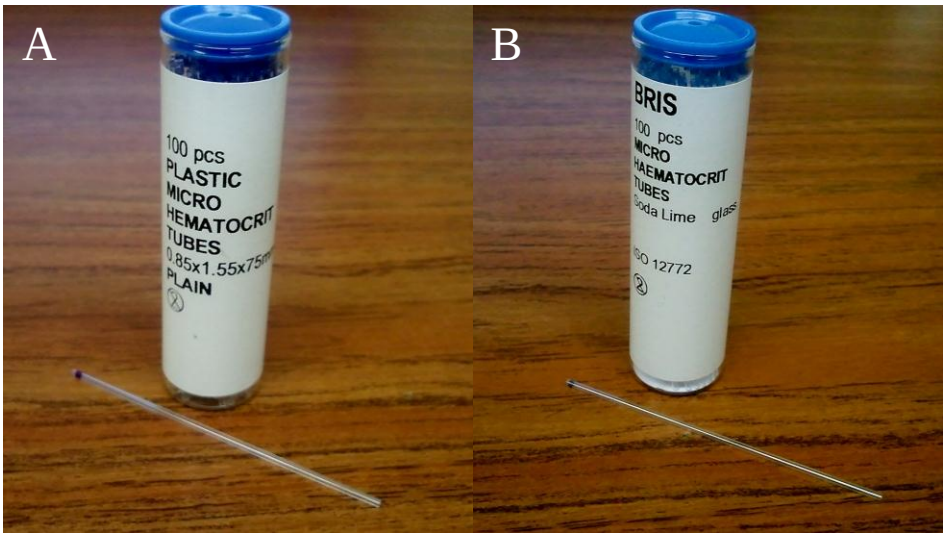

Figure 3.2-18: A) Plastic capillary tubes, **B)** Glass capillary tubes.

produces a clean finish with minimal surface defects, but it is rather difficult to get a straight perpendicular cut. For these reasons, the glass capillary tube was more closely investigated. One major advantage of using a glass capillary tube rather than a plastic capillary tube is its superior clarity. Conversely, the difficulties of producing a high quality end-face that is debris free and has a perpendicular cut with an accuracy of one thousandth of an inch is a major disadvantage. It is imperative that

the cleaved end has a smooth and perpendicular cut, because the capillary tube will be abutted next to the membrane filter. This will reduce the risk of the membrane being punctured by the cleaved the end.

Since glass capillary tubes are commonly used in the medical industry, there are a number of techniques used to help cut capillary tubes in order to produce a quality end-face. The optimal performance in many capillary applications is dependent upon the end-face quality[12]. There are four standard techniques for producing a quality end-face on a capillary tube as seen in Figure 3.2-20. The first technique is standard cleaving, which uses a ceramic scribe to score the around the outside of the capillary tube in order to create a stress concentration. This allows the capillary tube to produce a clean break that is used for general applications shown in as section A of Figure 3.2-20. The second technique is precision cleaving, which yields a nearly perpendicular end-face, while minimalizing debris and surface defects from the capillary's end-face as seen in section B of Figure 3.2-20. The technique is employed in high tolerance applications such as microfluidic interfaces. The third technique employs laser cutting, which produces an ultra-high quality precision cut

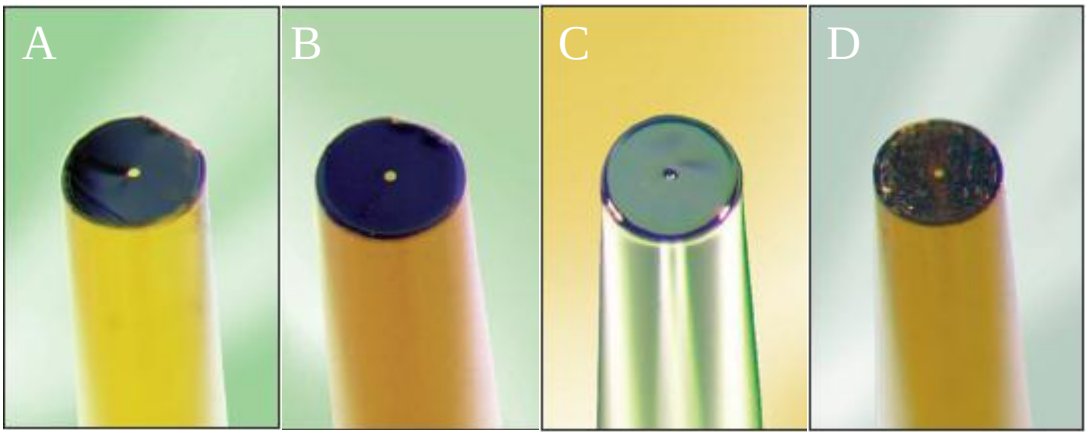

Figure 3.2-20: Four capillary cutting and cleaving techniques[12]; **A)** Standard Cleaving, **B)** Precision Cleaving, **C)** Laser Cutting, **D)** Saw Cutting.

that is defect free and yields a polished end-face. Section C of Figure 3.2-20 shows how the laser left the edges of the end-face rounded, to produce a defect free and smooth finish. This method is commonly used in applications where durability, high quality and low debris end-faces are required. The fourth technique is saw cutting, which often causes small micro-fractures and chips at the end-face as shown in section D of Figure 3.2-20. To help improve the end-face quality, the capillary ends are polished. This technique is often used in high volume applications in order to reduce the cost.

Due to the optical clarity that was required for this device, a glass capillary tube with an inside diameter of 1.15 mm and an outside diameter of 1.50 mm was implemented. This meant that it was necessary to develop a technique to overcome the challenges associated with a glass capillary tube. The end-face of the glass capillary tube needed to be debris free with no defects, while also ensuring a perpendicular cut that was accurate to one thousandth of an inch. The capillary cutting technique employed a combination of standard cleaving and precision cleaving due to its low-cost and high accuracy.

The cutting technique involved using a new capillary tube every time the end was cut, because the capillary tube would develop small fracture at the edges, which would increase the risk of the capillary tube breaking. A set of calipers was used to help determine the length of the capillary tube and also to ensure the accuracy of the cut to one thousandth of an inch. The capillary tube was lined-up along the side of the calipers at a set distance of 0.475 inch, so that the length could be marked with a

Sharpie as shown in section A of Figure 3.2-21. Then the capillary tube was placed alongside a ruler in order to ensure that the score mark of the ceramic cutting tool was perpendicular to the capillary tube. Using a ceramic cutting tool and the perpendicular lines on the ruler, the capillary tube was scored just above the mark around the outside as shown in section B of Figure 3.2-21. The capillary tube was then broken at the score mark. The cleaved end-face of the capillary tube was then viewed underneath a microscope, which produced an uneven and jagged end-face. The end-face of the capillary tube was then sanded down on a steel plate using 400 grit sandpaper, to produce a debris free and perpendicular end-face. The end-face

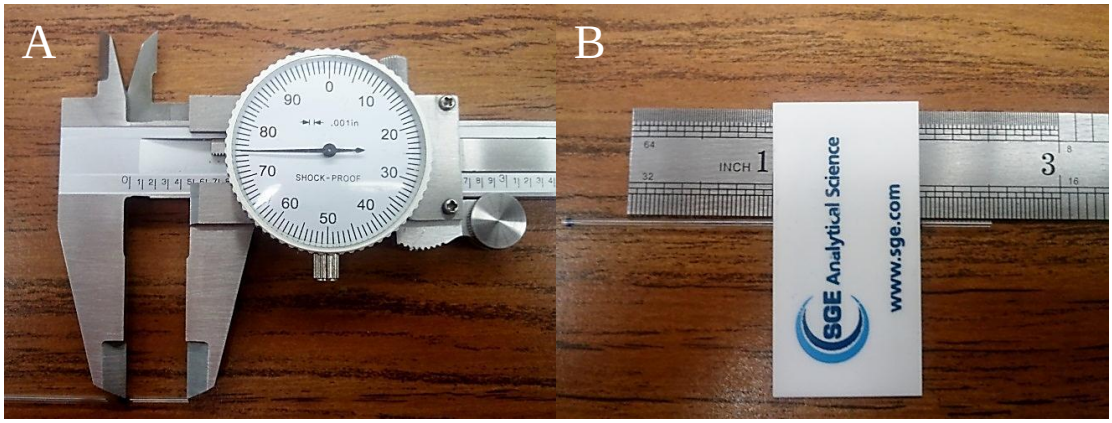

Figure 3.2-21: A) Lining-up the capillary tube alongside the calipers at 0.475 inch in order to mark the length with a Sharpie, **B)** Using a ruler to ensure that the score mark of the ceramic cutting tool is perpendicular to the capillary tube.

was then sanded to the length of 0.475 inch, using 1200 grit sandpaper. This cutting technique was able easily produce the exact length of the capillary tube needed, by only sanding off a thousandth of an inch at a time. The results of this cutting technique were compared to the standard cleaving technique by viewing with a

microscope, which produced a smooth and perpendicular end-face with no defects. This cutting technique was also able to produce the capillary's length with an accuracy of 0.001 of an inch as shown in Figure 3.2-22.

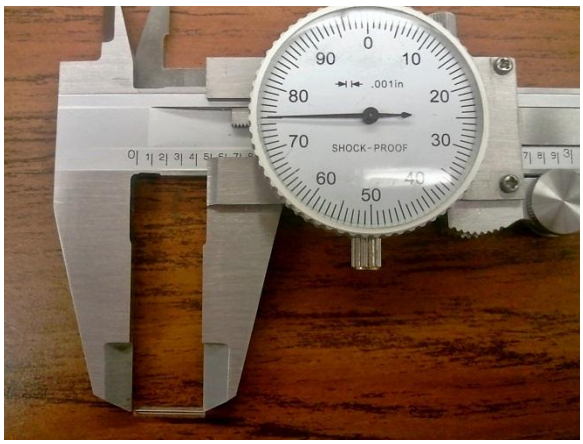

Figure 3.2-22: Using this cutting technique allowed the capillary tube to be cut to the exact specifications of 0.475 inch with a smooth and perpendicular end-face.

A whole was punched in the center of the latex gaskets using a sharp scribe, so that the newly made capillary tube could be assembled. The assembly of the capillary tube and the latex gaskets, fitted at both ends, are assembled first. Figure 3.2-23 shows how the capillary tube subassembly is set into place on the circular grooves in the slide before the chambers are press-fit into place. The gaskets hold the capillary tube in place during the assembly process, which keeps the tube from rolling off of the slide. This made the small notch to hold the capillary tube on top of the slide unnecessary, so modifications to the 3D AutoCAD model were made as shown in Drawing 3.2-9. Furthermore, the device is going to be viewed from the bottom, therefore this would eliminate viewing obstructions caused by the notch and create a

clearer viewing window. The final set of drawings that was made for the prototype slide is shown in Drawing 3.2-10.

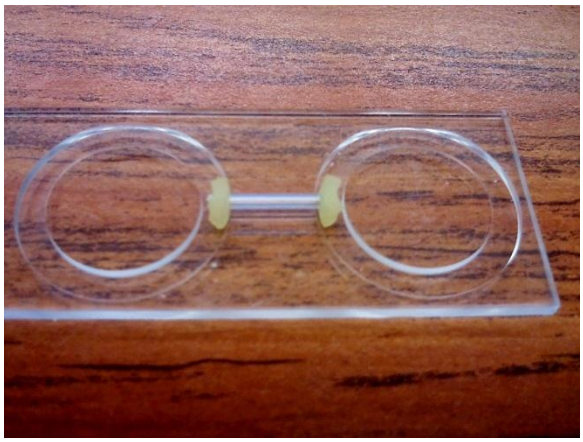

Figure 3.2-23: The subassembly of the glass capillary tube and the latex gaskets on top of the slide.

The device was then completely assembled together to test the overall function of the device; to see if it would work as intended without any leaks. The top of the right chamber was filled with water. The water flowed from the right chamber through the capillary tube to the left chamber, until each chamber reached equilibrium as shown in Figure 3.2-24. The device worked exactly as it was designed, flowing 10 µl of water through the capillary tube. The silicone grease prevented any leaks from occurring outside or between the chambers.

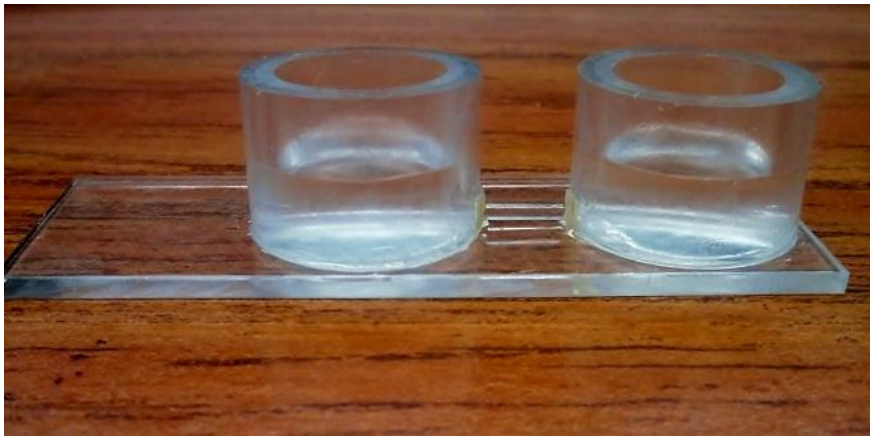

Figure 3.2-24: The device was assembled and then tested to see the overall function of the device.

The device fulfilled most of the customer's requirements including: the device does not leak outside or between the chambers, the membrane filter can be easily removed, the chambers are moved closer together in order to obtain the correct chemical gradient, the device is biocompatible with human tissue and cells, no adhesives are required to assemble the device, it is inexpensive to manufacture, the device can be easily packaged and disposed of after it is used, and it can withstand standard sterilization techniques.

Some of the requirements that the device does not fulfill are the optical clarity of the connecting channel between the two chambers and the ease of assembly of the device. Even though the glass capillary tube was used in this design for its high optical clarity, there was still some optical distortion caused by the curvature of the capillary tube. The assembly of the device was challenging, due to the number of small parts that were utilized in the design. The device incorporates 10 small parts, plus the use of the silicone grease. To assemble one metastatic device includes: 1

slide, 2 internal chambers, 2 external chambers, 2 membrane filters, 2 latex gaskets and 1 capillary tube. Adding to the challenge is assembling the capillary tube subassembly. It is hard to place the small gaskets at the very ends of the small capillary tube without the gaskets slipping off during the assembly process.

The final prototype design, as seen in Figure 3.2-25, was shown to Nikki Cheng and Wei Bin Fang. Both researchers were satisfied with the overall design of the device, but presented an additional requirement. The channel opening needs to be positioned at the very bottom of the chamber, not 0.075 inch above the bottom as shown in Drawing 3.2-8. These issues with the prototype design led to additional designs.

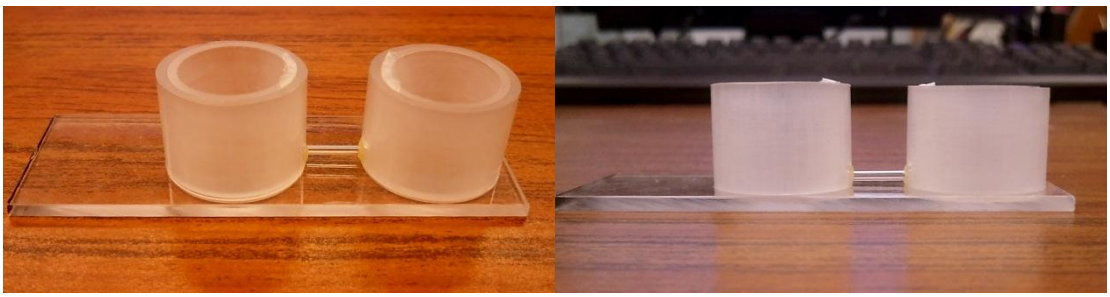

Figure 3.2-25: The final assembly of the prototype design.

3.3 Type I Design

This design satisfies all the original design requirements, plus helps resolve the issues with the optical distortion, the number of parts, and the position of the channel opening. The device is an integrated design rather than a modular design, where the specific features are combined into one complete device. The capillary tube subassembly was improved, by integrating the connecting channel into the polycarbonate slide as shown in Drawing 3.3-1. This allows the connecting channel to have a flat surface instead of being curved in order to reduce the optical distortion. The bottom of the channel is enclosed by fixing a rectangular polycarbonate cover plate to the back of the device. Drawing 3.3-2 shows the front of the device, where the positions of the channel openings were moved to the bottom-center of the chambers. An unaltered internal chamber with the same diameters as in the previous design is used to hold a 47 mm membrane filter at the bottom of the chamber. Using the silicone grease, the membrane filter can be easily inserted into the external chamber by wrapping the membrane filter around the bottom of the internal chamber. The wrinkles that are produced along the walls of the chamber are no longer significant, since the channel opening is placed in the bottom-center of the chamber. The external chambers will be permanently fixed to the top of the slide shown in Drawing 3.3-3. The slide and the external chambers will be made as one part. A set of drawings were produced as shown in Drawing 3.3-4, using the dimensions from the previous design and estimating the dimensions for the connecting channel.

An accurate 3D AutoCAD model of the slide was produced using the material properties of polycarbonate. Modifications were made to the model in order to increase the sizes of the channel openings from 0.15 inch to 0.20 inch, as shown in Drawing 3.3-5. This increases the number of cells that migrate through the channel. Also, the internal circular grooves on top of the slide were decreased to 0.746 inch, which increased to sizes of the circular grooves. This allowed for the external chambers to more easily be set in place. Additionally, the rectangular flow channel was modified to have a width of 0.20 inch and a height of 0.0315 inch, which can be viewed on the back of the slide in Drawing 3.3-6. This increases the flow through the channel to 7.5 ml. The Drawing 3.3-7 shows all of the alterations made to the slide, which details the exact specifications. These drawings were used to manufacture the slides from polycarbonate sheets.

Once the slides were received back from the machinist, it became apparent that tooling marks obstructed the view of the channel. Figure 3.3-1 shows the tooling marks in the front and back of the slide. This issue can be easily resolved when the slide and the external chambers are injection molded as one part, as shown in Drawing 3.3-3. Then the entire device would have the same optical clarity as glass.

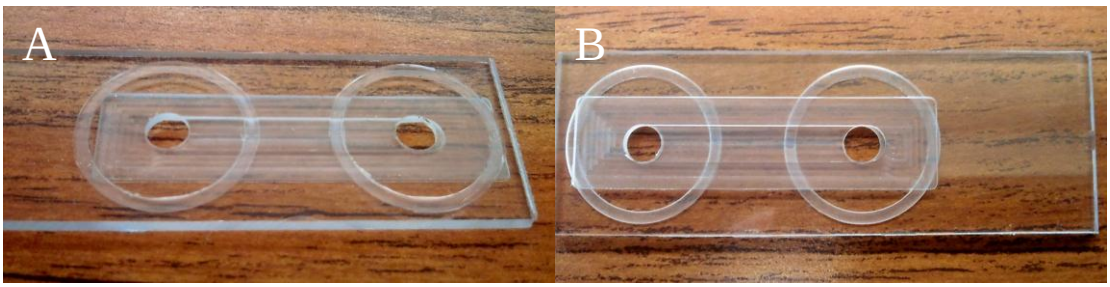

Figure 3.3-1: Shows the tooling marks from being machined; **A)** Front, **B)** Back.

The external chambers were placed in the circular grooves on top of the slide and permanently fixed into position by Weld-On® #4 adhesive. This adhesive is a water-thin, fast-setting solvent cement developed to form high-strength bonds between thermoplastics. It can bond polycarbonate pieces together, by first softening the surface of the plastic and then fusing the pieces together with the evaporation of the solvent, leaving a clear and residue free finish. The bond forms within minutes, but continues to significantly increase in strength over several hours.

The adhesive was applied, using a brush as the directions specified, to the pocket cut on the back of the slide in order to attach the cover plate. Even though the brush was hard to control, the adhesive was only applied to the surface of the pocket cut and not to the inside of the channel. After the cover plate was fixed in position, the Weld-On® adhesive started to quickly evaporate, leaving a white discoloration in the bond as seen in Figure 3.3-2. However, it was also observed in the areas where the solvent did not discolor, the tooling marks and the small scratches were removed. The white discoloration can occur when a fast evaporating solvent has been recently applied to a surface, which cools the coating below the dew point of the surrounding

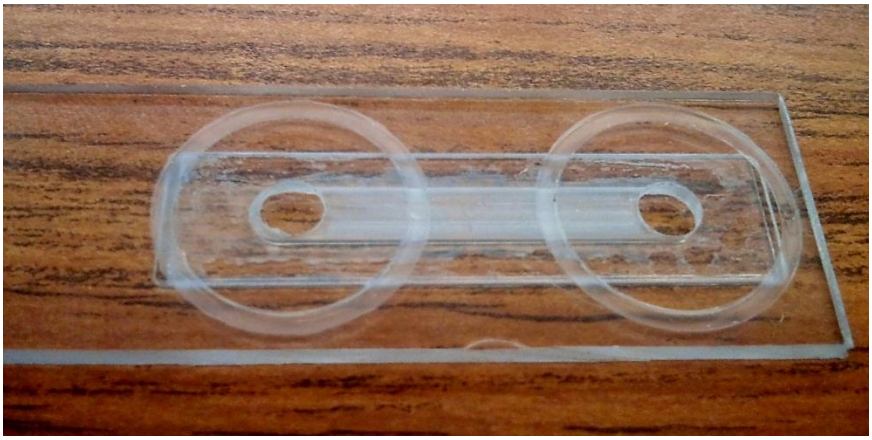

Figure 3.3-2: The Weld-On® adhesive left a white discoloration where the cover plate was bonded.

atmosphere, causing moisture to condense on the wet surface. This is commonly referred to as blushing and frequently happens during periods of high humidity. The problem can sometime be resolved by using a slower drying solvent or dehumidifying the surrounding air.

Several experiments were conducted to help resolve the issue of the solvent blushing and determine the best method to apply the solvent. A thin layer of Weld-On® adhesive was bonded to a machined surface and a finished surface, to see how the surface finish would affect the clarity of the bond. The machined surfaces formed small bubbles in the bond, leaving voids where the solvent was wicked into the micro-fractures and small pits in the material. The solvent did remove any scratches or tooling marks from the surface, which increased the clarity of the device. The bond between the finished surfaces did not form any bubbles or have any discoloration, because the pits in the surface were too small for the solvent to be wicked into, and the drying time was slower. Unfortunately, the solvent was only applied to areas where the surface had been machined.

It was determined through experimentation that the best method for applying the solvent was to use a 22 gauge syringe or a Weld-On® applicator bottle with a needle to control the flow of the solvent. The blushing was reduced only when a small amount of the solvent was used. Some of the flow channels were covered with a thin layer of solvent to remove the scratches and tooling marks. Using a 3 ml syringe, the solvent was dripped through the channel creating a thin layer, which increased the clarity of the viewing window as seen in Figure 3.3-3. Before the cover

plate and the slide were bonded, the two parts were clamped together in order to reduce the number of bubbles that formed. However, the bubble formation was localized in the pocket cut and not in the channel. This meant that the bubble formation in the pocket cut was not an issue, since the optical clarity of the device was focused on the flow channel. The flow channel was only obstructed by the tooling marks and small scratches, which can be easily resolved by using the solvent or having the part injection molded. The solvent was then wicked in between the parts using a syringe around the perimeter of the joint. This helped reduce the amount of air that came into contact with the evaporating solvent, which would not be able to blush.

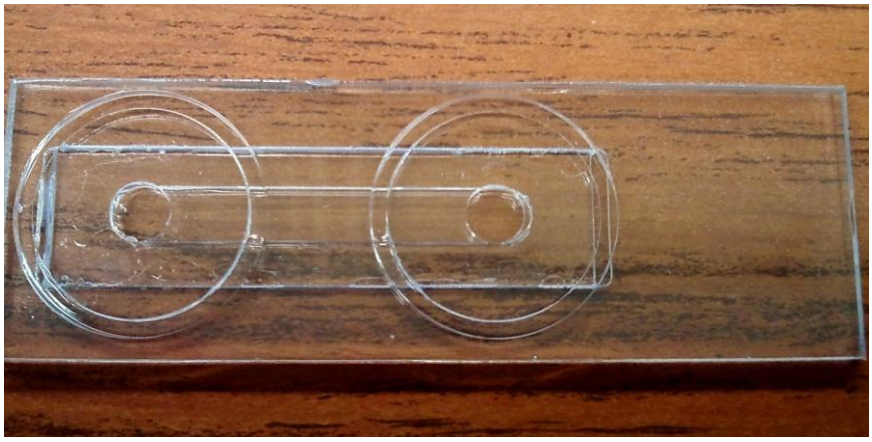

Figure 3.3-3: The solvent was used to remove all of the tooling marks and small scratches from the machined slide.

Using the syringe and clamp method, the device was assembled together with no discoloration and limited bubble formation, as shown in Figure 3.3-4. The cover plate was first placed in the pocket cut on the back of the slide and clamped into place. Using a syringe, small amounts of the solvent was injected around the

perimeter of the joint in order to make a hermetic seal. This created the bottom of the flow channel, with no bubbles forming and no discoloration. The inside surfaces of the external chambers were sanded down to 0.760 inch before being permanently affixed to the top of the slide. The outside surfaces of the internal chambers were sanded down to 0.740 inch in order to allow for ten thousands of an inch of clearance between the chamber walls. This permitted adequate room for the membrane filter to form wrinkles and easily let the internal chamber be removed. The silicone grease was later used to stop the water from leaking in between the inner and outer chamber walls. The external chambers were affixed on top of the slide by placing a small amount of the solvent in the circular grooves using a syringe and then pressing the chambers into place. If the solvent did not make a hermetic seal, the syringe was used to place the solvent around the outside perimeter of the chamber at the joint. Then the external chamber was tested for leaks, by filling the chamber with water. If a leak occurred, the chambers would first be dried and then the solvent would be injected with the syringe at the location of the leak until a hermetic seal was formed.

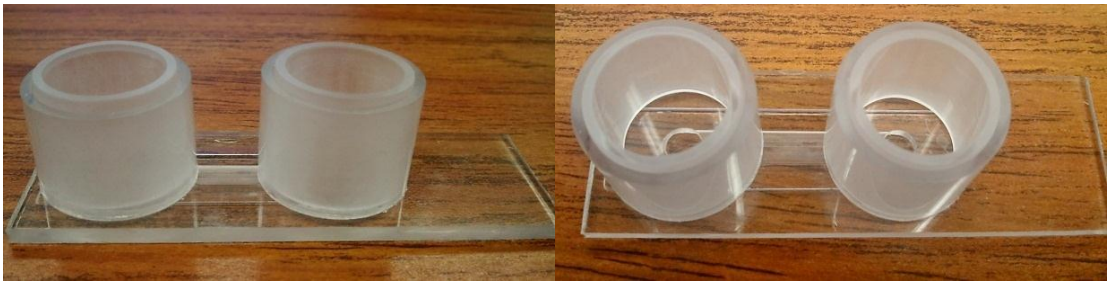

Figure 3.3-4: The device was assembled with no discoloration and limited bubble formation. The flow channel was not cleaned with the solvent to remove the tooling marks.

The number of parts was significantly reduced, to five parts in this design, to include: 1 slide, with the external chambers affixed on top and the cover plate affixed to the bottom, 2 membrane filters and 2 internal chambers. The rubber gaskets used in the previous design are not needed for the current design, because the flow channel was integrated into the slide by fixing the cover plate in order to reduce the amount of optical distortion. The optical clarity of the entire device would not be an issue if the external chamber and the slide were to be injection molded together. The metastatic device would then have the same high optical clarity as glass. Eventually, the back cover plate could be ultrasonically welded inside the pocket cut of the slide in order to create a watertight seal. This would eliminate the issues of discoloration and bubbles formation. With these design changes and the methods for manufacturing, the device would be to be inexpensive to produce.

The device was shown to the researchers, who noted that the Type I design had several improvements over the previous design, but mentioned some areas of concern. The positions of the channel openings needed to be aligned with the channel, so that the flow channel would directly open into the side of the external chamber, not through the bottom-center. This would allow the cells to better replicate the migration through the human body. Otherwise, the cells would have to make a 90° turn to migrate into the flow channel from the bottom-center of the chamber. Additionally, the flow channel was too large, which prevented only a few cells from migrating through the channel at a time. It was decided that the size of the flow channel needed to be a 1 mm square.

3.4 Type II Design

In this design, the device incorporates several features from the previous design, but also utilizes new features to resolve the issues with the flow channel. The size of the flow channel was reduced to a 1 mm square, which limits the number of cells that can migrate through the channel. But to have the flow channel open directly to the sides of the external chambers, two circular holes were cut through the slide to fix the external chambers in place, as shown in Drawing 3.4-1. The cover plate was utilized to create the bottom surfaces of the external chambers and the flow channel. The external chambers were be inserted into the circular holes and rest on top of the bottom cover plate, while being firmly held in place by the circular holes in the slide. Drawing 3.4-2 shows the exact dimensions used to manufacture the slides. Abutted against the channel opening was a 1 mm size hole in the side of the external chambers, while the internal chamber has a larger opening in order to control the flow rate, as seen in Drawing 3.4-3. The chambers were then manufactured to the dimensions from Drawing 3.4-4.

The slides that were manufactured had fewer tooling marks than the previous set of slides in the former design. This increased the clarity of the slides; however, several of the slides were cracked at the same location along the edge, caused by the high stresses from being machined. In Figure 3.4-1 the white arrow is pointing to the location of where a stress fracture occurred. The cracked slides were easily bonded together using the Weld-On® #4 adhesive.

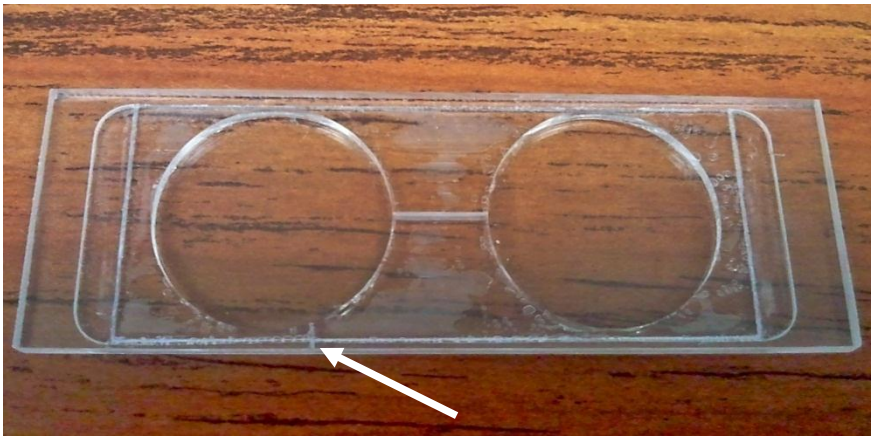

Figure 3.4-1: The white arrow points to the location of where the stress fracture occurred from being machined.

The device was then assembled together using the syringe and clamp method developed from the Type I design. The back cover plate was first sanded along the edges in order to remove any burrs that formed while being cut to the specifications in Drawing 3.4-5. Section A of Figure 3.4-2 shows how the cover plate was inserted inside the back pocket cut of the slide and firmly held in position with two binder clips. This reduced the amount of bubbles that formed between the two surfaces. A syringe was used to control the flow of the Weld-On® adhesive in order to wick the solvent between the cover plate and the slide. This prevented the solvent from blushing, which can cause a decrease in clarity. The solvent was injected along both ends of the cover plate until the solvent stopped wicking in between the two surfaces. The tooling marks were still visible where the solvent did not cover, due to the larger surface area of the cover plate. The solvent has a limited range of how far it would wick in between the two surfaces. The two clamps were then removed, and a single clamp was positioned along the side of the slide as shown in section B of

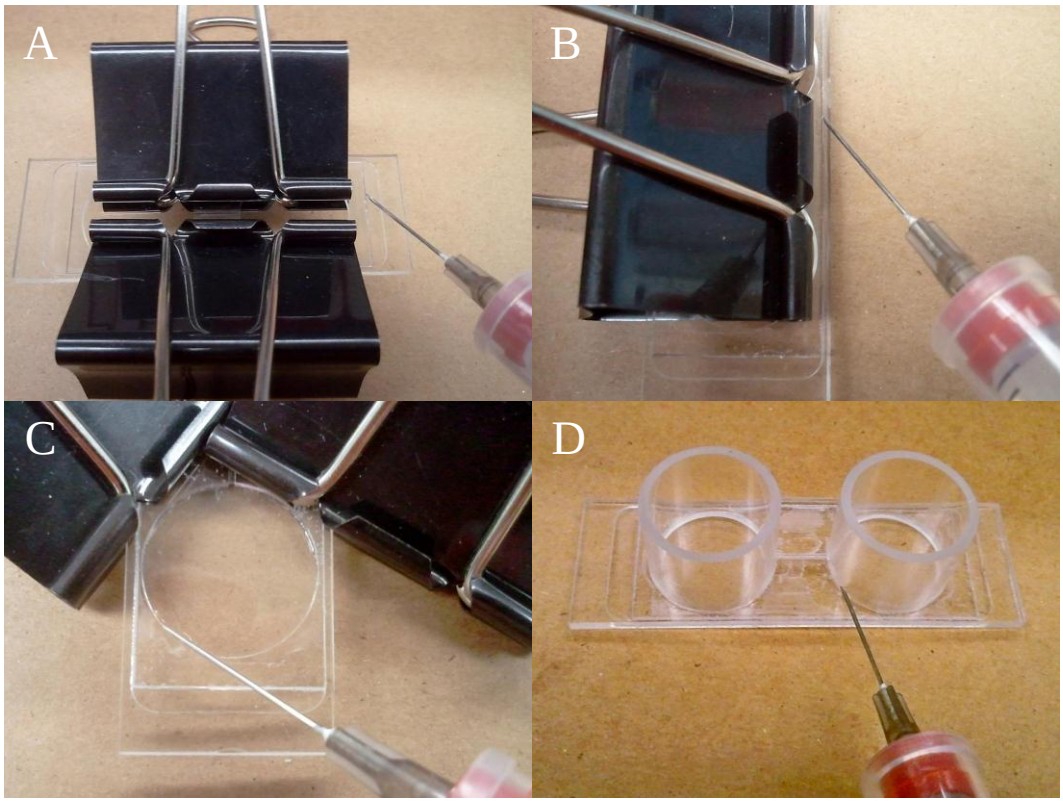

Figure 3.4-2: A) The solvent was wicked in-between both ends of the cover plate, **B)** The syringe was used to inject the solvent along the length of the joint, **C)** The syringe was used around the circumference of the through hole to wick the solvent, **D)** The solvent was injected around the bottom edges of the chambers.

Figure 3.4-2. The syringe was used to inject the solvent along the length of the joint until the solvent stopped wicking in between the joint. The clip was repositioned along the other side of the slide so that the procedure could be repeated. Then the slide was flipped over, and the clips were repositioned around one of the through holes, as shown in section C of Figure 3.4-2. The syringe was used around the circumference of the through hole to wick the solvent in between the slide and the cover plate. The solvent was carefully injected near the channel opening in order to ensure that the opening was not completely sealed. Capillary action pulled the

solvent along the sides of the flow channel, affixing the channel to the cover plate. The clips were removed and repositioned at the other through hole so that the procedure could be repeated. The inside diameters of the external chambers needed to be sanded down to 0.760 inch before being permanently affixed to the through hole on top of the slide. The outside surfaces of the internal chambers were also sanded down to 0.740 inch, in order to increase the amount of clearance between the chamber walls. This allowed plenty of space for the 25 mm membrane filters to be easily wrapped along the sides of the internal chambers and be easily removed. Then the external chambers were inserted into the through hole, and the channel openings were aligned with the flow channel. Section D of Figure 3.4-2 shows how the syringe was used to inject solvent around the bottom edge of the chambers until the chambers were hermetic seal. In Figure 3.4-3 shows the final assembly of the device being tested for leaks.

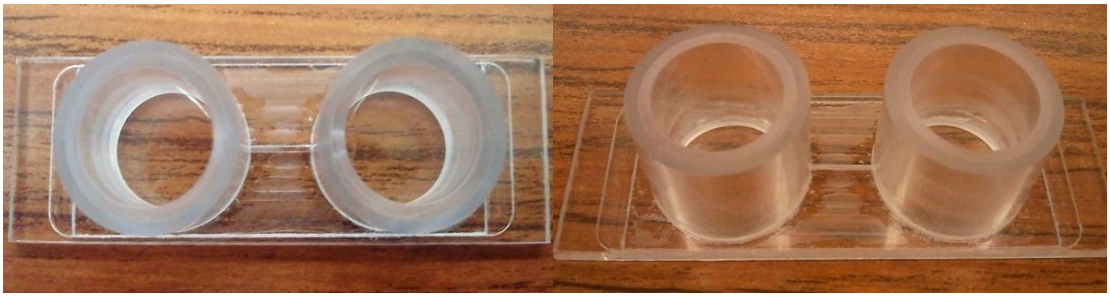

Figure 3.4-3: The final assembly of the device being tested for leaks.

The assembled devices were tested for leaks using the membrane filters with the silicone grease in between the chamber walls. But feedback from the researchers suggested that the silicone grease was stopping the growth of the cells. However, the

grease could still be used if it is not placed around the channel opening. A method was devised, so that the silicone grease could still be used without getting it near the channel openings. The silicone grease was brushed along the bottom edge of the inside surface in the external chamber, with the exception of a 0.125 inch surrounding the chamber opening. Then the 25 mm membrane filter was wrapped around the side of the internal chamber, and the silicone grease was only brushed along the top portion of the filter, 0.125 inch above the chamber opening, which helped to hold the membrane filter in place. When the internal chamber was inserted into the top of external chamber, with the membrane filter, the silicone grease only spread directly above the chamber opening and in between the bottom of the walls. This would roughly leave a 0.25 inch square area that surrounded the channel opening, where it was not covered with the silicone grease.

Final changes were made to the 3D AutoCAD model of the slide in order to reduce the number of slides cracking while being manufactured and to increase the diameter of the through hole, as seen in Drawing 3.4-6. The total width of the slide needed to be increased by 0.25 inch in order to increase the amount of material where the stress fracture was occurring. The slide's width was increased by 0.125 inch on either side, as seen in Drawing 3.4-7. The external chambers no longer needed to be press-fit inside the slide, since the Weld-On® adhesive was used to permanently seal and affix the external chambers to the slide. The diameter of the through hole was increased from 0.868 inch to 0.873 inch, in order for the external chambers to be

more easily assembled, as seen in Drawing 3.4-7. The chambers were manufactured with the final sets of drawings shown in Drawing 3.4-4.

The final set of machined slides was received back with numerous tooling marks on the surface of the pocket cut, shown in Figure 3.4-4. This significantly decreased the visibility through the slide and the flow channel. The solvent could not be used to remove the tooling marks from the flow channel, because the capillary forces were too strong. The solvent was not able to drip through the flow channel when the slide was tilted, in order to create a thin layer of solvent on the surface. The small amount of solvent would stay in the channel until it hardened and then blocked the flow channel.

Figure 3.4-4: The tooling marks in the modified slides significantly decreased the visibility of the slide and the flow channel.

Additional changes were made to the device in order to increase the ease of manufacturing, by redesigning the back cover plate. Modifications were made to the 3D AutoCAD model in Drawing 3.4-8 to produce a back cover plate such as Drawing

3.4-9 illustrates. Instead of the cover plate having sharp perpendicular corners, as shown in section A of Figure 3.4-5, the corners were be manufactured at an angle to lessen the degree of accuracy of the cut, as shown in in section B of Figure 3.4-5. This allowed the back cover plate to make a watertight seal and be self-aligning to easily insert into the pocket cut without having to line-up the corners when the slide was being assembled. Drawing 3.4-10 shows the exact specifications used to manufacture the back cover plate.

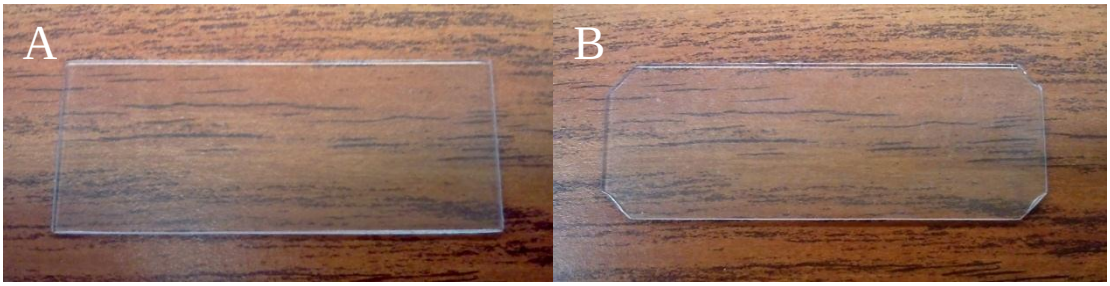

Figure 3.4-5: A) Cover plate with perpendicular corners, **B)** Cover plate with angled corners.

The final device was assembled together, shown in Figure 3.4-6, using the clamp and syringe method, but the tooling marks still obstructed the viewing window of the flow channel. The solvent was quickly wicked into the small pits in the pocket cut, creating several small bubbles. A white discoloration was caused by the tooling marks that were are left in the device where the solvent did not reach.

Figure 3.4-6: The final assembly of the type II design.

The final device would employ injection molding as a manufacturing techniques and ultrasonic welding for the assembly. Injection molding is the most common method of part manufacturing, which is ideal for producing high volumes of the same object[3]. Injection molding is governed by economies of scale, which means that the average cost per unit decreases as the scale of the output is increased. The cost of injection molding can vary, but it can also be very cost effective as long as there are high volume production rates. Some advantages of injection molding are high production rates, repeatable high tolerances, the ability to use a wide range of materials, low labor cost, minimal scrap losses, and little need to finish parts after molding[3]. The polycarbonate slide and external chambers would be injection molded as one piece, in order to reduce the cost and the number of parts in the device, and produce a device with the highest optical clarity. Using injection molding as a means of manufacturing, the device could easily be mass-produced while minimizing the cost per unit.

Ultrasonic welding is commonly used in the healthcare and other industries as a means of joining plastic pieces together[13]. The back cover plate would be ultrasonically welded to the slide assembly as a means of hermetically sealing the device without using any adhesives or solvents. This will eliminate the risk of contaminants and will not compromise the integrity of the biocompatibility of the device. Ultrasonic welding is increasing in popularity due to the fact that it is fast, reproducible, clean, easily automated, requires minimal capital expenditure, and its only raw material requirements are an electrical outlet and a pressurized air source[13].

Design II was sent to Sonobond® Ultrasonics to test the viability of ultrasonically welding the device together. Ultrasonic welding involves using high frequency vibrational energy at the interface of two thermoplastic parts, to cause the surfaces of the materials to soften and flow together, which create a high strength bond upon solidification. The frictional heat generated is confined to at the interface area and immediately dissipates after welding. Ultrasonic welding accomplishes this by the use of a power supply, transducer, booster and a horn. The power supply takes electricity at 50 or 60 Hz and changes the energy to ultrasonic frequencies of 20,000 Hz or more. The transducer contains piezoelectric crystals that change the incoming high-frequency electrical signals to mechanical vibrations of the same frequency[6]. The booster distributes the vibrational energy, while it increases the amplitude. And the horn makes contact with the parts in order to deliver the vibrational energy to create the bond.

For the device to be ultrasonically welded together, the joints in the design needed to be modified to ensure that the assembly is bonded correctly. Joint design needs to be considered at the initial design stage of the device by determining: the material to be bonded, the ultimate use of the device, the cost and ease of molding, and the location of the joint surface relative to the horn[6]. One type of joint design is a shear joint, which is used when the walls of the parts are to be joined. This type of joint is preferred for parts that require a hermetic seal, such as creating the bottom of the flow channel with the back cover plate. Design changes to the drawings were recommended by Janet Devine, president of Sonobond® Ultrasonics, in order to incorporate this continuous shear joint around the edge of the pocket cut, as shown in the top drawing of Drawing 3.4-11. The part must not fit so tightly before bonding that it inhibits the vibration needed to induce welding[6]. Therefore, a small clearance of at least 0.002 of an inch is given between the two parts.

Another common joint design is a triangular protrusion called an energy director, which concentrates the ultrasonic energy and rapidly plasticizes the joining surfaces. The triangular energy directors can have an angle of 60° or 90° and a height of 0.008 to 0.04 inch, depending on the material, wall thickness, joint requirements and the possibility that excess melted plastic formed along the molded part line, called flash[6]. In the bottom drawing of Drawing 3.4-11 is the side view of the slide and external chamber with an energy director placed on the bottom of the chamber. The choice of which molded part carries the energy director is rarely important. The

drawing shows the triangular energy director with a height of 0.020 inch and at a 60° angle, which is often preferred for polycarbonate materials.

Individual components were sent to Sonobond® Ultrasonics to make four completely assembled devices. Two of the sets were needed to calibrate the ultrasonic welder to the proper settings, which were thrown away afterwards. The other two sets were ultrasonically welded together, but unfortunately the components did not contain any joint designs. The parts were still able to bond together, but produced spotty welds where the plastic solidified before it flowed across the joint to form a seal. A Sonobond® Ultrasonics laboratory report was produced to specify the exact equipment and parameters used to ultrasonically weld the parts together, as seen in Table 7. Additional notes were made by the technician about the ultrasonic welds; the parts would need dedicated tooling. The horn that was used to ultrasonically weld the parts was not the correct tool for this type of device. The appropriate horn size and shape was not available, so a standard horn size was used. The proper tool needed was a horn with a flat surface to allow the device to rest on top, in order to ensure an even weld. Since energy directors were not used on these parts, the technician noted that better energy directors were needed to maintain a more consistent weld. Overall, the joint design updates from Sonobond® Ultrasonics can be easily incorporate into the injection mold by several iterative processes. These two manufacturing techniques of injection molding the parts and ultrasonic welding the assembly together are recommended methods of manufacturing the device with the highest optical clarity.

3.5 Type III-V Designs

The motivation behind these three designs was to eliminate the issues with the visibility of the device, specifically the flow channel. The previous design, Type II, achieved all of the required specifications set by the researchers, except for the optical clarity due to the parts being machined. These sets of designs will eliminate the need for the parts to be machined by removing the flow channel entirely. Instead of the device being an integrated design, such as the previous designs, it will be more modular in design. The design will allow the user to place different sized internal chambers inside the device to regulate the flow. The device will use a new approach by incorporating a polystyrene Petri dish into the design. Petri dishes are typically made from glass; however polystyrene Petri dishes have the same clarity and are widely used in disposable or reusable applications. The Petri dish is commonly used in cell microscopy, but it does not have flow system such as a channel or reservoir to apply a defined flow. However, these designs will create a flow system by regulating the flow from the inside chamber to the outside in the Petri dish.

The device was constructed with both the internal and external chambers sitting inside of a Petri dish. The membrane filter sits in between the chambers, which will be used to measure the cell interaction from intracellular fluid, inside the chambers, to the extracellular fluid in the Petri dish. The researchers specified that the external chamber would have an opening of 0.1575 inch in diameter, while the openings in the internal chambers would vary in size. The internal chambers would

be interchangeable with the external chambers in order to control the flow using various chamber openings such as 0.03 inch, 0.0787 inch and 0.1575 inch.

Design Type III and Type IV were constructed using similar techniques, except for the diameter of the Petri dish. In both designs, the external chamber was permanently affixed to the center of the Petri dish using the Weld-On® adhesive. A chamber opening of 0.1575 inch was drilled into the side on the bottom, before it was permanently affixed to the 10 cm or 6 cm diameter Petri dish. The various sizes of internal chambers could be easily inserted and swiveled to the side in the external chamber in order to control the flow rate. Figure 3.5-1 shows the assembled devices with the 10 cm Petri dish in section A and the smaller 6 cm Petri dish in section B.

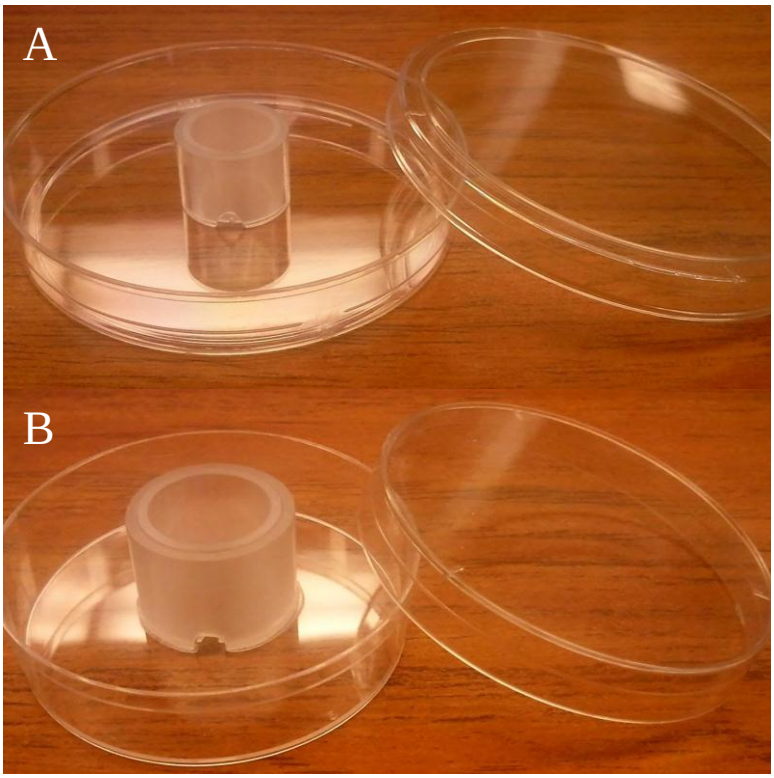

Figure 3.5-1: A) Type III; the chambers were placed in the 10 cm Petri dish, **B)** Type IV; the chambers were placed in the 6 cm Petri dish.

Design Type V was constructed with a detachable chamber, which could be used in the 10 cm or 6 cm diameter Petri dish. The bottom of the external chamber was sealed with a thin layer of plastic. Several types of plastic sheeting were investigated that had thicknesses of 0.001 inch and were optically clear. Drop cloths and plastic wrap were considered, but only the plastic wrap had the correct thickness and clarity. The plastic wrap is made from polyethylene plastic, which was be used to make the chambers portable. The plastic wrap was stretched and taped on a flat surface to remove all of the wrinkles. Then the bottom end of the external chamber was covered with the Weld-On® adhesive and carefully placed on top of the stretched plastic wrap. Using an X-Acto® Knife, the excess plastic wrap was cut away from the chamber as seen in section A of Figure 3.5-2. The final assemble of the Type V device is shown in section B of Figure 3.5-2.

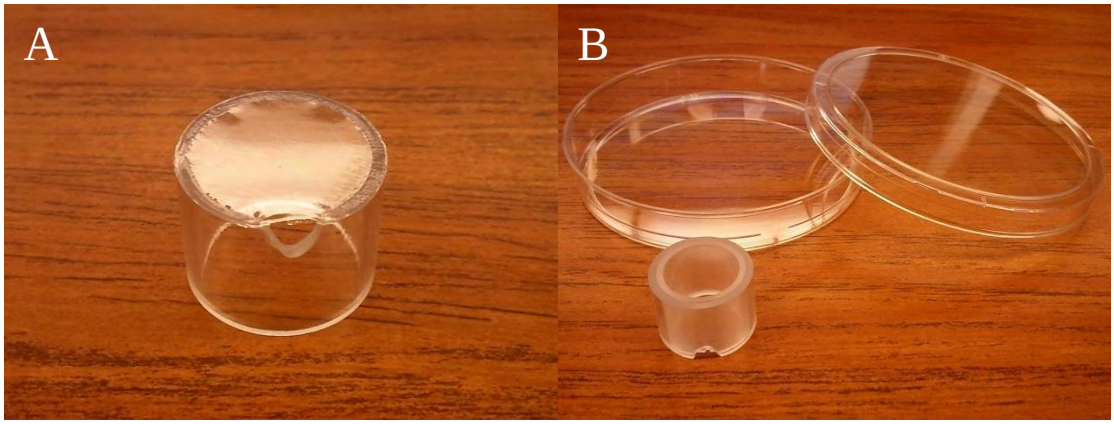

Figure 3.5-2: A) The bottom of the chamber after the sealed plastic wrap was cut out, **B)** The final assembly of the portable Type V device.

Chapter 4
Testing and Results

4.1 Type I Design

The testing of the device took 4 days to complete, and the cells were imaged with an inverted phase contrast microscope model Motic AE31 at 24 and 48 hours. On day one, an 8 micron pore membrane filter was inserted in between the internal and external chambers. Then, 300,000 MCF7 breast cancer cells were plated on top of the membrane filter inside chamber 1, Figure 4.1-1. On day two, 3 ml of serum free medium was pipetted into the flow channel, and then 300 µl of fetal bovine serum was plated in chamber 2. The device was placed in a 10 cm covered tissue culture and incubated up to 48 hours. On days three and four, the cells were imaged, so the membrane filter was removed and fixed in a 10% neutral formalin buffer and stained with a 0.1% crystal violet. The cells on top of the membrane filter were

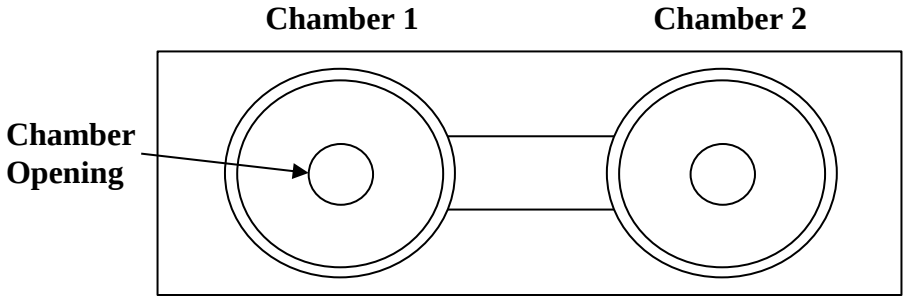

Figure 4.1-1: Diagram depicting the orientation of the Type I device. The design is similar to the µ-Slide I from Ibidi LLC in Figure 1.1-2.

removed with a cotton swab, so that the cells that migrated underneath the membrane filter could be viewed. The membrane filter was placed on a transparent slide to allow the cells to be imaged with the Motic AE31 microscope at 24 and 48 hours.

In Figure 4.1-2 shows the images of the cells migration at 48 hours in the presence and absence of serum, in which the incubated cells resulted in no cells appearing in the flow channel or in chamber 2. The cells did not appear to adhere to the membrane filter consistently or detach and migrate through the flow channel into chamber 2. The serum did result in an increase of the number of cells that migrated underneath the membrane filter.

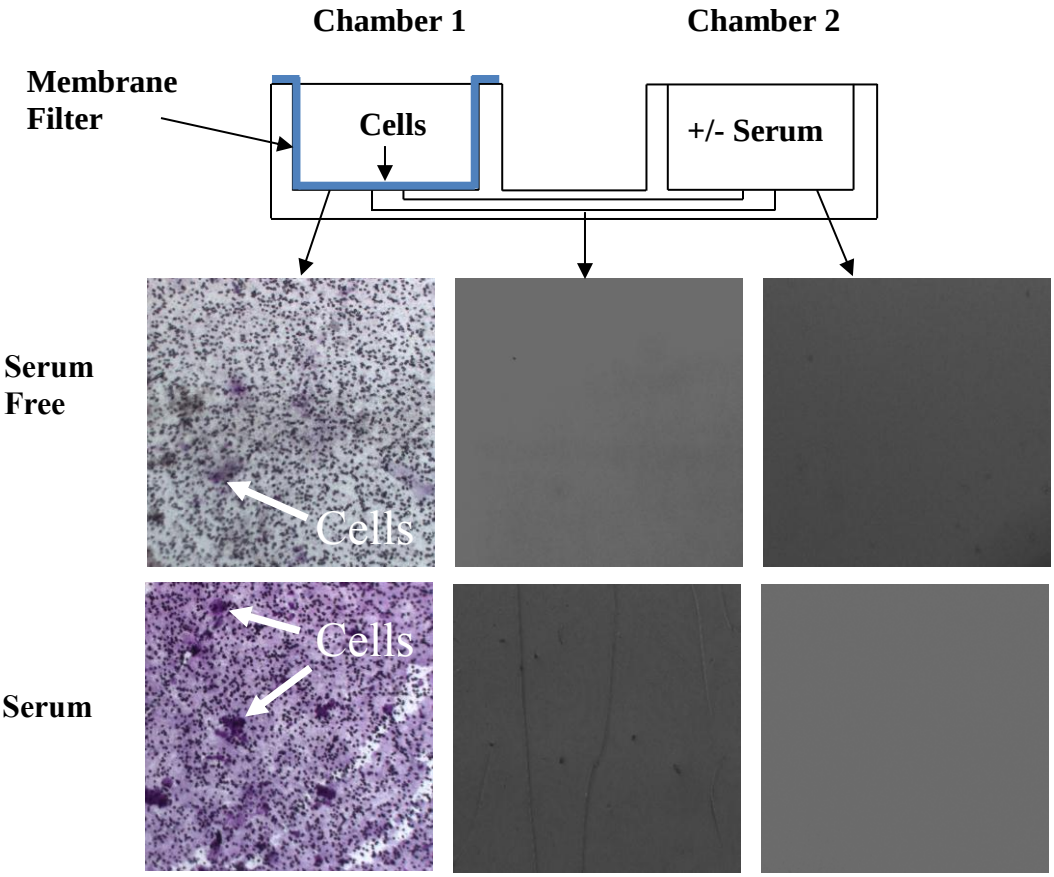

Figure 4.1-2: The result from testing the Type I device, which shows no cell migration through the flow channel or into chamber 2. The serum did result in an increase of the number of cells that migrated underneath the membrane filter. Tests were performed by Nikki Cheng.

4.2 Type II Design

The testing of the device was completed within 4 days, and the cells were imaged with an inverted phase contrast microscope model Motic AE31 at 24 and 48 hours. On day one, before the cells could be plated, the opening in chamber 1 was sealed, by swiveling the internal chamber to the side in order to close off the flow channel. Then, 300,000 MCF7 breast cancer cells were plated inside chamber 1, Figure 4.2-1. On day two, an 8 micron pore membrane filter was inserted in between the internal and external chambers. Then, 3 ml of serum free medium was pipetted into the flow channel as well 300 µl of fetal bovine serum was plated in chamber 2. The device was placed in a 10 cm covered tissue culture and incubated up to 48 hours. On days three and four, the cells were imaged, so the membrane filter was removed and fixed in a 10% neutral formalin buffer and stained with a 0.1% crystal violet. The membrane filter was placed on a transparent slide to allow for the cells to be imaged with the Motic AE31 microscope at 24 and 48 hours. The cells that were still on the device after the experiments were removed by using 0.25% trypsin. The

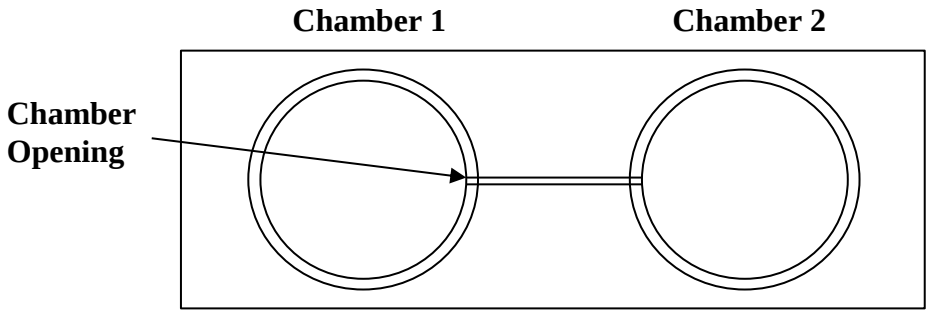

Figure 4.2-1: Diagram depicting the orientation of the Type II device.

device was cleaned by flushing it with PBS and sterile water, and then exposing the device under a UV light for 2 minutes for sterilization. The experiments were repeated for a total of 3 times.

The images of Figure 4.2-2 show the cells migration at 48 hours in the presence and absence of serum, in which the serum did induce the MCF7 breast cancer cells to migrate through the membrane filter across the flow channel and into chamber 2. The serum free incubated cells did result in the cells migrating through the membrane filter into the flow channel, but not into chamber 2. The cells were still

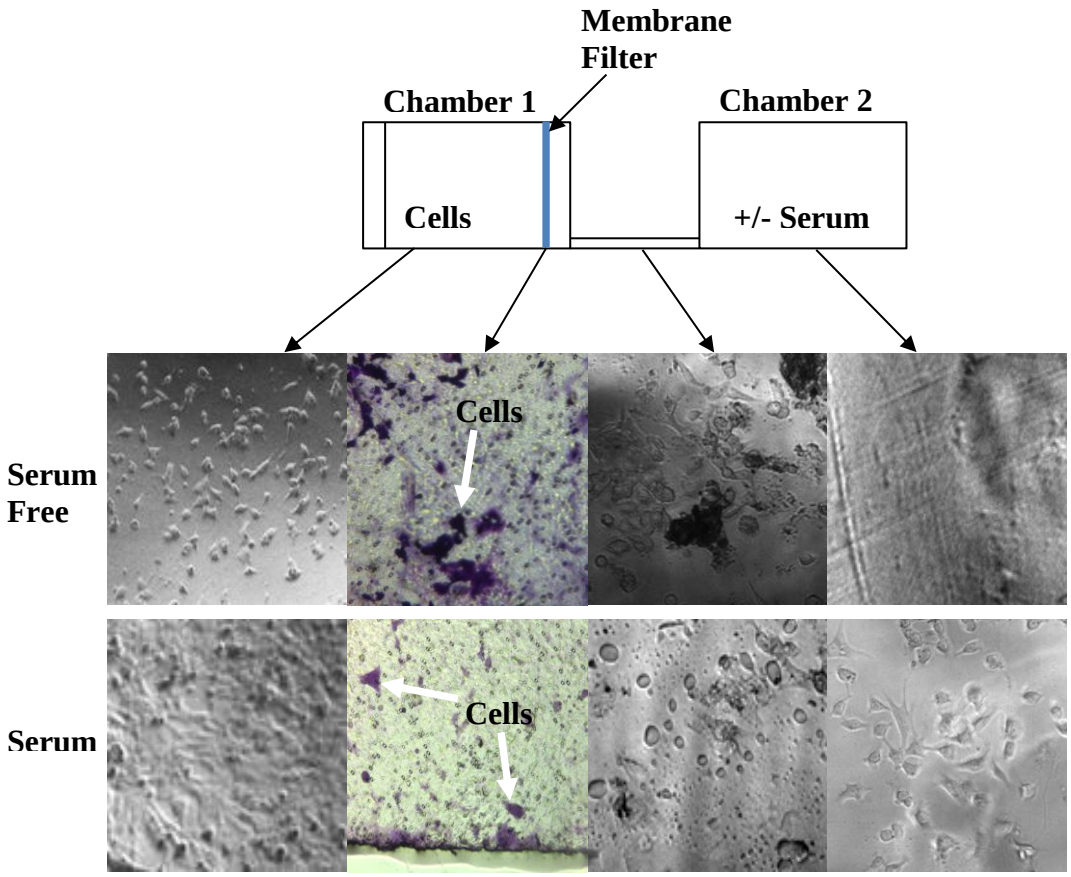

Figure 4.2-2: The results from testing the Type II device, which shows the cells did migrate into chamber 2 with the serum. The serum free incubated cells migrated through the flow channel but not into chamber 2. And the results were reproducible. Tests were performed by Nikki Cheng.

viable, but the cell deaths in chamber 1 were due to a lack of nutrients in the serum free media, which may have resulted in a lower cell density at 48 hours. The cells were plated at equal densities of 95% cells at the beginning of the experiments. The cells that incubated with the serum had a higher density after 48 hours, which is due to cell proliferation. The results of the experiments were reproducible. After the first experiment, cracks in the slide were observed along the channel. The silicon grease was used to seal the cracks for the next two experiments, but the media was still leaking in the subsequent experiments. However, the cells were still observed migrating through the flow channel and into chamber 2.

4.3 Type III Design

It took 5 days to test the device and the cells were imaged with an inverted phase contrast microscope model Motic AE31 daily. On day one, before the cells could be plated, the opening to the chamber was sealed, by swiveling the internal chamber to the side of the external chamber. Then, 300,000 MCF7 breast cancer cells labeled with CellTracker™ Green CMFDA dye were plated inside the chamber, Figure 4.3-1. On day two, the 8 micron pore membrane filter was coated with Matrigel and mammary fibroblasts, and then labeled in a 10 cm tissue culture dish for 24 hours. On days three through five, the membrane filter was inserted in between the internal and external chambers. Then, 3 ml of serum free medium was pipetted into the device as well 300 µl of fetal bovine serum was plated inside the Petri dish. The device was placed in a 10 cm covered tissue culture and incubated up to 72 hours. The cells were imaged daily, but on day five the membrane filter was removed and fixed in a 10% neutral formalin buffer and stained with a 0.1% crystal violet.

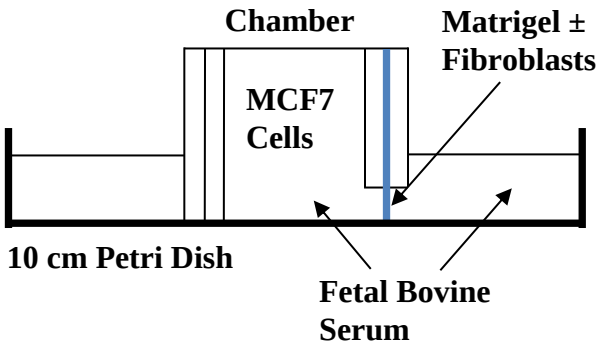

Figure 4.3-1: Diagram depicting the orientation of the Type III device.

The membrane filter was placed on a transparent slide to allow for the cells to be imaged with the Motic AE31 microscope. The cells that were still on the device after the experiments were removed by using 0.25% trypsin. The device was cleaned by flushing it with PBS and sterile water, and then exposing the device under a UV light for 2 minutes for sterilization. The experiments were repeated for a total of 3 times.

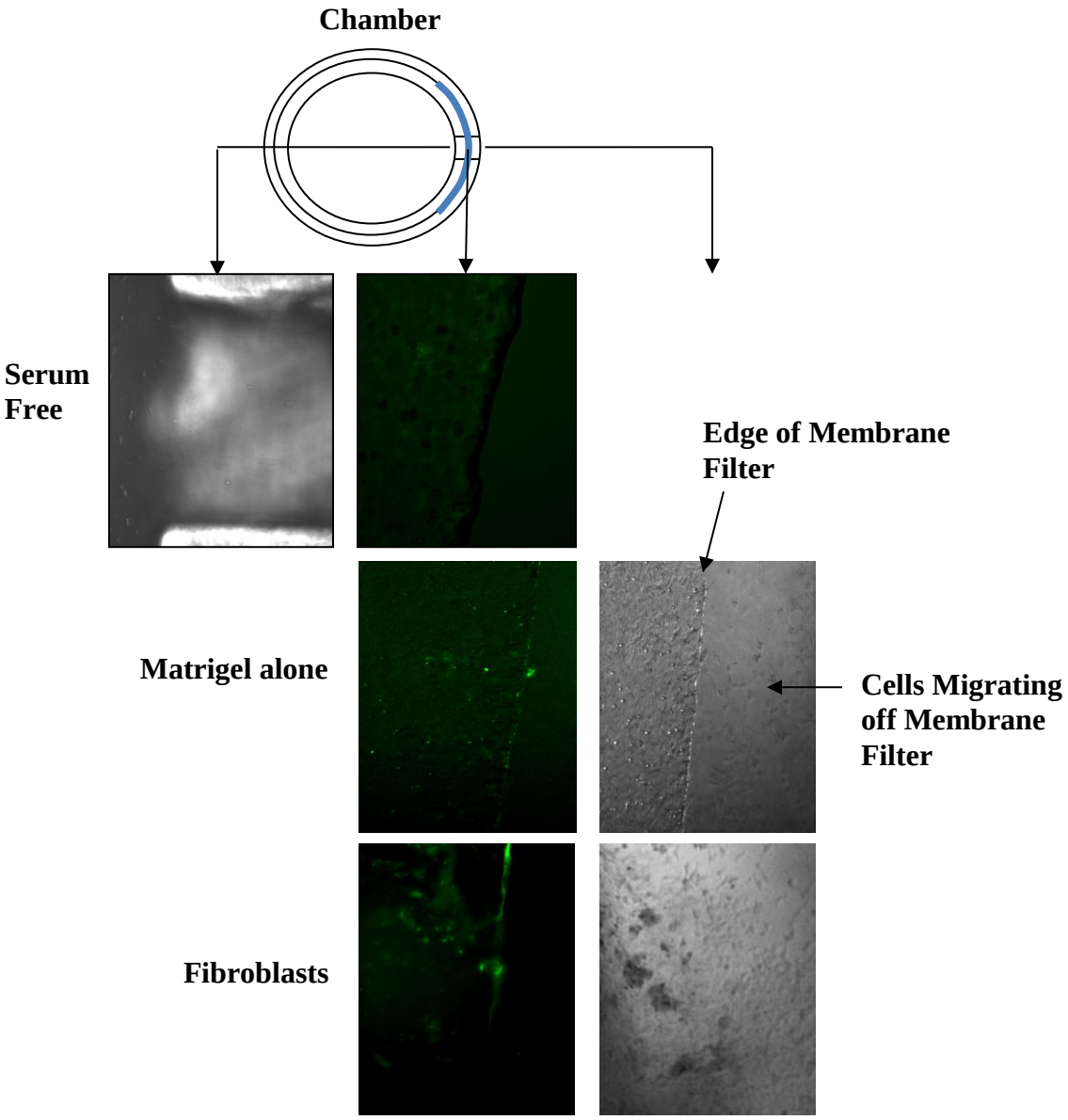

Figure 4.3-2: The results from testing the Type III device, which shows the cells migrating out of the device with or without the mammary fibroblasts and Matrigel. Tests were performed by Nikki Cheng.

The images of Figure 4.3-2 show the cells migrating out of the device with or without the mammary fibroblasts and Matrigel. The data indicates that the cells can migrate outside of the chamber in response to external stimulus. Some of the MCF7 breast cancer cells leaked out around the sides of the chamber after the initial plating. These cells were scraped off prior to the incubation with the serum. The silicon grease was used around the sides to reduce the leaking. Future experiments will be conducted to test if the cells can migrate into the chamber containing stimulus.

4.4 Type IV Design

The testing of the device took 5 days to complete and the cells were imaged with an inverted phase contrast microscope model Motic AE31 daily. On day one, before the cells could be plated, the opening to the chamber was sealed, by swiveling the internal chamber to the side of the external chamber. Then, 300,000 MCF7 breast cancer cells labeled with CellTracker™ Green CMFDA dye were plated inside the chamber, Figure 4.4-1. On day two, the 8 micron pore membrane filter was coated with Matrigel and mammary fibroblasts, and then labeled in a 6 cm tissue culture dish for 24 hours. On days three through five, the membrane filter was inserted in between the internal and external chambers. Then, 3 ml of serum free medium was pipetted into the device as well 300 µl of fetal bovine serum was plated inside the Petri dish. The device was placed in a 6 cm covered tissue culture and incubated up to 72 hours. The cells were imaged daily, but on day five the membrane filter was removed and fixed in a 10% neutral formalin buffer and stained with a 0.1% crystal

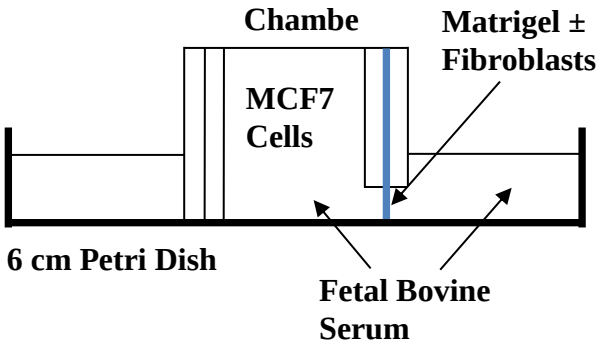

Figure 4.4-1: Diagram depicting the orientation of the Type IV device.

violet. The membrane filter was placed on a transparent slide to allow for the cells to be imaged with the Motic AE31 microscope. The cells that were still on the device after the experiments were removed by using 0.25% trypsin. The device was cleaned by flushing it with PBS and sterile water, and then exposing the device under a UV light for 2 minutes for sterilization. The experiments were repeated for a total of 3 times.

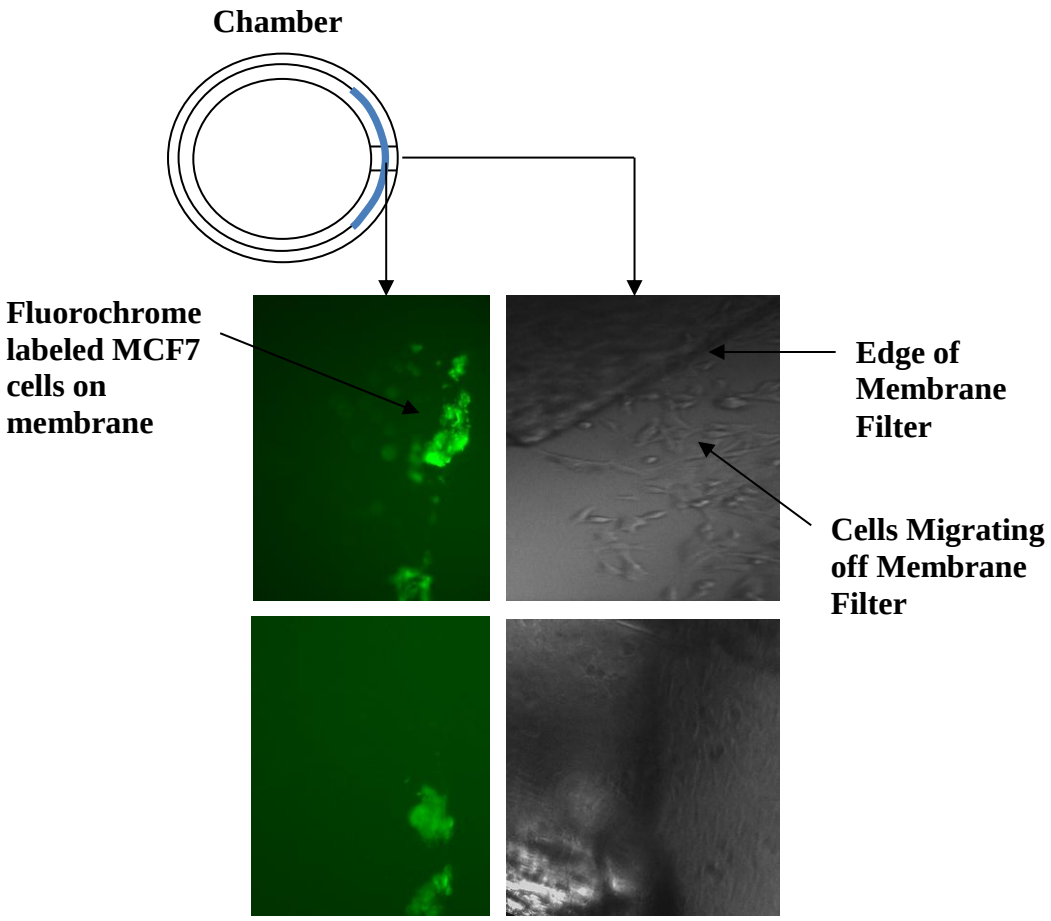

Figure 4.4-2: The results from testing the Type IV device, which shows the cells migrating out of the device with the mammary fibroblasts or Matrigel. The data indicates that the cells can migrate outside of the chamber in response to external stimulus. Tests were performed by Nikki Cheng.

The images of Figure 4.4-2 show the cells migrating out of the device with the mammary fibroblasts or Matrigel. The data indicates that the cells can migrate outside of the chamber in response to external stimulus. A longer time period would result in an increase in the number of cells migrating to the outside through the membrane filter. Some of the MCF7 breast cancer cells leaked out around the sides of the chamber after the initial plating. These cells were scraped off prior to the incubation with the serum. The silicon grease was used around the sides to reduce the leaking. Future experiments will be conducted to test if the cells can migrate into the chamber containing stimulus.

4.5 Type V Design

The testing of the device took 5 days to complete and the cells were imaged with an inverted phase contrast microscope model Motic AE31 daily. On day one, before the cells could be plated, the opening to the chamber was sealed, by swiveling the internal chamber to the side of the external chamber. Then, 300,000 MCF7 breast cancer cells labeled with CellTracker™ Green CMFDA dye were plated inside the chamber, Figure 4.5-1. On day two, the membrane filter was inserted in between the internal and external chambers. Then, 3 ml of serum free medium was pipetted into the device as well 300 µl of fetal bovine serum was plated inside the Petri dish. The device was placed in a 6 cm covered tissue culture and incubated up to 72 hours. On days three through five, the cells were imaged daily, but on day five the membrane filter was removed and fixed in a 10% neutral formalin buffer and stained with a 0.1% crystal violet. The membrane filter was placed on a transparent slide to allow for the cells to be imaged with the Motic AE31 microscope. The cells that were still on the device after the experiments were removed by using 0.25% trypsin. The

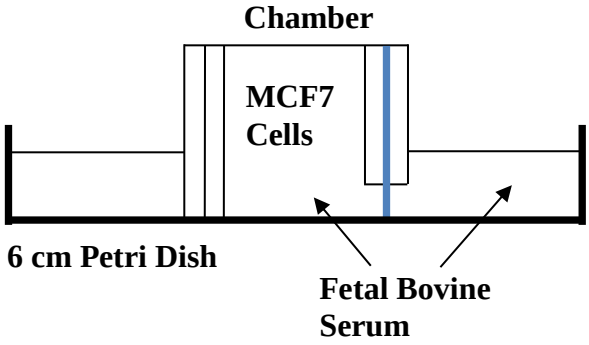

Figure 4.5-1: Diagram depicting the orientation of the Type V device.

device was cleaned by flushing it with PBS and sterile water, and then exposing the device under a UV light for 2 minutes for sterilization. The experiments were repeated for a total of 3 times.

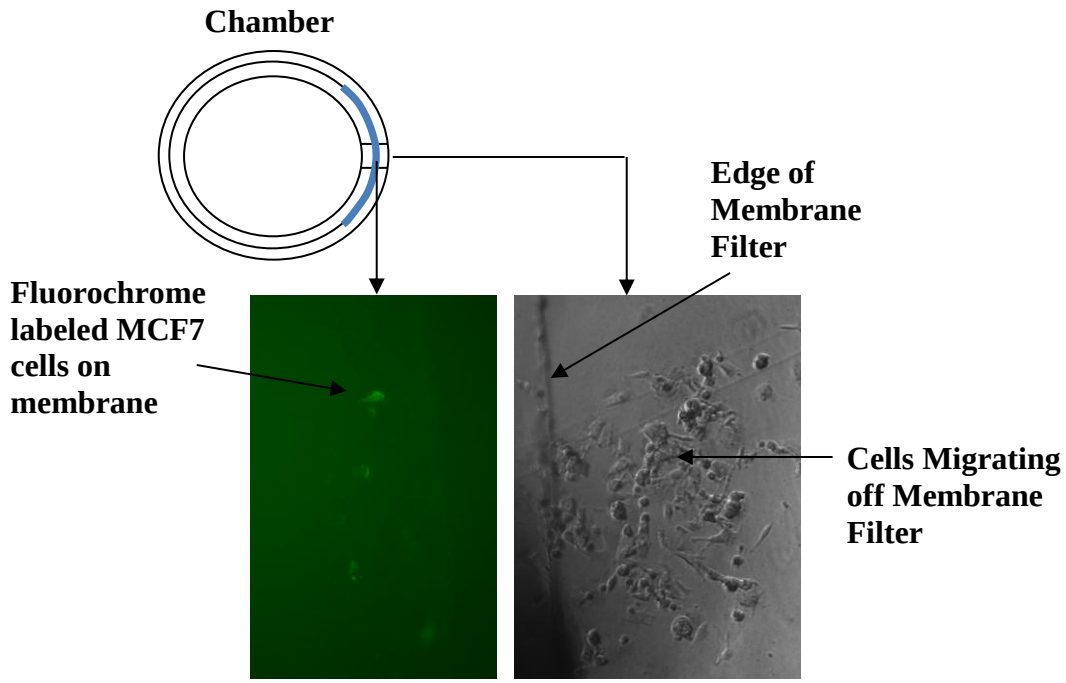

Figure 4.5-2: The results from testing the Type V device, which shows the cells migrating out of the device with the bottom end of the chamber sealed with plastic. The data indicates that the cells can migrate outside of the chamber in response to external stimulus. Tests were performed by Nikki Cheng.

The images of Figure 4.5-2 show the cells migrating out of the device with the bottom end of the chamber sealed with plastic. The data indicates that the cells can migrate outside of the chamber in response to external stimulus. There were no leaks observed in this device. Future experiments will be conducted to test if the cells can climb over the lip of the plastic edge to reach the chamber containing the stimulus.

Chapter 5
Conclusions and Recommendations

5.1 Conclusions

In this thesis, the development of six distinct designs of metastatic devices has been presented. These devices will give researchers several unique advantages to analyze multiple aspects of metastatic cell behavior, and mimicking multiple steps of the metastatic process. All of the designs presented, were able to accurately replicate the multiple steps of the progression of metastatic cancer such as cell proliferation, migration, invasion, intravasation, extravasation, and colonization of other tissues. The porous membrane at each end of the channel enabled researchers to measure transendothelial invasion of tumor cells, by controlling the molecular diffusion and also serving as a scaffold for coating endothelial cells to mimic part of the blood vessel. These devices are a significant advancement in technology to model metastatic cancer cells during the disease.

Each device was tested using a set of experiments involving the analysis of breast cancer cell migration using the MCF7 human cancer cell line. An 8 micron membrane was inserted in between the chambers and the cells were analyzed for the

migration through the membrane filter in response to 24 hour treatment with the fetal bovine serum. The presence of the 10% fetal bovine serum created a chemical gradient to force the cells through the flow channel. The chemical gradient was sustained long enough to induce the cell migration into or out of the chambers. Additionally, the size of the opening in the chambers affected the number of cells entering and exiting through the flow channel. The 3 ml of serum free medium pipetted into the device was used to force the air bubbles out of the flow channel. The presence of air bubbles in a microfluidic perfusion culture system is undesirable as it obstructs the fluid flow and kills cells at the gas-liquid interface. Air bubbles can arise from residual air due to incomplete priming of the system or spontaneous formations at defect sites[9]. There were no issues with biocompatibility in any of the devices. The cells were able to adhere to the bottom of the chambers without the use of coating matrix. The sterilization method of flushing the device with sterile water and using the UV light was able to eliminate all of the contaminants.

The results indicate that the serum enhanced the cell migration to the second chamber within 24 hours. Even though, the Type II device had an issue with leaking media, the cells were still able to migrating through the flow channel to the second chamber. No leaks were observed in the portable Type V device, but the cells did take more time to exit the chamber, due to the lip of the plastic seal that the cells had to traverse over. The cells were able to adhere properly to the bottom of the plastic seal. The Type II and Type V device worked the best, due to the greatest number of cells that migrated to the other side and the most consistent results. It is currently

unknown whether the cells can migrate into the chamber with the slight lip due to the plastic seal on the bottom. Future experiments will be performed to determine if the cells can migrate into the chamber containing stimulus. Also, the device has the potential to be fabricated into a multi-well format for high-throughput screening of drug compounds towards a specific target or screening for novel drug targets.

5.2 Recommendations

After all the devices were tested, the researchers had some recommendations to improve upon the designs. The cells that were imaged near the walls of the chambers were overshadowed, which created part of the image to be obscured. The walls of the chambers need to be transparent, so the light can pass through the walls and not create a shadow over the imaging area. Also, the media forms a meniscus at the top of the chamber, which touches the cover plate when the device was placed in the tissue culture plate. The chambers need to be made shorter, so the device can easily fit inside the tissue culture plate without touching the top cover. This would mean the device can be no taller than 0.5 inch. The device should have an additional set of internal chambers that extends beyond the external chambers for when the device is not being incubating. The taller set of internal chambers would be used during the experiments, which would allow the user to easily swivel the internal chambers to open or close the chambers. Modifications to the slide could be made, so the cover plate would be elevated above the surface to prevent it from becoming scratched. The slide would sit on top of a frame created from the surface of the base plate, by increasing the thickness of the slide and the depth of the pocket cut. This would allow the cover plate to be recessed into the slide and not touch the surface.

References

1. Christine M. Salerni, Engineering Adhesives for Repeated Sterilization, Application Engineering Chemist for Loctite ® Corporation, page 2, http://www.henkelna.com/us/content_data/99736_Engineering_Adhesives_for_Repeated_Sterilization.pdf

2. Chunhung Zheng, Liang Zhao, Gui'e Chen, Ying Zhou, Yuhong Pang, Yang Huang, Quantitaive Study of the Dynamic Tumor-Endothelial Cell Interactions through an Integrated Microfluidic Coculture System, Analytical Chemistry, 2012

3. Engineers Edge, LLC, Injection Molding Applications, © Copyright 2000 - 2012 Retrieved October 2012 from http://www.engineersedge.com/manufacturing/injection-molding-applications.htm

4. Henkel Corporation, The Design Guide for Bonding Plastics, The Loctite® Design Guide for Bonding Plastics, Volume 6 pages 18, 42, 66, http://www.henkelna.com/us/content_data/237471_LT2197_Plastic_Guide_v6_LR7911911.pdf

5. Ibidi, LLC, Cells in Focus µ-Slide I, 2012, Retrieved May 2011 from http://www.ibidiusa.com/product/m-slide-i/

6. Janet Devine, President of Sonobond® Ultrasonics, Ultrasonic Rx for Medical Device Assembly, Sonobond® Ultrasonics, Inc. © 2012. http://www.sonobondultrasonic.com/articles.asp?Article_Id=18

7. Johan-Valentin Kahl, Ibidi GmbH, Flow Chamber, United States Patent, Pat. No. 7,517,499 B2, April 14, 2009.

8. Johan-Valentin Kahl, Roman Zantl, Ibidi GmbH, Device for Microfluid Analyses, United States Patent, Pat. No. 7,582,264 B2, Sept. 1, 2009.

9. Lily Kim, Yi-Chin Toh, Joel Voldman, Hanry Yu, A Practical Guide to Microfluidic Perfusion Culture of Adherent Mammalian Cells, Lab on a Chip, The Royal Society of Chemistry, May 11, 2007.

10. Nikki Cheng, Ph.D. Metastasis Mimetic Device Invention Disclosure, The Center for Technology Commercialization, The University of Kansas, April 2010.

11. Nikki Cheng, Ph.D. Metastasis Mimetic Device IAMI Grant Proposal, The University of Kansas Medical Center, Sept. 2010.

12. Polymicro Technologies, Cutting Edge technologies, Flexible Fused Silica Capillary Tubing, 2008. http://www.polymicro.com/products/capillarytubing/products_capillarytubing_CET.htm

13. R. Kingsbury, Ultrasonic Weldability of a Broad Range of Medical Plastics, The Dow Chemical Company, The Society of Plastics Engineers. Volume 49, page: 1844-1848, May 1991.

14. Stephanie Toetsch, Peter Olwell, Adriele Prina-Mello, Yuri Volkov, The evolution of chemotaxis assays from static models to physiologically relevant platforms, Integrative Biology, Royal Society of Chemistry, Dec. 12, 2008b

Appendix A: List of Materials

Capillary Tube

Tygon S-54-HL Microbore Tubing: *USplastics.com*

ID:	0.04”	x	**OD**:	0.07”	**Wall**:	0.015”
	0.05”	x		0.09”		0.020”

Note: Medical and laboratory application tubing that is non-toxic, non-pyrogenic and bio-compatible. Sterilize by autoclave, radiation, ethylene oxide, steam or chemical methods.

Ethyl Vinyl Acetate Microbore Tubing: *Coleparmer.com*

ID:	0.03”	x	**OD**:	0.09”	**Wall**:	0.030”
	0.04”	x		0.07”		0.015”
	0.05”	x		0.09”		0.020”

Note: Ideal for clinical and biological testing that is biologically stable, nontoxic, and non-contaminating. Sterilize by autoclave, ethylene oxide, gamma irradiation, or dry heat

Glass Capillary Tubes: *Amazon.com*

ID:	1.10 mm	x	**OD**:	1.30 mm	**Wall**:	0.20 mm
	1.20 mm	x		1.50 mm		0.20 mm

Kimax-51 Glass Capillary Tubes: *Amazon.com*

ID:	0.80 mm	x	**OD**:	1.05 mm	**Wall**:	0.125 mm
	0.90 mm	x		1.15 mm		0.125 mm
	1.00 mm	x		1.25 mm		0.125 mm
	1.10 mm	x		1.35 mm		0.125 mm
	1.50 mm	x		1.70 mm		0.100 mm
	1.60 mm	x		1.80 mm		0.100 mm

Micro-Hematocrit Glass Capillary Tubes Ammonium Heparinized: *Pulmolab.com*

ID:	1.15 mm	x	**OD**:	1.50 mm

Micro-Hematocrit Glass Capillary Tubes: *Pulmolab.com*

ID:	1.15 mm	x	**OD**:	1.50 mm

Micro-Hematocrit Plastic Capillary Tubes Ammonium Heparinized: *Pulmolab.com*

ID:	1.15 mm	x	**OD**:	1.50 mm

Micro-Hematocrit Plastic Capillary Tubes: *Pulmolab.com*

ID:	1.15 mm	x	**OD**:	1.50 mm

Acrylic (PMMA) Capillary Tubes: *Paradigmoptics.com*

ID:	500 μm	x	**OD**:	7500 μm
	1400 μm	x		1800 μm

Polycarbonate Capillary Tubes: *Paradigmoptics.com*

ID:	600 μm	x	**OD**:	1200 μm
	500 μm	x		1000 μm
	1000 μm	x		2000 μm

Polystyrene Capillary Tubes: *Paradigmoptics.com*

ID:	250 μm	x	**OD**:	550 μm

Polypropylene Capillary Tubes: *Paradigmoptics.com*

ID:	270 μm	x	**OD**:	360 μm

Zeonex 480R Capillary Tubes: *Paradigmoptics.com*

ID:	250 μm	x	**OD**:	500 μm

PTFE Capillary Tubes: *Paradigmoptics.com*

ID:	1067 μm	x	**OD**:	1676 μm
	864 μm	x		1473 μm

***Tygon LFL Microbore Tubing**: *Coleparmer.com*

ID:	0.89 mm	x	**OD**:	2.62 mm
	1.14 mm	x		2.87 mm
	1.42 mm	x		3.15 mm

Tygon Microbore Tubing: *Coleparmer.com*

ID:	0.04”	x	**OD**:	0.07”	**Wall**:	0.015”
	0.05”	x		0.09”		0.020”

Thin Wall Single Barrel Glass Capillary Tubes: *Store.wiinc.com*

ID:	0.75 mm	x	**OD**:	1.00 mm
	0.90 mm	x		1.20 mm
	1.12 mm	x		1.50 mm

Borosilicate Single Barrel Glass Capillary Tubes: *Store.wiinc.com*

ID:	0.68 mm	x	**OD**:	1.20 mm
	0.84 mm	x		1.50 mm

** Will need to be machined to correct the dimensions*

Patch Clamp Single Barrel Glass Capillary Tubes: *Store.wiinc.com*

ID:	0.75 mm	x	**OD**:	1.50 mm
	1.00 mm	x		1.50 mm
	1.10 mm	x		1.65 mm

Chemfluor FEP Tubing: P*rofessionalplastics.com*

ID:	0.031"	x	**OD**:	0.062"
	0.062"	x		0.125"

FEP Tubing: P*rofessionalplastics.com*

ID:	0.062"	x	**OD**:	0.125"

Note: FEP has several properties PTFE does not have and is one of the clearest plastics available on the market. Inert Tubing that is Chemical and Corrosion Resistance and will not absorb moisture.

Tygon 2075 Ultra Chemical Resistant Tubing: P*rofessionalplastics.com*

ID:	0.062"	x	**OD**:	0.125"

Note: Its exceptionally smooth inner surface inhibits particulate buildup and reduces the potential for contamination. And offers unequaled combination of chemical resistance, clarity and flexibility.

Tygon 2275 High-Purity Tubing: P*rofessionalplastics.com*

ID:	0.062"	x	**OD**:	0.187"

Note: Ideal for handling sensitive fluids such as pharmaceutical or biological solutions. There is virtually no absorption into the tubing material. Sterilized by radiation, ethylene oxide, steam or chemical methods. Frequently, incineration is used to dispose of contaminated materials. Many tubing's release hazardous by-products when burned, Tygon High-Purity Tubing only releases carbon dioxide and water when properly incinerated, providing safe disposal.

Tygon B-44-3 Beverage Tubing: P*rofessionalplastics.com*

ID:	0.062"	x	**OD**:	0.125"

Note: Non-wetting surface permits thorough cleaning and complete drainage. And broad chemical resistance to virtually all non-solvent chemicals.

Tygon B-44-4X Food, Milk & Dairy Tubing: P*rofessionalplastics.com*

ID:	0.031"	x	**OD**:	0.093"

Note: Its smooth, non-porous bore will not trap particulates or promote bacterial growth.

Tygon R-3603 Laboratory Tubing: P*rofessionalplastics.com*
ID: 0.062" x **OD**: 0.125"

Note: Crystal-clear and non-oxidizing and non-contaminating. Glassy-smooth inner bore helps prevent buildup so that cleaning is facilitated. Outstanding chemical resistance lot-to-lot consistency for reproducible results.

Tygon S-50-HL Medical/Surgical Tubing: P*rofessionalplastics.com*
ID: 0.062" x **OD**: 0.125"

Note: Tubing's consistent quality provides dependable performance in medical device applications. Ideal for contact with blood. Sterilized by radiation, ethylene oxide, steam or chemical methods.

Tygon PTFE SE-200 Inert Tubing: P*rofessionalplastics.com*
ID: 0.062" x **OD**: 0.125"

Note: Its FEP inner liner provides the ultimate in chemical resistance and will not extract or contaminate fluids being transferred. Crystal clear for easy visual flow monitoring.

Vinyl Tubing: P*rofessionalplastics.com*
ID: 0.062" x **OD**: 0.125"

Teflon PTFE Tubing - Extruded AWG Sizes: P*rofessionalplastics.com*
AWG: #14 SW ~ 1.63 mm
#15 SW ~ 1.45 mm
#16 SW ~ 1.30 mm
#17 SW ~ 1.10 mm

Note: Provides chemical resistance, biocompatibility, and precision extruded tolerances. Excellent Lubricity - Lowest coefficient of friction of any polymer and Teflon tubing is chemically Inert.

F&D Fabricated (Borosilicate) Capillary Tubing: *FDglass.com*
ID: 1.00 mm x **OD**: 1.40 mm
0.90 mm x 1.30 mm

***Heraeus HSQ 300 Quartz:** *FDglass.com*
ID: 1.00 mm x **OD**: 2.00 mm

** Will need to be machined to correct the dimensions*

Chambers

Acrylic (PMMA) Extruded Tubing: *USplastics.com*

	ID:			**OD**:	
	0.625”	x		0.750”
	0.750”	x		0.875”
	0.625”	x		0.875”
	0.875”	x		1.00”
	0.750”	x		0.875”
	0.875”	x		1.00”

Tygon S-50-HL Medical/Surgical Tubing: *USplastics.com*

	ID:			**OD**:	
	0.375”	x		0.500”
	0.500”	x		0.750”
	0.375”	x		0.625”
	0.625”	x		0.875”
	0.500”	x		0.750”
	0.750”	x		1.00”
	0.5625”	x		0.750”
	0.750”	x		1.00”
	0.4375”	x		0.625”
	0.625”	x		0.875”

Tygon R-3603 Laboratory Tubing: *USplastics.com*

	ID:			**OD**:	
	0.500”	x		0.625”
	0.625”	x		0.8125”
	0.500”	x		0.625”
	0.625”	x		0.875”
	0.625”	x		0.875”
*	0.750”	x		1.00”

Tygon High Purity Plasticizer Free Tubing 2275: *USplastics.com*

	ID:			**OD**:	
	0.625”	x		0.875”
*	0.750”	x		1.00”

Heraeus HLQ 200 Quartz Tubing: *FDglass.com*

	ID:			**OD**:	
	15 mm	x		17 mm
	17 mm	x		19 mm
	16 mm	x		18 mm
	18 mm	x		20 mm
*	16 mm	x		18 mm
	17 mm	x		19 mm
	17 mm	x		19 mm
	19 mm	x		21 mm

** Will need to be machined to correct the dimensions*

Heraeus HSQ 300 Quartz: *FDglass.com*

ID:	14 mm	x	**OD**:	17 mm
	17 mm	x		19 mm
	15 mm	x		18 mm
	18 mm	x		20 mm
	17 mm	x		19 mm
	19 mm	x		21 mm

Polycarbonate Tubing - Extruded: P*rofessionalplastics.com*

ID:	0.625”	x	**OD**:	0.750”
	0.750”	x		0.875”

Appendix B: Tables

Table 1: Standard Sterilization Methods[1].

Sterilization Method	Description
Steam Autoclave	• Steam under pressure (15-20 pounds steam pressure) • Temperatures between 110 – 135°C • Estimated 80% of market • Potential effect of adhesive bond strengths • *Potential candidate for use with reusable/resposable devices*
Ethylene Oxide	• Toxic gas which requires 24 hours of aeration following exposure • Temperatures: ~ 55°C • Minimal effect on adhesive bond strengths
Gamma	• Cobalt-60 radiation source • Temperatures: ambient • Minimal effect on adhesive bond strengths
Electron Beam	• Electron accelerator, radiation source • Temperatures: ambient • Minimal effect on adhesive bond strengths
Hydrogen Peroxide	• Typically low temperature plasma • Temperatures: ambient to 50°C (vapor phase temperatures slightly higher) • Minimal effect on adhesive bond strengths • *Potential candidate for use with reusable/resposable devices*
Chemical Immersion	• Liquid sterilant solutions such as glutaraldehyde or peroxyacetic acid • Temperatures: ambient to 50°C • Minimal effect on adhesive bond strengths • *Potential candidate for use with reusable/resposable devices*

Table 2: Common materials used for the fabrication of microfluidic networks in microfluidic perfusion culture systems[9].

	Properties relevant to microfluidic perfusion culture systems					
Materials	Fabrication techniques	Visible light transmittance[a]	Autoclavable[b]	Water diffusion coefficient[c] $\times 10^9$/m^2 s^{-1}	Gas permeability[c] $\times 10^{10}$/cm^3 (STP) cm (cm^2 s cm Hg)$^{-1}$	Young's Modulus[d]/GPa
Poly(dimethylsiloxane) (PDMS)	Soft lithography	Clear	Yes	3–6 (Heo *et al.*[35])	N_2: 280 CO_2: 340 O_2: 600 (Mark[39])	3.6×10^{-4}–8.7×10^{-4} (Armani *et al.*[40])
Silicon	Micro-electronics fabrication	Opaque	Yes	N/A	N/A	165 (Dolbow *et al.*[44])
Glass	Micro-electronics fabrication	Clear	Yes	N/A	N/A	63–73 (Smith[47])
Poly(methyl-methacrylate) (PMMA)	Hot embossing, injection molding, laser photoablation	Clear	Yes	0.002 (Rodriguez *et al.*[38])	N_2: 0.039 CO_2: 0.78 O_2: 0.23 (Nakai *et al.*[49])	3.3 (Brandrup *et al.*[50])
Polysulfone	Hot embossing, injection molding, laser photoablation	Clear	Yes	0.009 (Schult *et al.*[52])	N_2: 0.2 CO_2: 8 O_2: 1.5 (Hu *et al.*[53])	2.47 (Brandrup *et al.*[50])

[a] Affects compatibility with live-cell imaging during microfluidic perfusion culture. [b] Sterilization of microfluidic perfusion culture system at 121 °C, 20 min. [c] Affects culture conditions within the microfluidic perfusion culture system. [d] Elasticity affects chip-to-world interface and integration of other microfluidic components *e.g.* valves.

Table 3: Material Properties of Acrylic (PMMA) [4].

Typical Properties of Acrylic (PMMA)		
	American Engineering	SI
Processing Temperature	350°F to 570°F	117°C to 299°C
Linear Mold Shrinkage	0.003 to 0.007 in./in.	0.003 to 0.007 cm/cm
Melting Point	266°F	130°C
Density	65.6 to 76.2 lb./ft.^{3}	1.05 to 1.22 g/cm^3
Tensile Strength, Yield	1.5 to 10.5 lb./in.^{2} x 10^3	1.1 to 7.4 kg/cm^2 x 10^2
Tensile Strength, Break	1.3 to 12.8 lb./in.^{2} x 10^3	0.9 to 9.0 kg/cm^2 x 10^2
Elongation, Break	0.5 to 75.0%	0.5 to 75.0%
Tensile Modulus	1.5 to 7.0 lb./in.^{2} x 10^5	1.1 to 4.9 kg/cm^2 x 10^4
Flexural Strength, Yield	1.7 to 3.1 lb./in.^{2} x 10^3	1.2 to 2.2 kg/cm^2 x 10^2
Flexural Modulus	0.1 to 6.2 lb./in.^{2} x 10^5	0 to 4.4 kg/cm^2 x 10^4
Compressive Strength	6.0 to 18.5 lb./in.^{2} x 10^3	4.2 to 13.0 kg/cm^2 x 10^2
Izod Notched, R.T.	0.2 to 2.0 ft.-lb./in.	0.9 to 10.8 kg cm/cm
Hardness	M65 - M100 Rockwell	M65 - M100 Rockwell
Thermal Conductivity	1.3 to 1.5 BTU-in./hr.-ft.^{2}-°F	0.19 to 0.22 W/m-°K
Linear Thermal Expansion	3.3 to 5.6 in./in.-°F x 10^{-5}	5.9 to 10.1 cm/cm-°C x10^{-5}
Deflection Temperature @ 264 psi	150°F to 225°F	66°C to 107°C
Deflection Temperature @ 66 psi	176°F to 217°F	80°C to 103°C
Continuous Service Temperature	170°F to 190°F	77°C to 88°C
Dielectric Strength	260 to 760 V/10^{-3} in.	1.0 to 3.0 V/mm x 10^4
Dielectric Constant @ 1 MHz	2.2 to 3.9	2.2 to 3.9
Dissipation Factor @ 1 MHz	0.025 to 0.045	0.025 to 0.045
Water Absorption, 24 hr.	0.1 to 0.5%	0.1 to 0.5%

Table 4: Material Properties of Polycarbonate (PC) [4].

Typical Properties of Polycarbonate (PC)		
	American Engineering	SI
Processing Temperature	500°F to 575°F	260°C to 302°C
Linear Mold Shrinkage	0.003 to 0.007 in./in.	0.003 to 0.007 cm/cm
Melting Point	–	–
Density	70.5 to 80.5 lb./ft.^{3}	1.13 to 1.29 g/cm^3
Tensile Strength, Yield	8.4 to 9.6 lb./in.^{2} x 10^3	5.9 to 6.7 kg/cm^2 x 10^2
Tensile Strength, Break	7.4 to 10.9 lb./in.^{2} x 10^3	5.2 to 7.7 kg/cm^2 x 10^2
Elongation, Break	97.0 to 136.0%	97.0 to 136.0%
Tensile Modulus	3.1 to 3.5 lb./in.^{2} x 10^5	2.2 to 2.5 kg/cm^2 x 10^4
Flexural Strength, Yield	12.4 to 14.0 lb./in.^{2} x 10^3	8.7 to 9.8 kg/cm^2 x 10^2
Flexural Modulus	3.2 to 3.5 lb./in.^{2} x 10^5	2.2 to 2.5 kg/cm^2 x 10^4
Compressive Strength	9.9 to 11.1 lb./in.^{2} x 10^3	7.0 to 7.8 kg/cm^2 x 10^2
Izod Notched, R.T.	11.3 to 17.0 ft.-lb./in.	60.8 to 91.8 kg cm/cm
Hardness	R120 - R125 Rockwell	R120 - R125 Rockwell
Thermal Conductivity	1.3 to 1.6 BTU-in./hr.-ft.^{2}-°F	0.19 to 0.23 W/m-°K
Linear Thermal Expansion	2.9 to 3.9 in./in.-°F x 10^{-5}	2.2 to 7.0 cm/cm-°C x10^{-5}
Deflection Temperature @ 264 psi	200°F to 350°F	98°C to 177°C
Deflection Temperature @ 66 psi	280°F to 350°F	138°C to 177°C
Continuous Service Temperature	240°F to 275°F	116°C to 135°C
Dielectric Strength	375 to 500 V/10^{-3} in.	1.5 to 2.0 V/mm x 10^4
Dielectric Constant @ 1 MHz	2.7 to 3.2	2.7 to 3.2
Dissipation Factor @ 1 MHz	0.009 to 0.010	0.009 to 0.010
Water Absorption, 24 hr.	0.1 to 0.3%	0.1 to 0.3%

Table 5: Material Properties of Polystyrene (PS) [4].

Typical Properties of Polystyrene (PS)		
	American Engineering	SI
Processing Temperature	300°F to 500°F	149°C to 260°C
Linear Mold Shrinkage	0.002 to 0.008 in./in.	0.002 to 0.008 cm/cm
Melting Point	212°F to 545°F	100°C to 241°C
Density	63.7 to 66.2 lb./ft.^{3}	1.02 to 1.06 g/cm^3
Tensile Strength, Yield	2.4 to 6.2 lb./in.^{2} x 10^3	1.7 to 4.4 kg/cm^2 x 10^2
Tensile Strength, Break	2.7 to 7.6 lb./in.^{2} x 10^3	1.9 to 5.3 kg/cm^2 x 10^2
Elongation, Break	2.0 to 80.0%	2.0 to 80.0%
Tensile Modulus	2.2 to 4.8 lb./in.^{2} x 10^5	1.5 to 3.4 kg/cm^2 x 10^4
Flexural Strength, Yield	4.3 to 13.0 lb./in.^{2} x 10^3	3.0 to 9.1 kg/cm^2 x 10^2
Flexural Modulus	2.0 to 4.8 lb./in.^{2} x 10^5	1.4 to 3.4 kg/cm^2 x 10^4
Compressive Strength	7.0 to 12.0 lb./in.^{2} x 10^3	4.9 to 8.4 kg/cm^2 x 10^2
Izod Notched, R.T.	0.2 to 2.2 ft.-lb./in.	1.1 to 11.9 kg cm/cm
Hardness	M50 - M100 Rockwell	M50 - M100 Rockwell
Thermal Conductivity	1.4 to 3.0 BTU-in./hr.-ft.^{2}-°F	0.20 to 0.43 W/m-°K
Linear Thermal Expansion	3.7 to 8.4 in./in.-°F x 10^{-5}	6.7 to 15.1 cm/cm-°C x10^{-5}
Deflection Temperature @ 264 psi	150°F to 275°F	66°C to 135°C
Deflection Temperature @ 66 psi	170°F to 275°F	77°C to 135°C
Continuous Service Temperature	–	–
Dielectric Strength	300 to 575 V/10^{-3} in.	1.2 to 2.3 V/mm x 10^4
Dielectric Constant @ 1 MHz	2.5 to 2.6	2.5 to 2.6
Dissipation Factor @ 1 MHz	0.0001 to 0.0010	0.0001 to 0.0010
Water Absorption, 24 hr.	0.05 to 0.10%	0.05 to 0.10%

Table 2: Bill of Materials

Bill of Materials					
Quantity	**Part Name**	**Description**	**Purchased**	**Vendor**	**Cost**
100	Glass Capillary Tubing	ID: 1.10 mm OD: 1.50 mm	Yes	Amazon.com	$10.95
100	Kimble, Kimax Glass Capillary Tubing	ID: 0.80 mm OD: 1.10 mm	Yes	Amazon.com	$10.72
100	Kimble, Kimax Glass Capillary Tubing	ID: 1.50 mm OD: 1.80 mm	Yes	Amazon.com	$9.04
1	Natural Amber Latex Tubing	ID: 0.125 inches, OD: 0.250 inches Wall: 0.0625 inches, Length: 10 ft.	Yes	Amazon.com	$16.31
1	White Silicon Tubing	ID: 0.125 inches, OD: 0.1875 inches Wall: 0.03125 inches, Length: 10 ft.	Yes	Amazon.com	$24.88
1	Clear Tygon S-50-HL Medical Tubing	ID: 0.03125 inches, OD: 0.09375 inches Wall: 0.03125 inches, Length: 10 ft.	Yes	Amazon.com	$30.66
1	Lubrifilm Plus Tube	4 oz. Tube	Yes	Amazon.com	$4.00
1	Haynes Silicon Grease Tube	4 oz. Tube	Yes	Amazon.com	$10.00
1	Ethyl Vinyl Acetate Microbore Tubing	ID: 0.04 inches, Wall: 0.15 inch OD: 0.07 inches, Length: 1 ft.	No	Coleparmer.com	$0
1	Tygon Microbore Tubing	ID: 0.04 inches, Wall: 0.15 inch OD: 0.07 inches, Length: 1 ft.	No	Coleparmer.com	$0
20	Polystyrene Petri Dishes	60 mm x 15 mm	Yes	Edmond Scientifics.com	$3.95
20	Polystyrene Petri Dishes	100 mm x 15 mm	Yes	Edmond Scientifics.com	$5.95
2	Lexan Clear Polycarbonate Sheeting	12 inches x 24 inches x 0.093 inch	Yes	Home Depot	$14.78
2	Three Flute Carbide End Mill	1/32 inch Mill Diameter bit 1/8 inch Shank Diameter	Yes	McMasterCarr.com	$23.92
1	Clear Extruded Polycarbonate Tubing	ID: 0.625 inches OD: 0.750 inches, Length: 8 ft.	Yes	Profesional Plastics.com	$20.00
1	Clear Extruded Polycarbonate Tubing	ID: 0.750 inches OD: 0.875 inches, Length: 8 ft.	Yes	Profesional Plastics.com	$26.44
100	Micro-Hematocrit Glass Tubing	ID: 1.15 mm OD: 1.50 mm, Volume: 75µL	Yes	Pulmolab.com	$4.50
100	Micro-Hematocrit Plastic Plain Capillary Tubing	ID: 0.85 mm OD: 1.55 mm, Volume: 45µL	Yes	Pulmolab.com	$12.50
100	Micro-Hematocrit Glass Ammonium Heparinized Tubing	ID: 1.15 mm OD: 1.50 mm, Volume: 75µL	Yes	Pulmolab.com	$4.50
100	Micro-Hematocrit Plastic Ammonium Heparinized Tubing	ID: 0.85 mm OD: 1.55 mm, Volume: 45µL	Yes	Pulmolab.com	$12.50
1	Clear Polycarbonate Sheeting	24 inches x 48 inches x 0.03125 inch	Yes	Ridout Plastics ePlastics.com	$16.09
1	Weld-on #4	4 oz. Can	Yes	Ridout Plastics ePlastics.com	$8.80
1	FDA Silicon Sheeting	5 ft. x 3 ft. x 0.0625 inch	Yes	Rubber-Cal.com	$134.75
5	Capillary Ceramic Cutter	3 inches x 1 inch Wafers	No	SGE Analytical Science	$0
25	Plastic Microscope slides	Acrylic 75 mm x 25 mm x 1.1 mm	Yes	Tedpella.com	$16.75
1	ETFE Tubing	ID: 0.030 inches OD: 0.063 inches	No	Zeus.com	$0
1	PTFE Tubing	ID: 0.042 inches OD: 0.054 inches, AWG: 18	No	Zeus.com	$0
1	PTFE Tubing	ID: 0.038 inches OD: 0.050 inches, AWG: 19	No	Zeus.com	$0
1	PFA Tubing	ID: 0.042 inches OD: 0.054 inches, AWG: 18	No	Zeus.com	$0
1	FEP Tubing	ID: 0.038 inches OD: 0.050 inches, AWG: 19	No	Zeus.com	$0
Total					$421.99

Table 7: Sonobond® Ultrasonics Laboratory Report

SONOBOND® ULTRASONICS

NDA ☐

APPLICATION LABORATORY REPORT

Company	University of KS	**AE No.**	19052
Contact	Preston White	Date In	2-17-12
Phone	785-864-3181 Ext.	Date Out	2-21-12
Address	1530 W. 15th St	Date Mailed	
		NO GO?	
City	Lawrence	Textile/Plastic	X Metal
State	KS Zip 66045	I.S.R.	JD
Country		Lab Tech	PT
Email	prestonw@ku.edu	Sales Rep	

APPLICATION:			MATERIAL:		
			Upper		Lower
Customer Specification:					
EQUIPMENT USED					
Model No.:	Standard 3000				
Tooling:	Horn	2 ¾" X ¾" Flat face	Fixture	Clamp to hold parts	
PARAMETERS USED					
Amplitude	2000W	Power draw	5%		
Down Pressure	60 Psi	Booster 1.5 X 1.0			
Time:	Delay/Trigger	1.0 Sec	Sonics	1.0 Sec	
	Hold	1.5 Sec	Speed	2	

Notes:
Parts would need dedicated tooling and better energy directors to maintain a consistent weld

Appendix C: Drawings

Drawing 3.2-1: The 3D AutoCAD model of the slide using dimensions from the experiment.

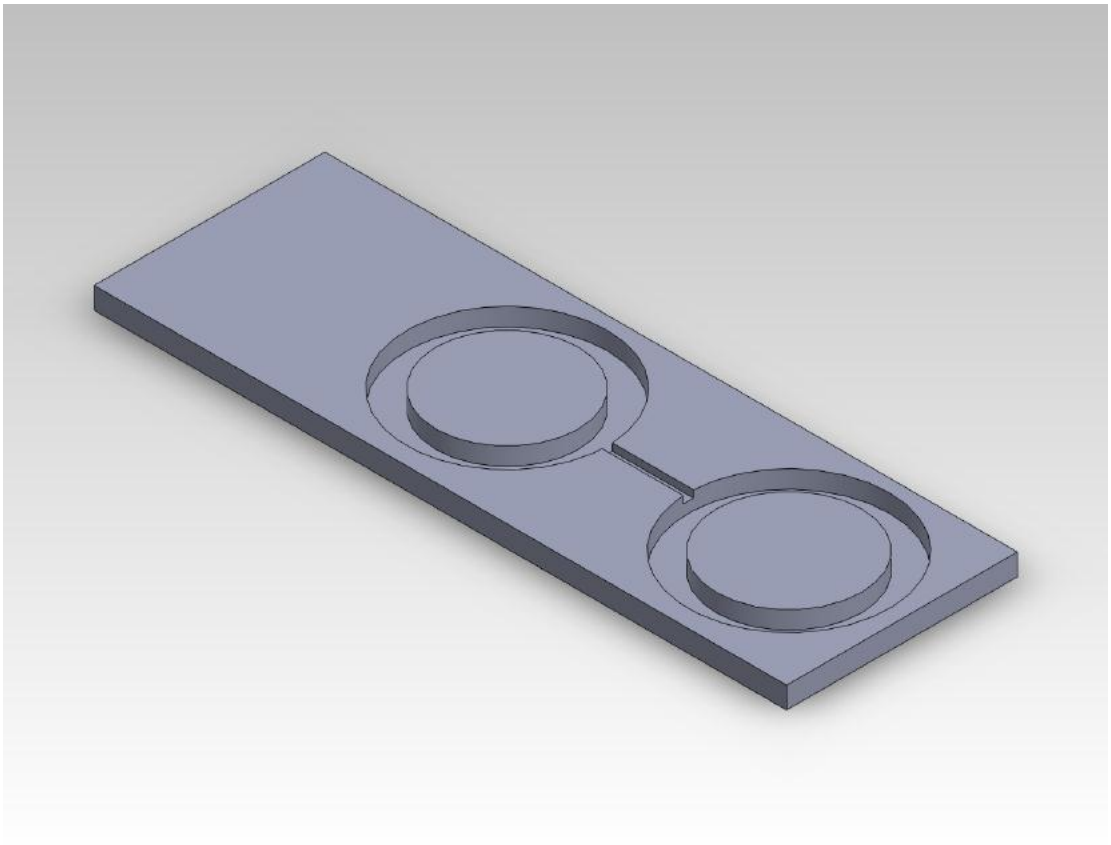

Drawing 3.2-2: The correct dimensions of the inner and outer circular groove diameters.

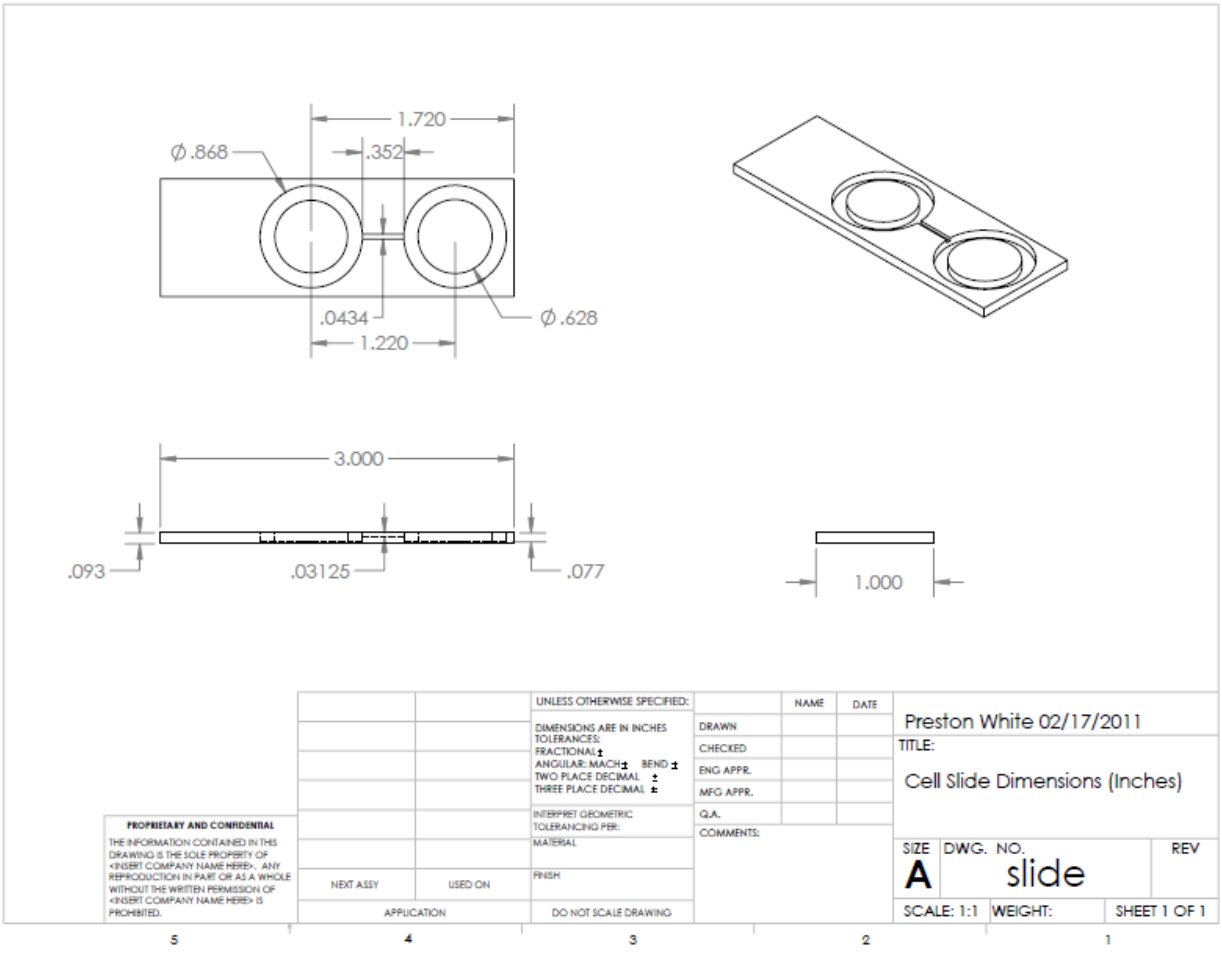

Drawing 3.2-3: Modifications were made to the 3D AutoCAD model to increase the amount of material between the circular grooves and the bottom of the slide.

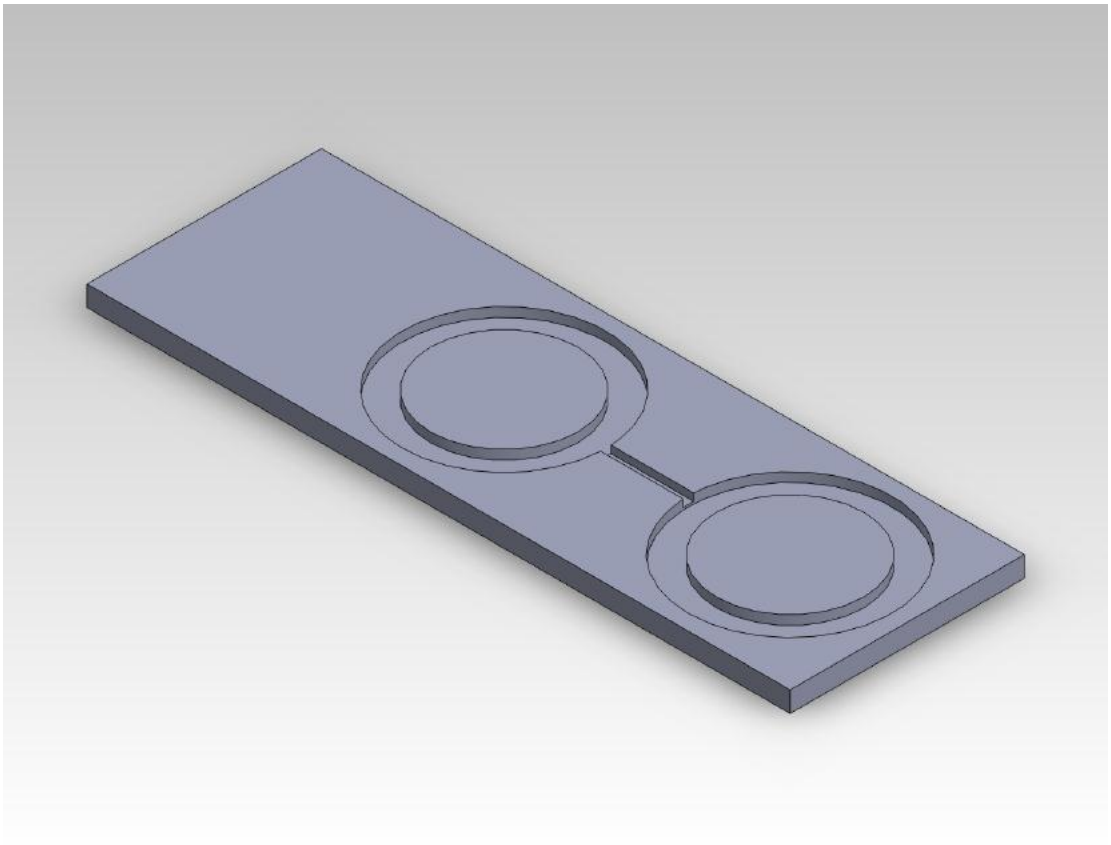

Drawing 3.2-4: Shows the change in dimensions to the slide from the previous drawings.

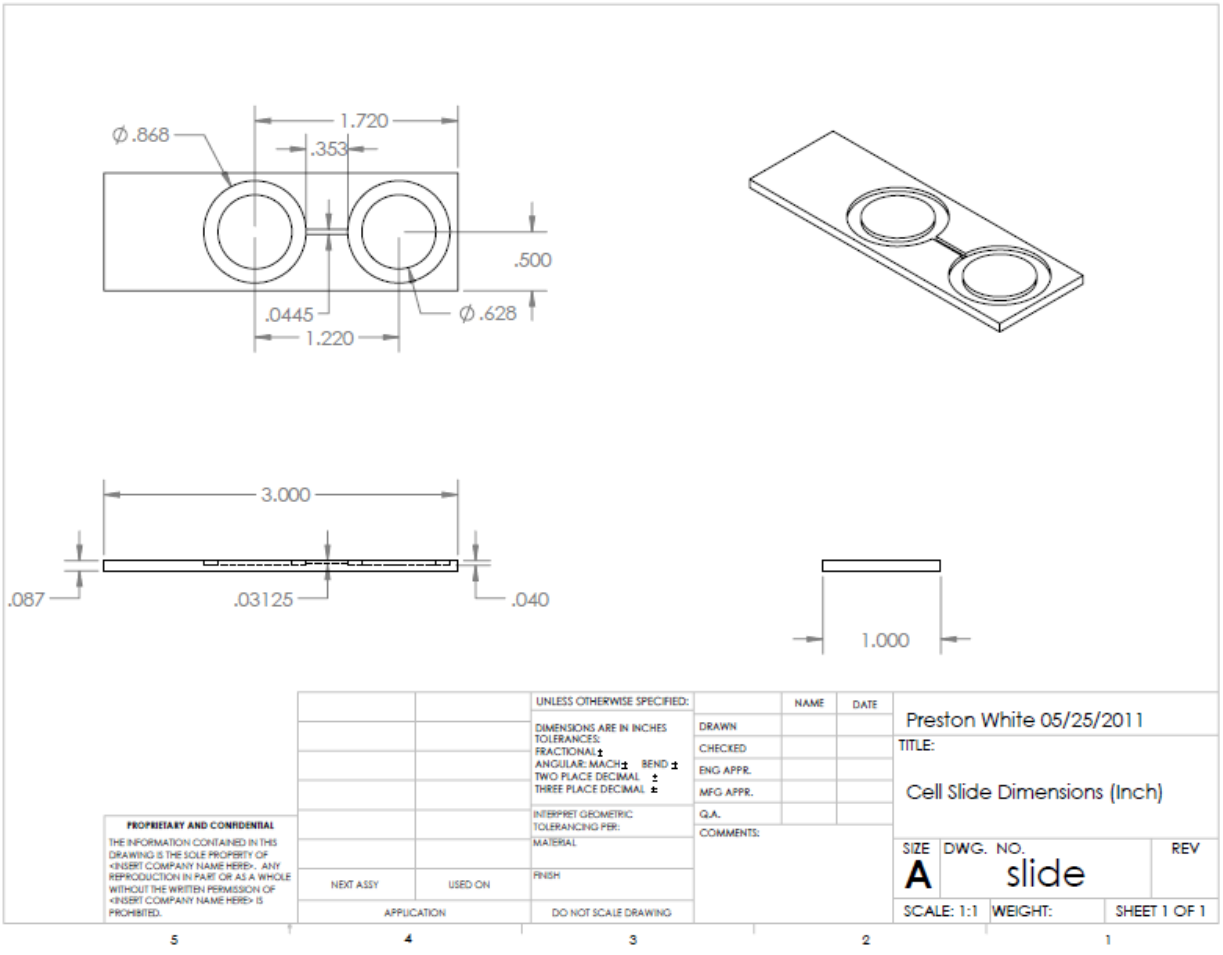

Drawing 3.2-5: The 3D AutoCAD model of the internal and external chambers used to test the gasket for leaks.

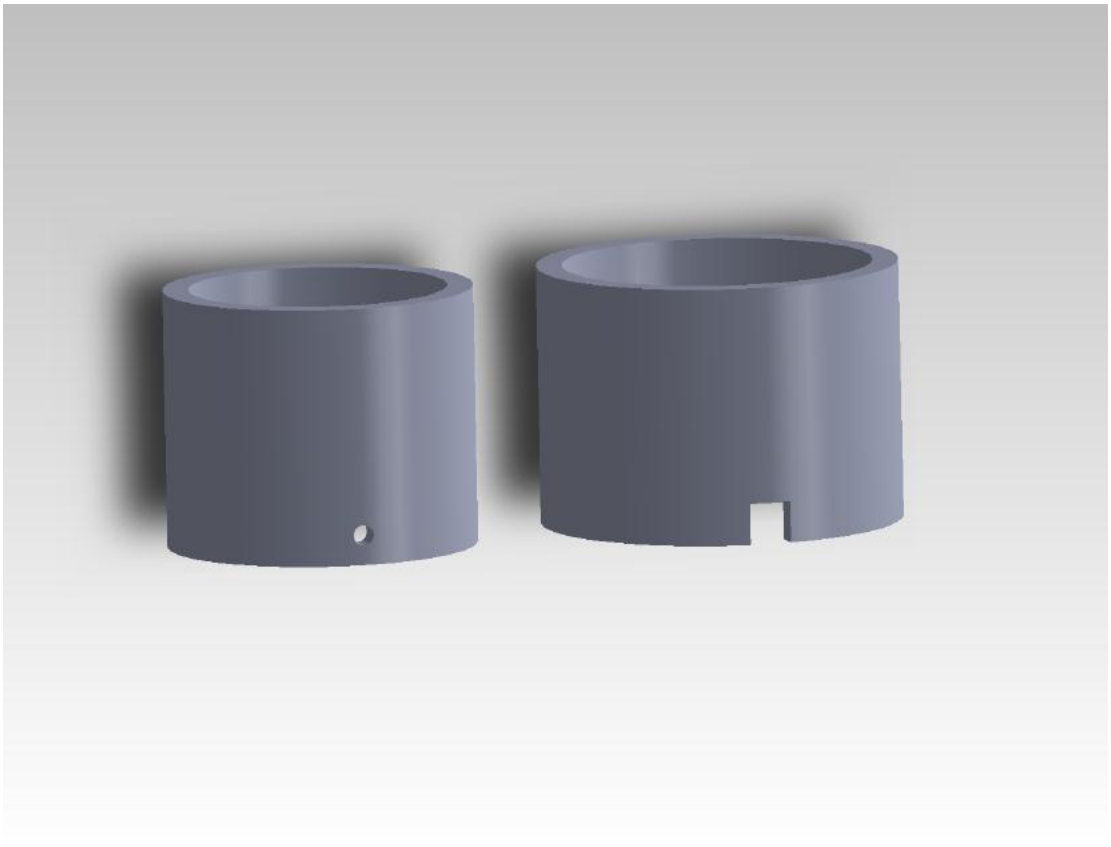

Drawing 3.2-6: Shows the exact dimensions used to machine the hole sizes in each of the chambers.

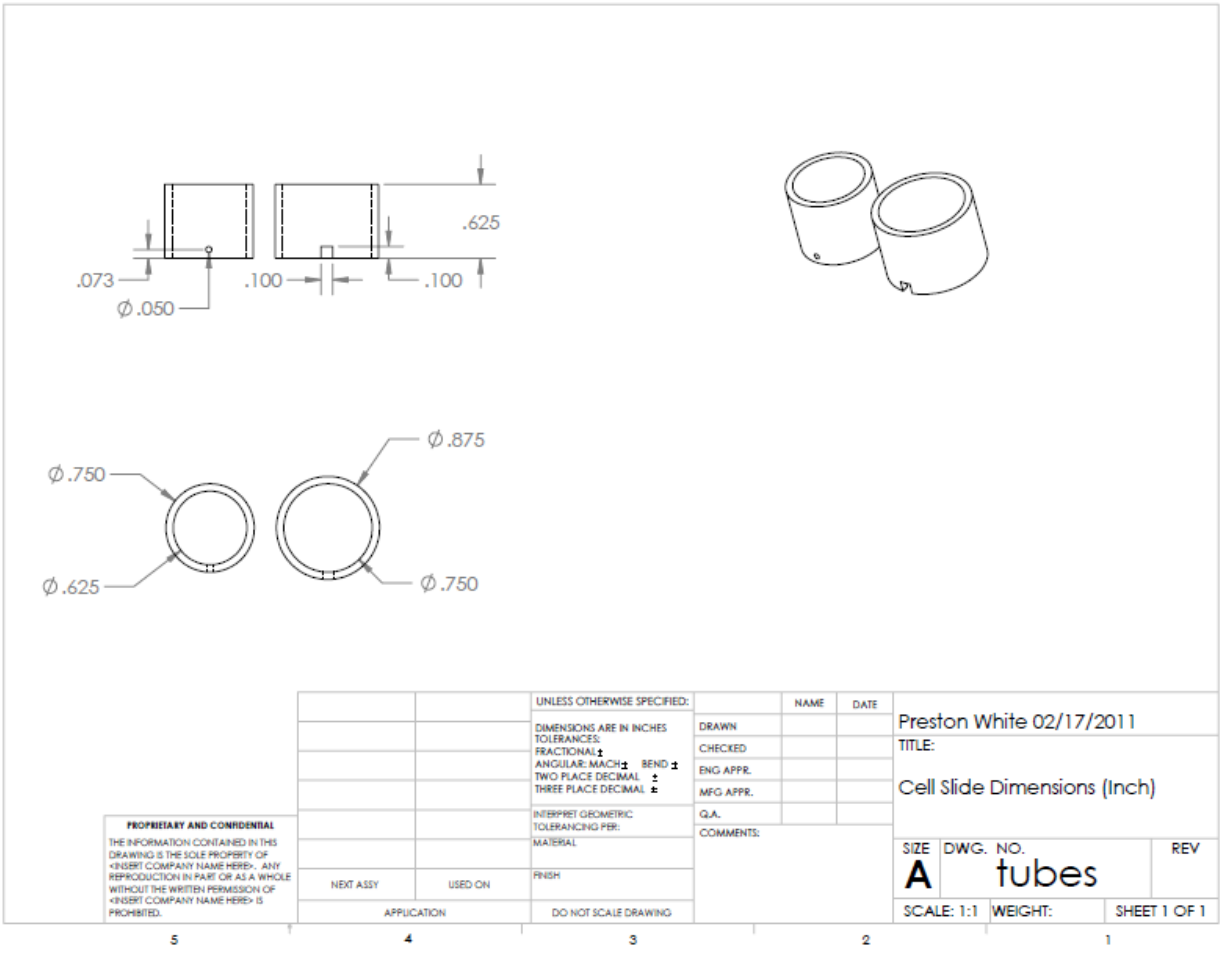

Drawing 3.2-7: Modifications were made to the 3D AutoCAD model using the measurements obtained from the capillary tube.

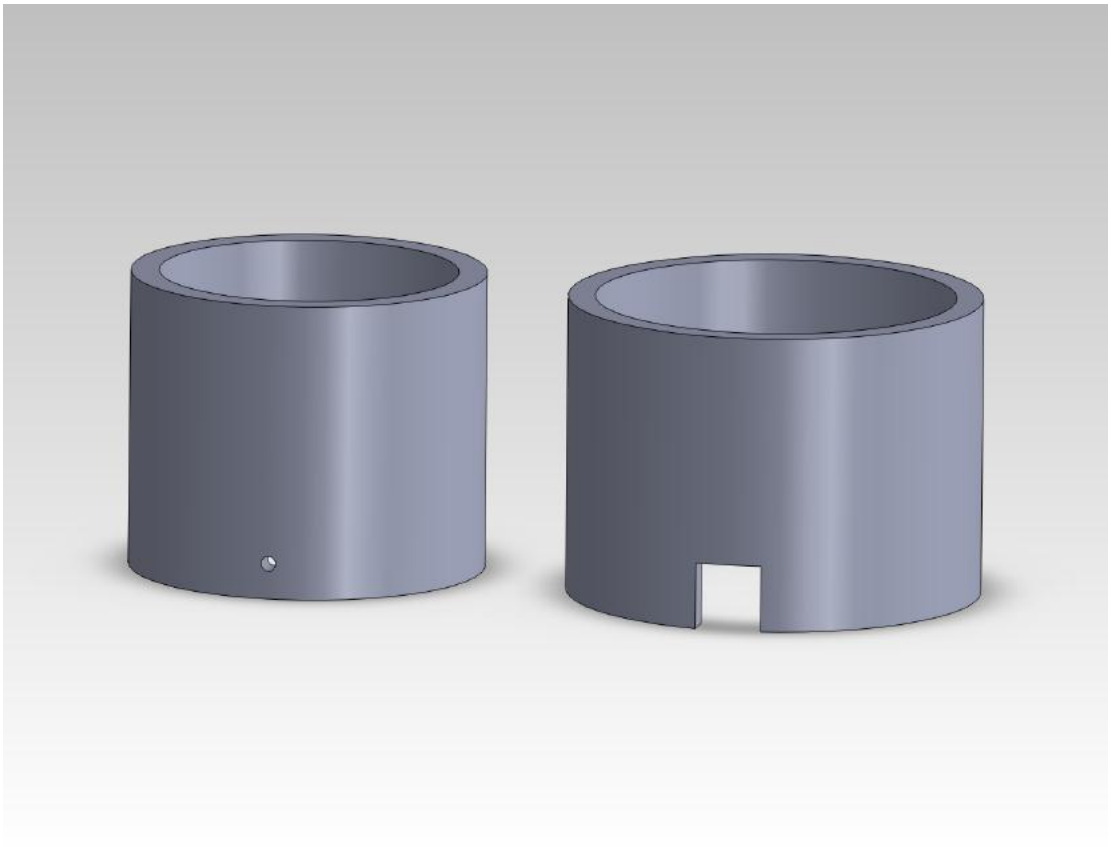

Drawing 3.2-8: Shows the final dimensions of the hole sizes in the internal and external chamber.

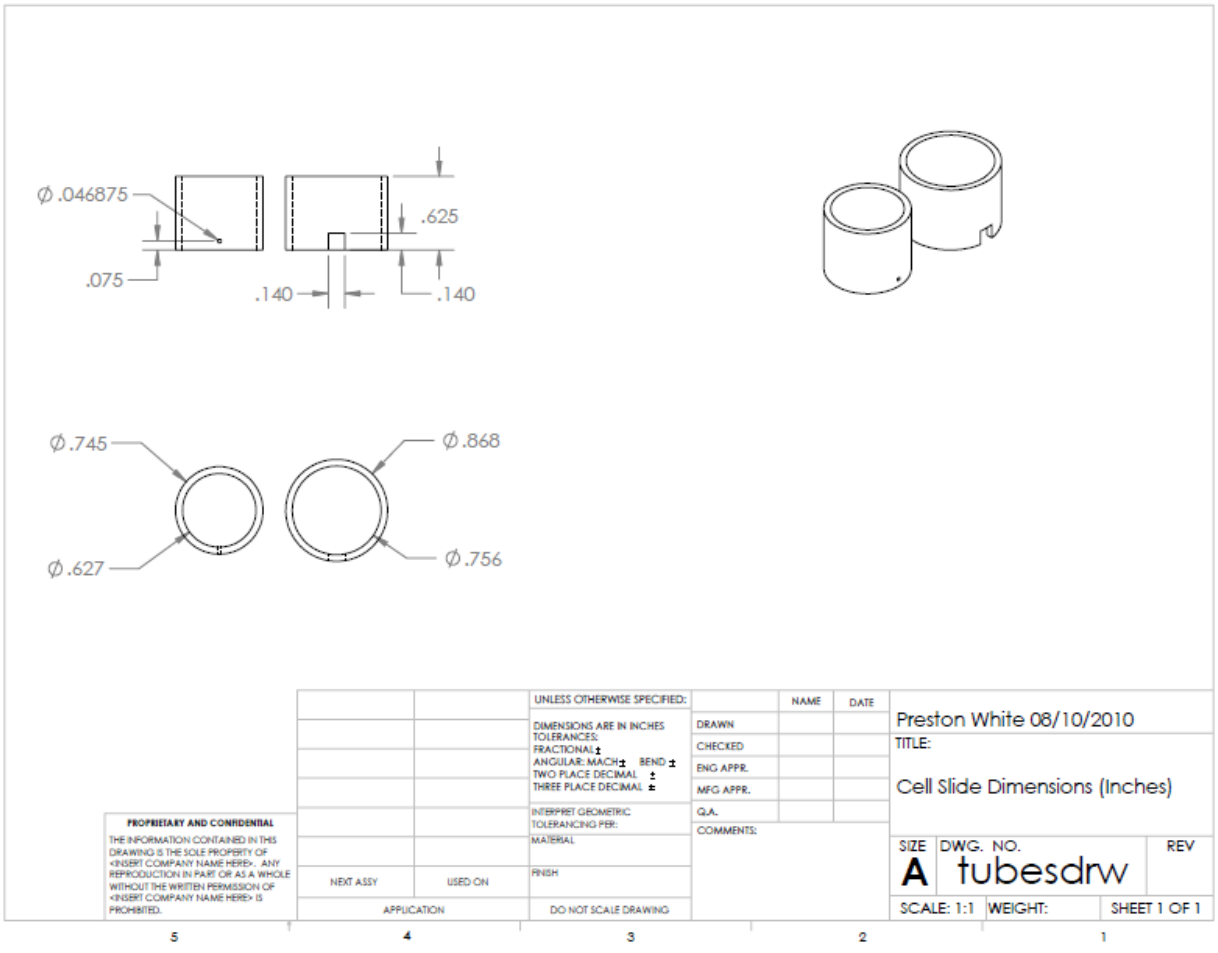

Drawing 3.2-9: Modifying the 3D AutoCAD model by removing the notch from the top of the slide, which held the capillary tube in place.

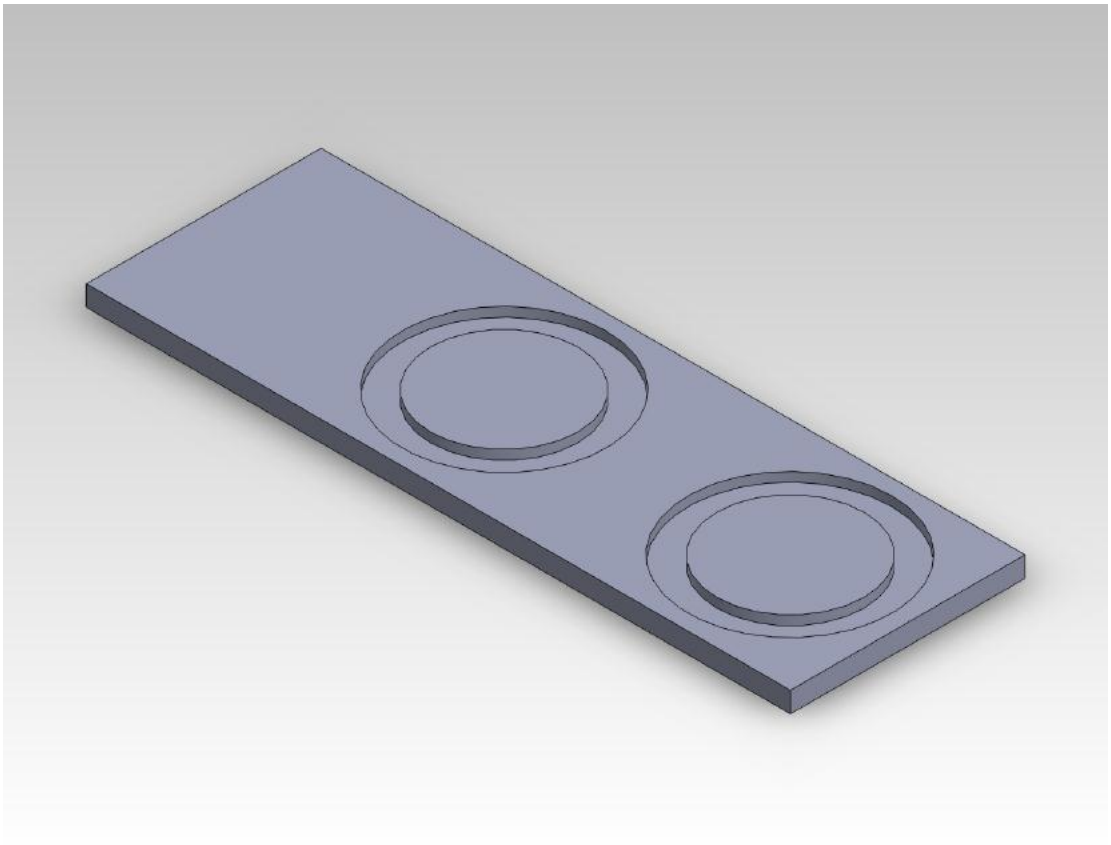

Drawing 3.2-10: The final set of drawings for the prototype slide.

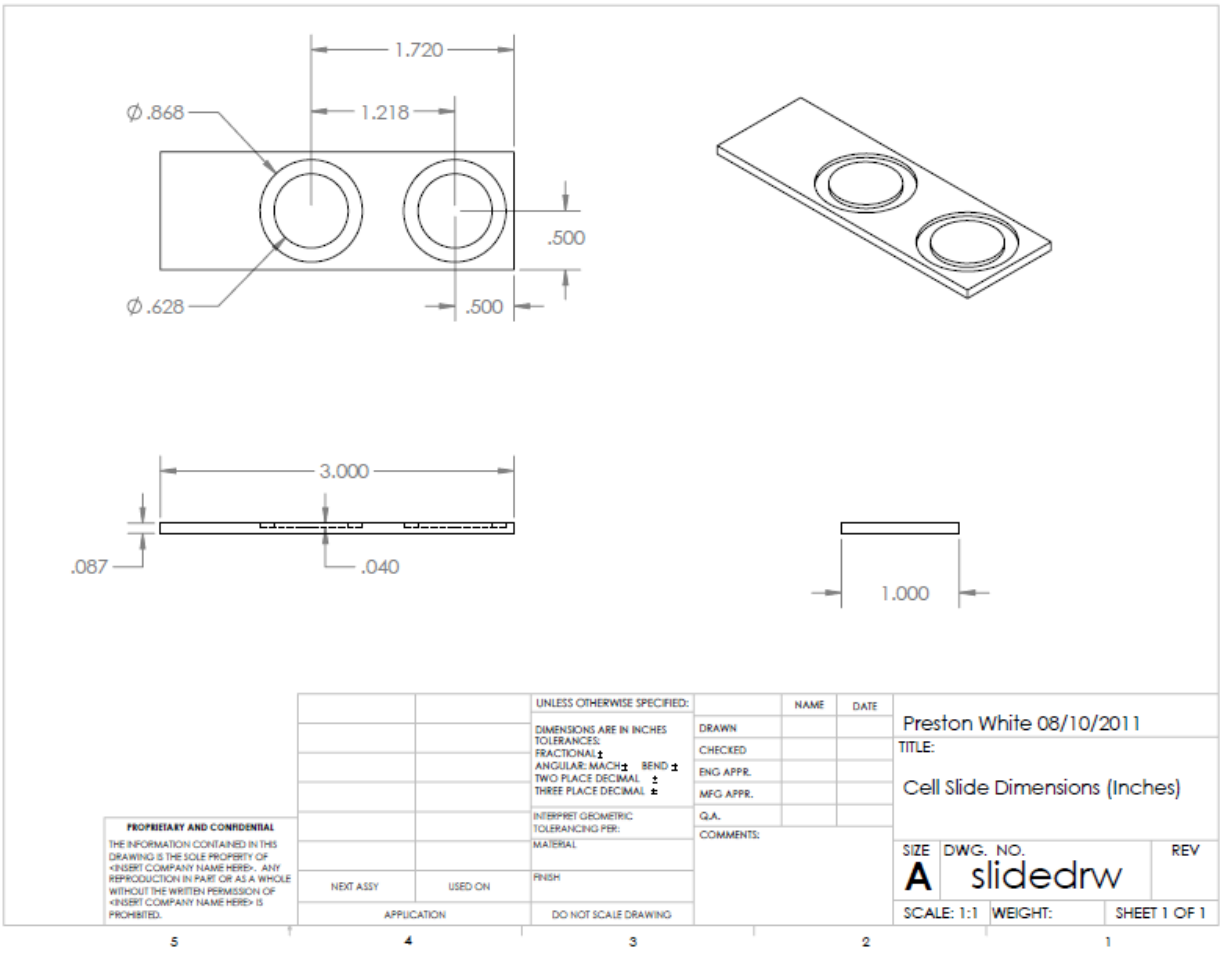

Drawing 3.3-1: Integrating the connecting channel into the polycarbonate slide.

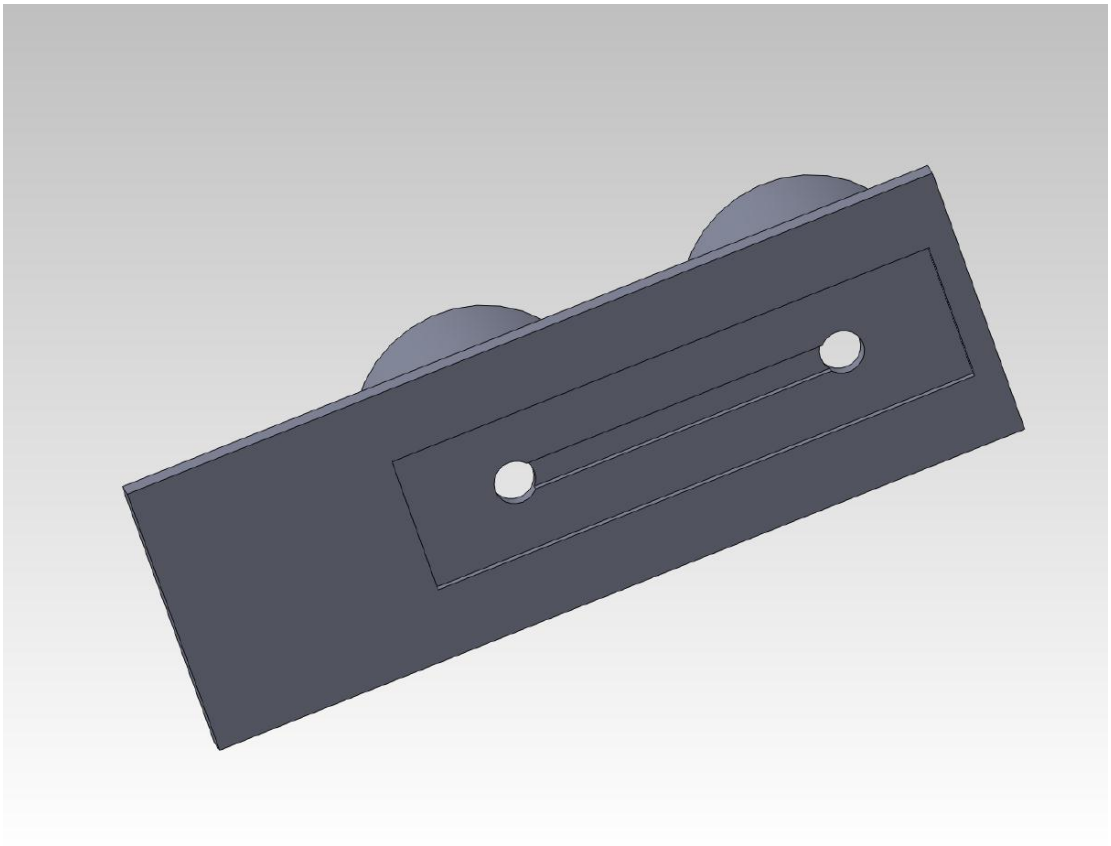

Drawing 3.3-2: The channel openings are positioned at the bottom of the chambers.

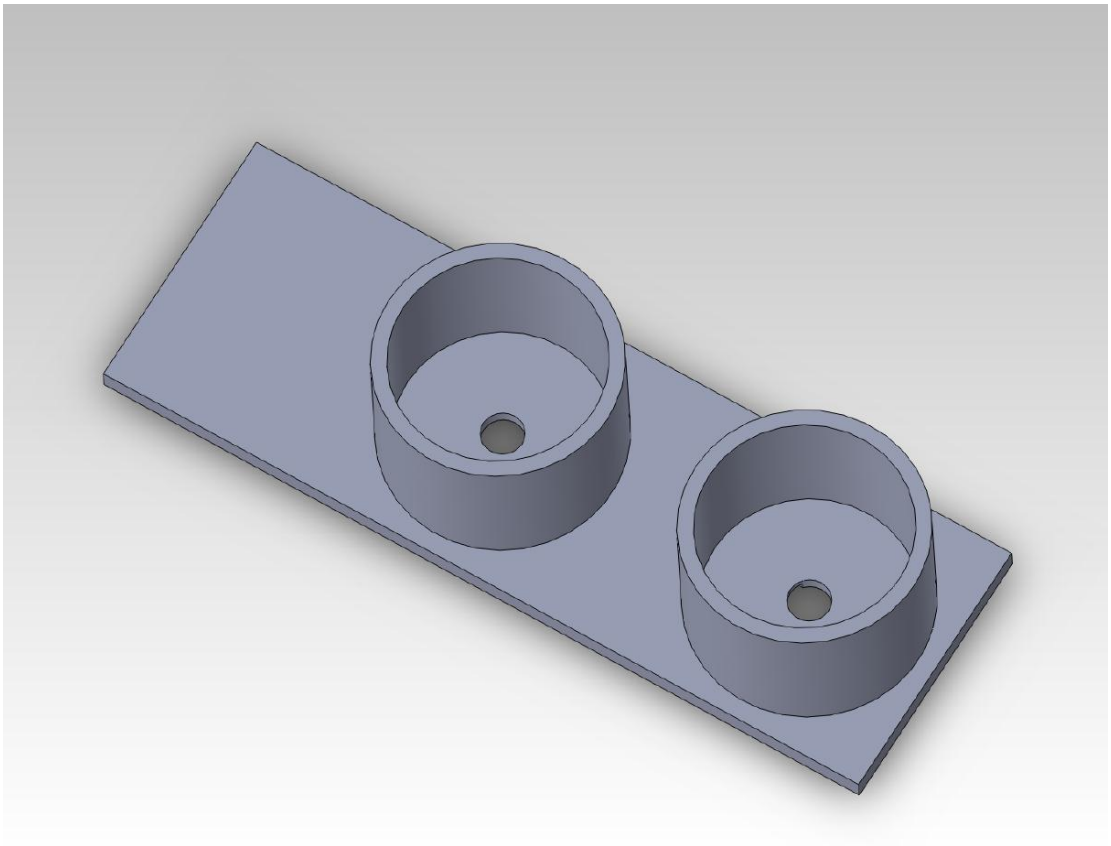

Drawing 3.3-3: The external chambers are permanently fixed to the top of the slide.

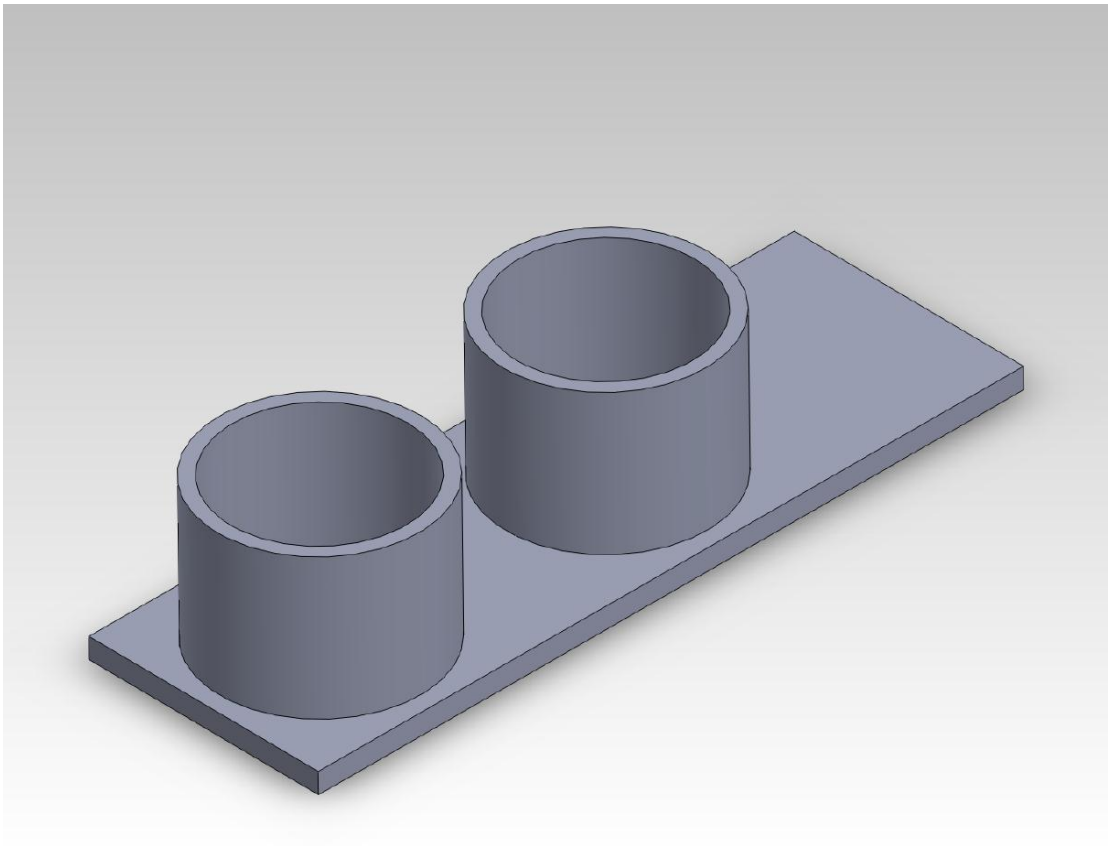

Drawing 3.3-4: Using the dimensions from the previous design and fabricating the dimensions for the connecting channel, a set of drawing were produced for the machinist.

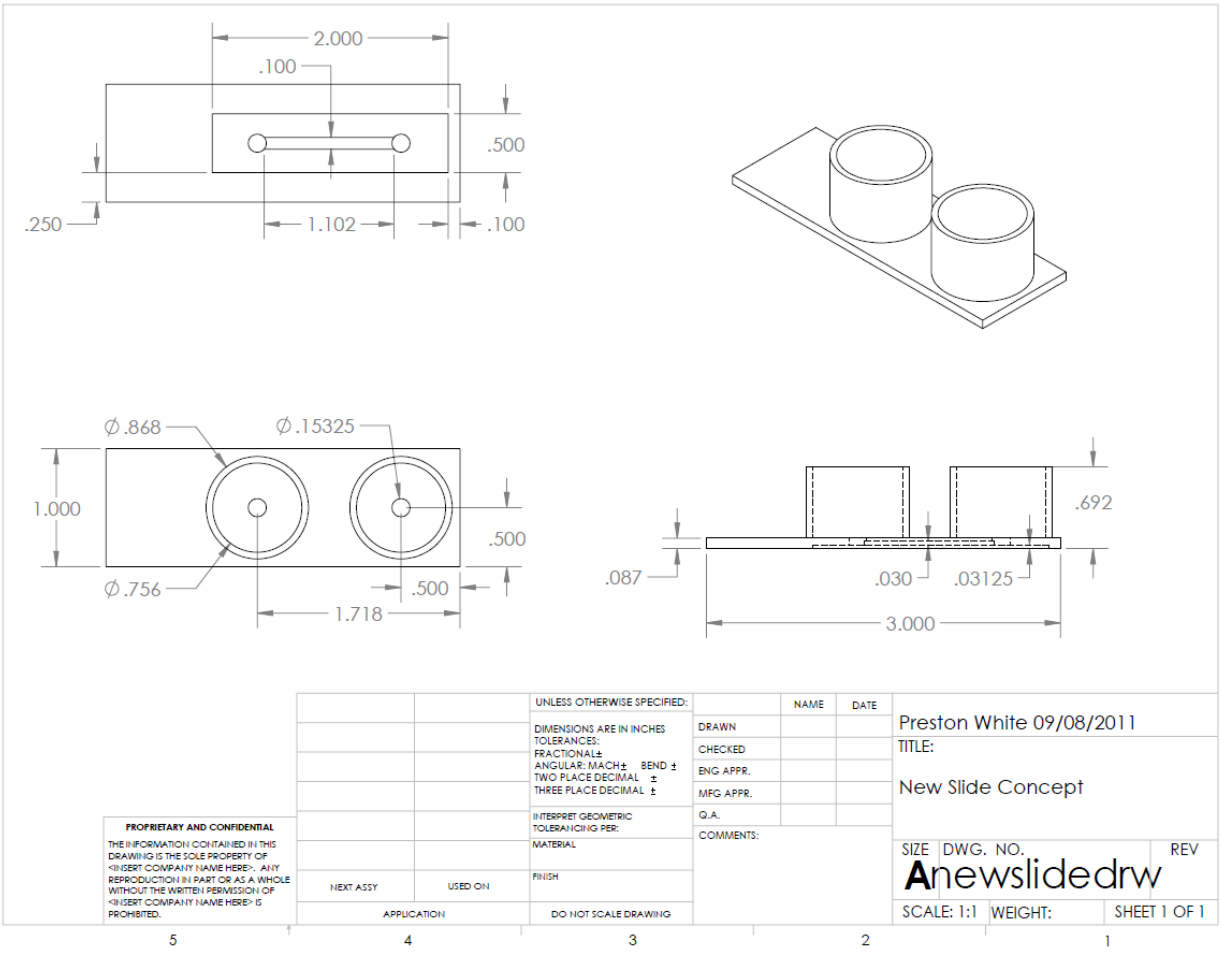

Drawing 3.3-5: Shows the front side of the 3D AutoCAD model, which uses the material properties of polycarbonate. Increased the size to channel openings and the circular grooves.

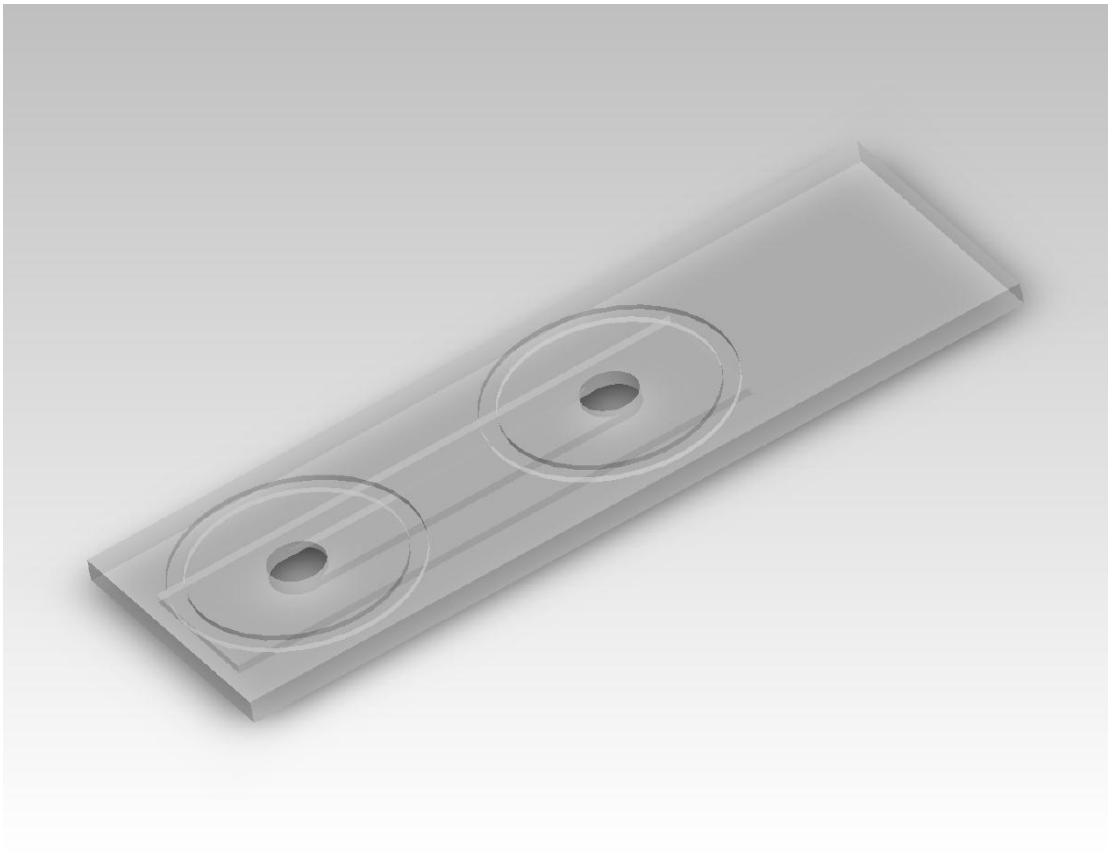

Drawing 3.3-6: Shows the back side of the slide model to point out the increased size of the flow channel.

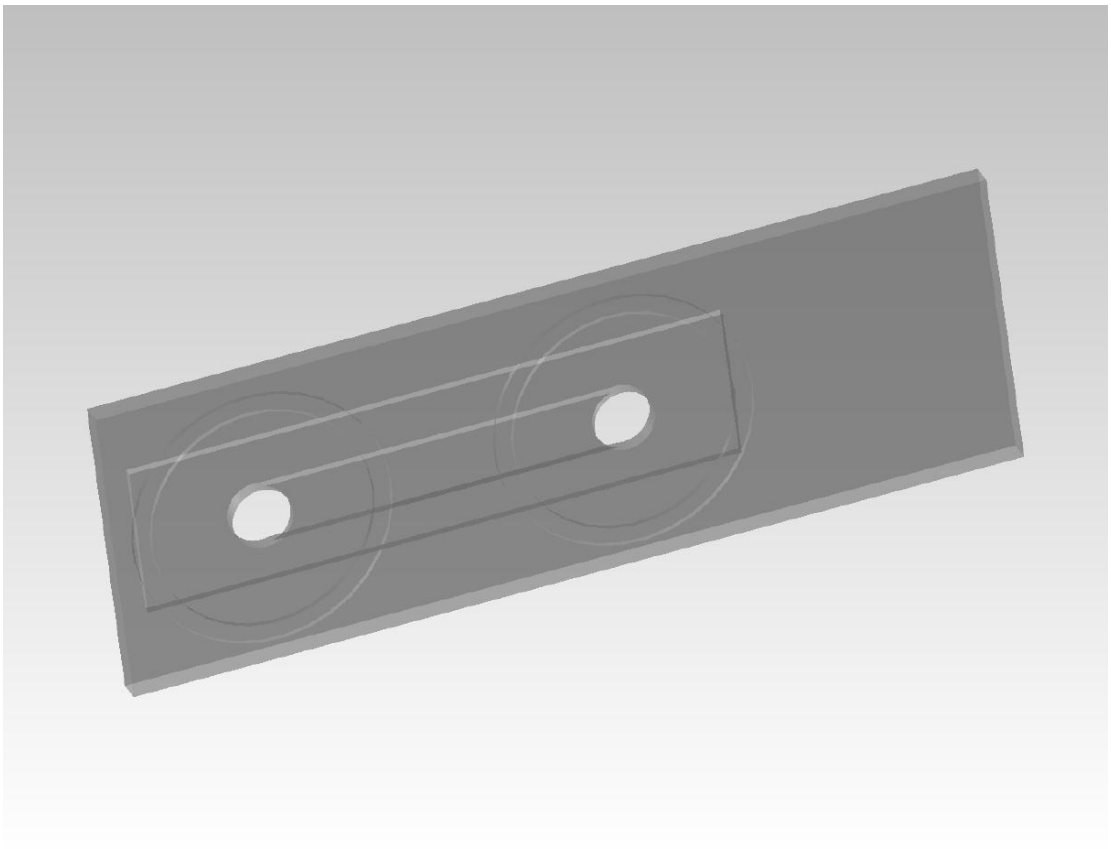

Drawing 3.3-7: Final set of drawings, detailing all the alterations.

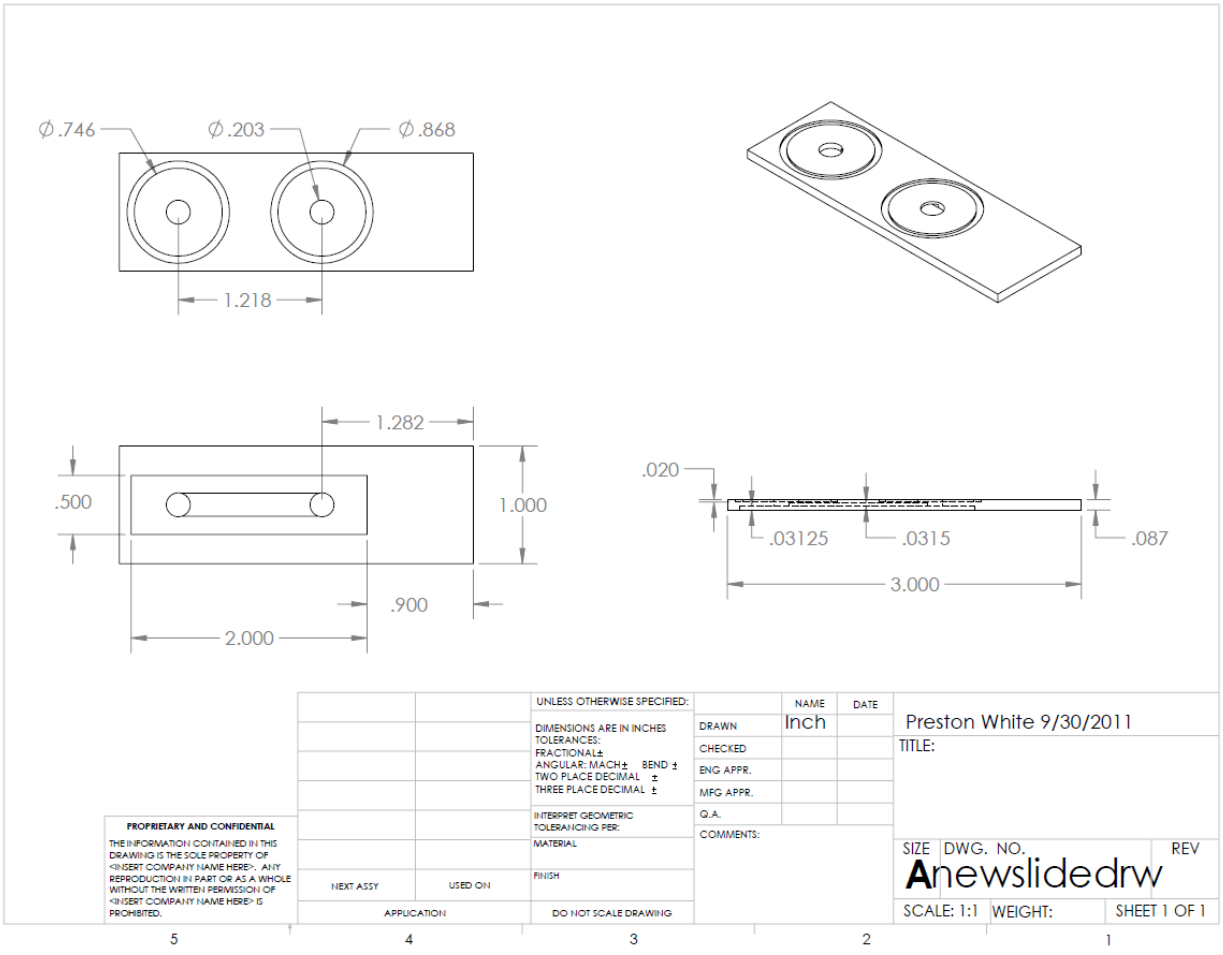

Drawing 3.4-1: Underneath of the slide to show the flow channel and the circular through holes to fix the external chambers in place.

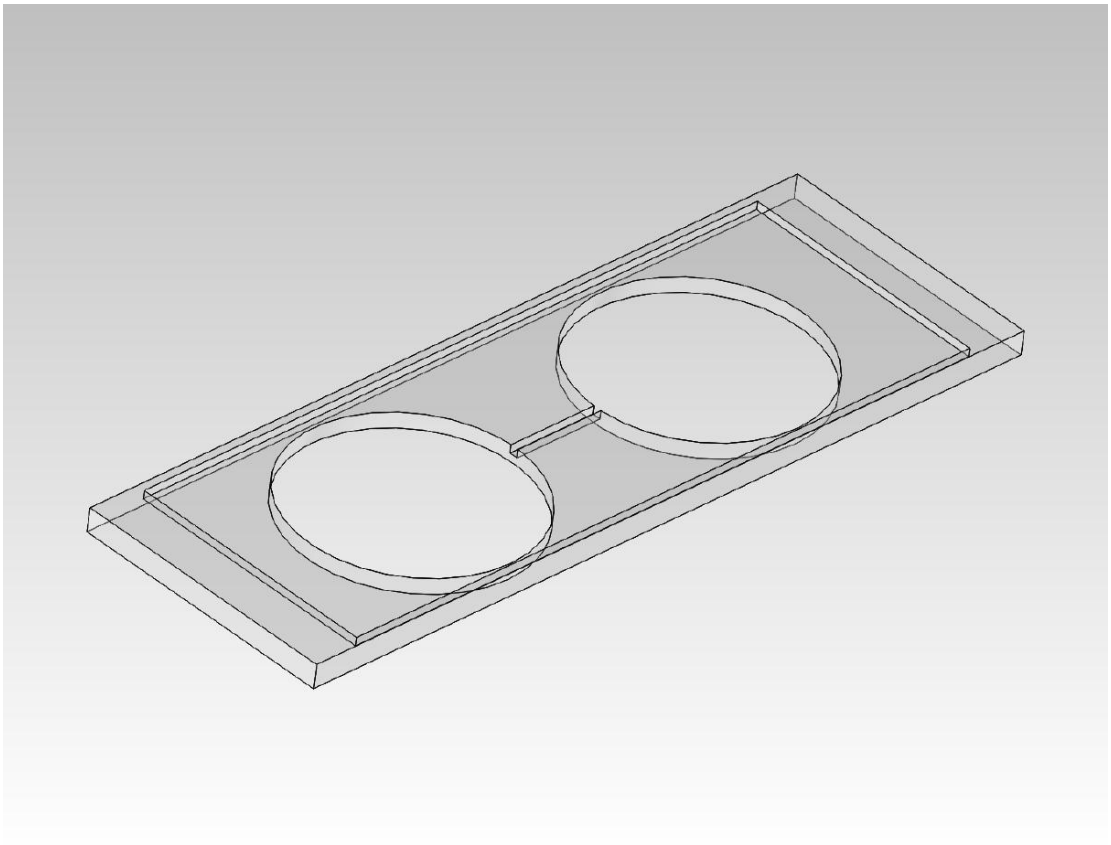

Drawing 3.4-2: Shows the exact dimensions used to manufacture the slides.

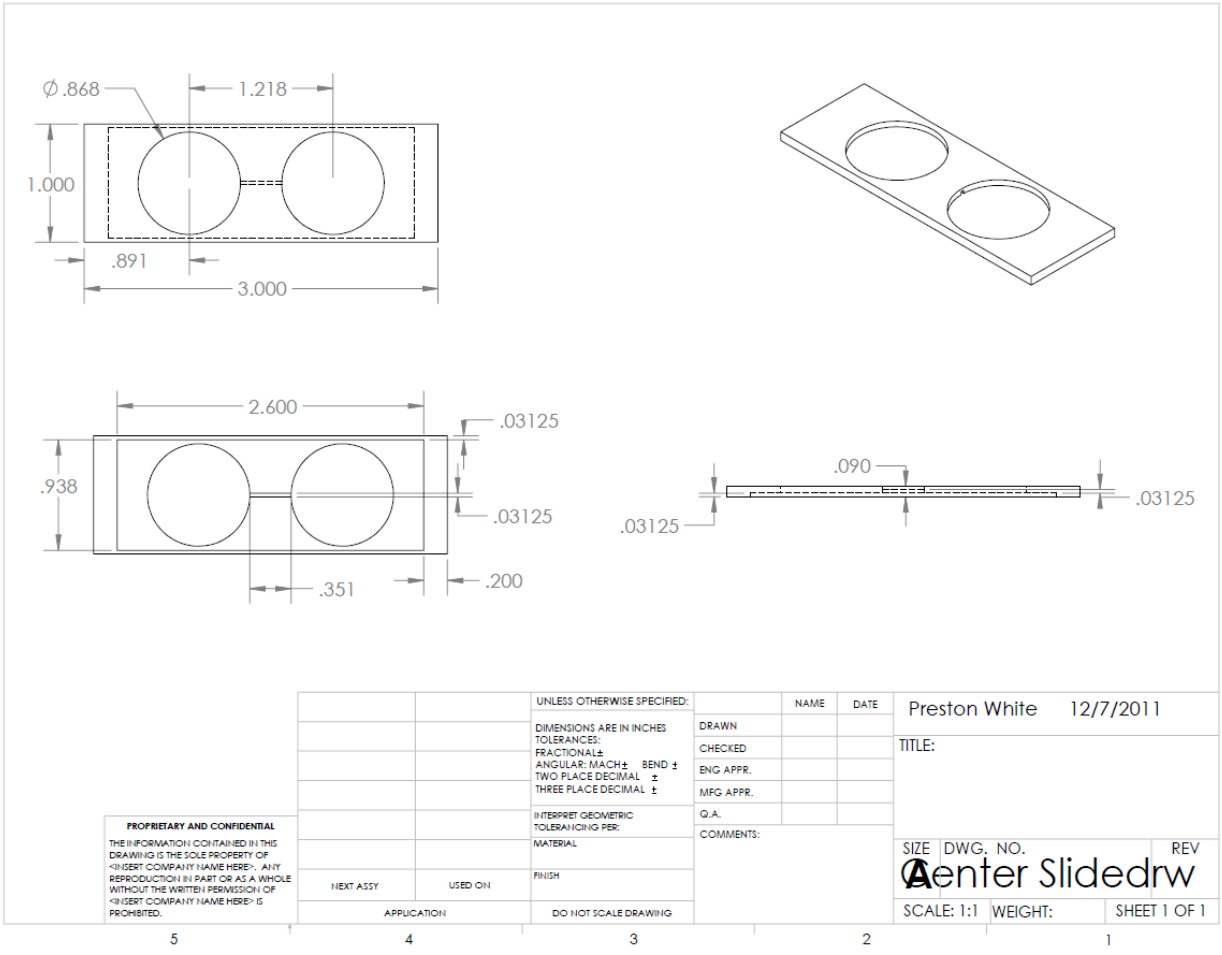

Drawing 3.4-3: Shows the sizes and where the openings are positioned on both the internal and external chambers.

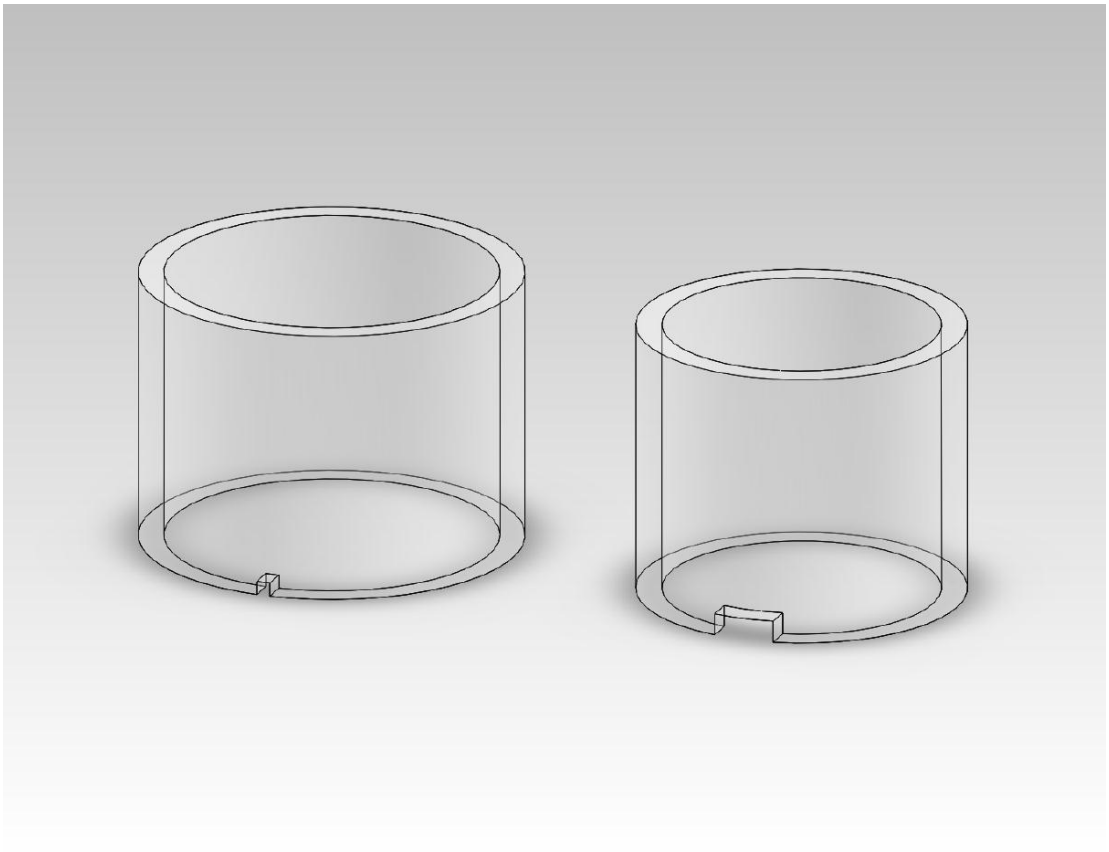

Drawing 3.4-4: The chambers were then manufactured to specifications using these dimensions.

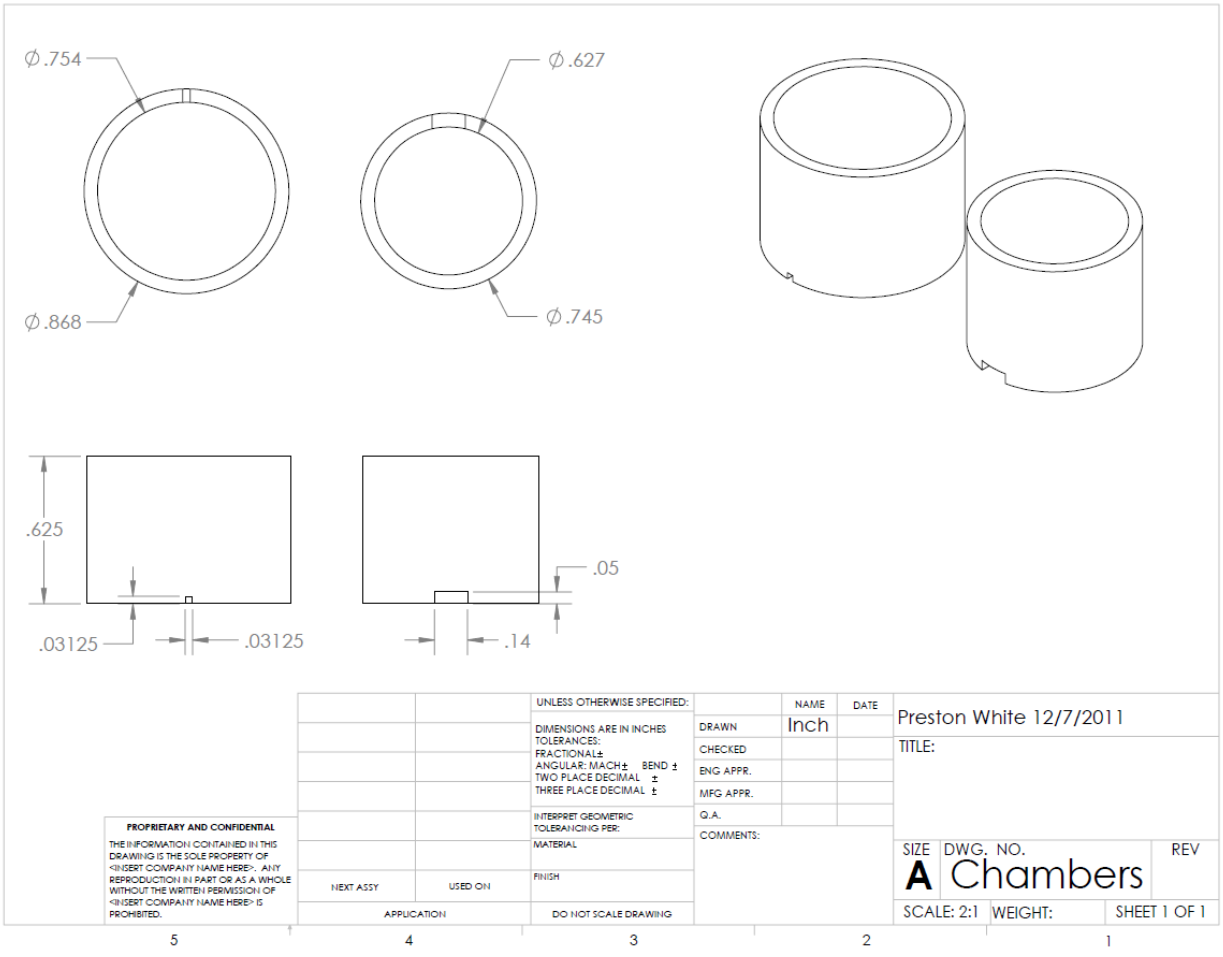

Drawing 3.4-5: The dimensions used to manufacture the back cover plate.

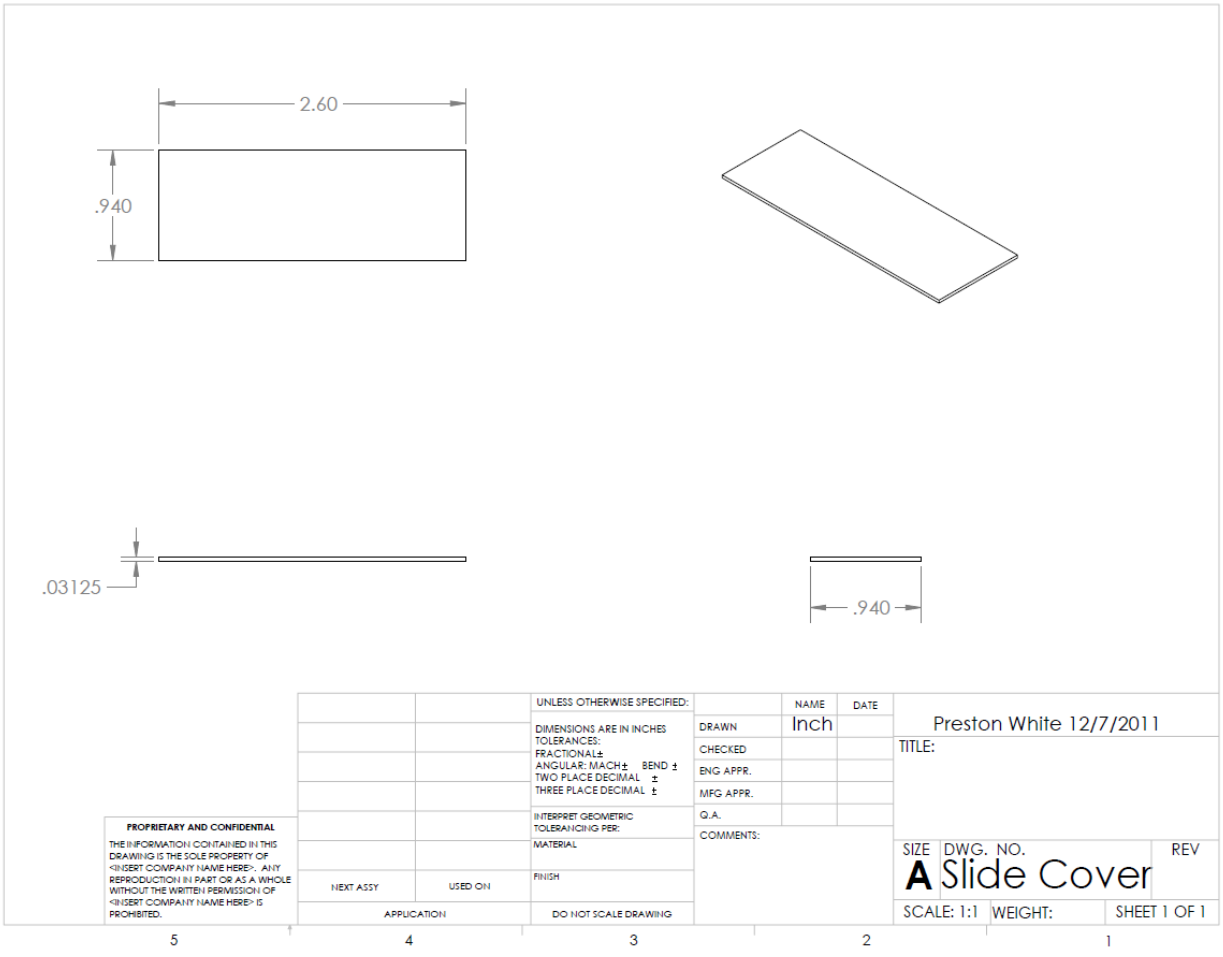

Drawing 3.4-6: Final changes the 3D AutoCAD model to increase the total width and diameter of the through holes.

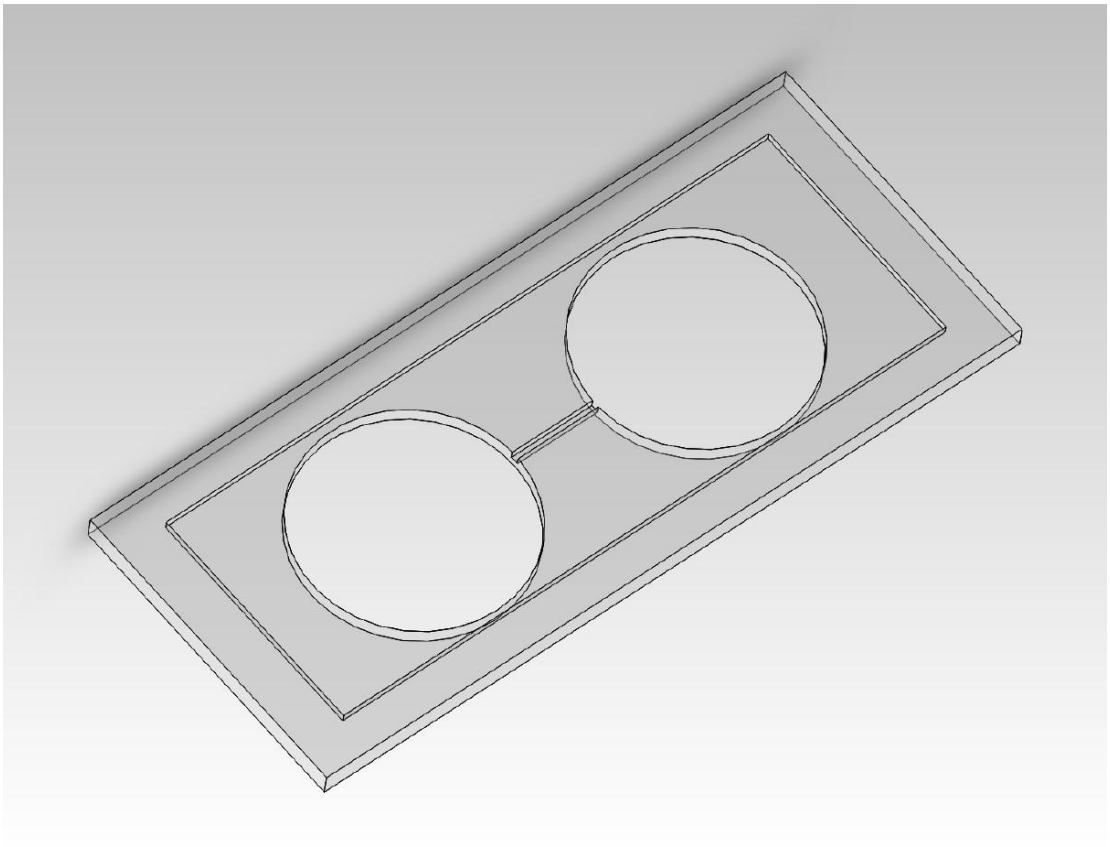

Drawing 3.4-7: The slides width was increased by 0.125 inch on either side and the diameter of the through hole was increased from 0.868 inch to 0.873 inch.

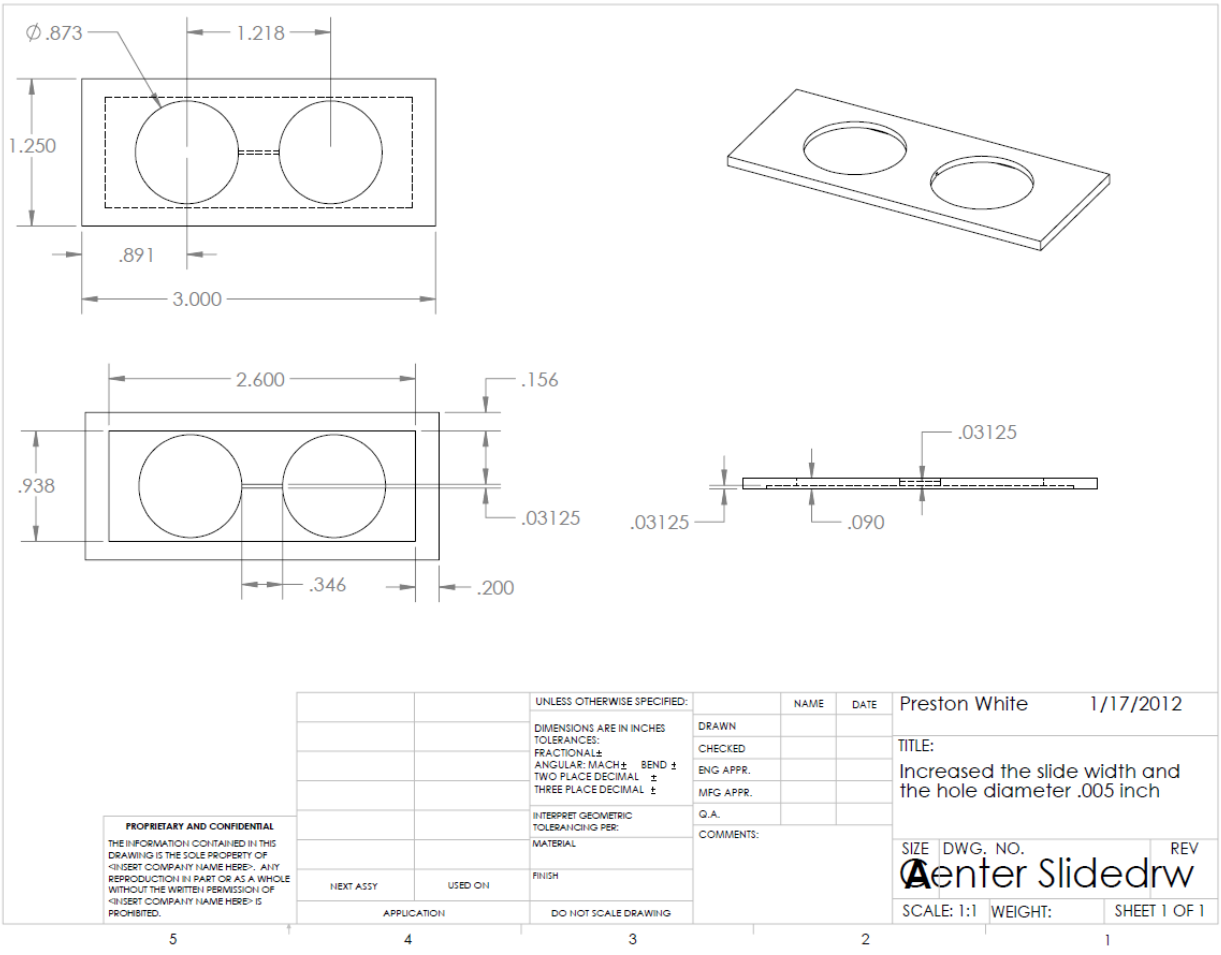

Drawing 3.4-8: The back cover plate with straight perpendicular corners.

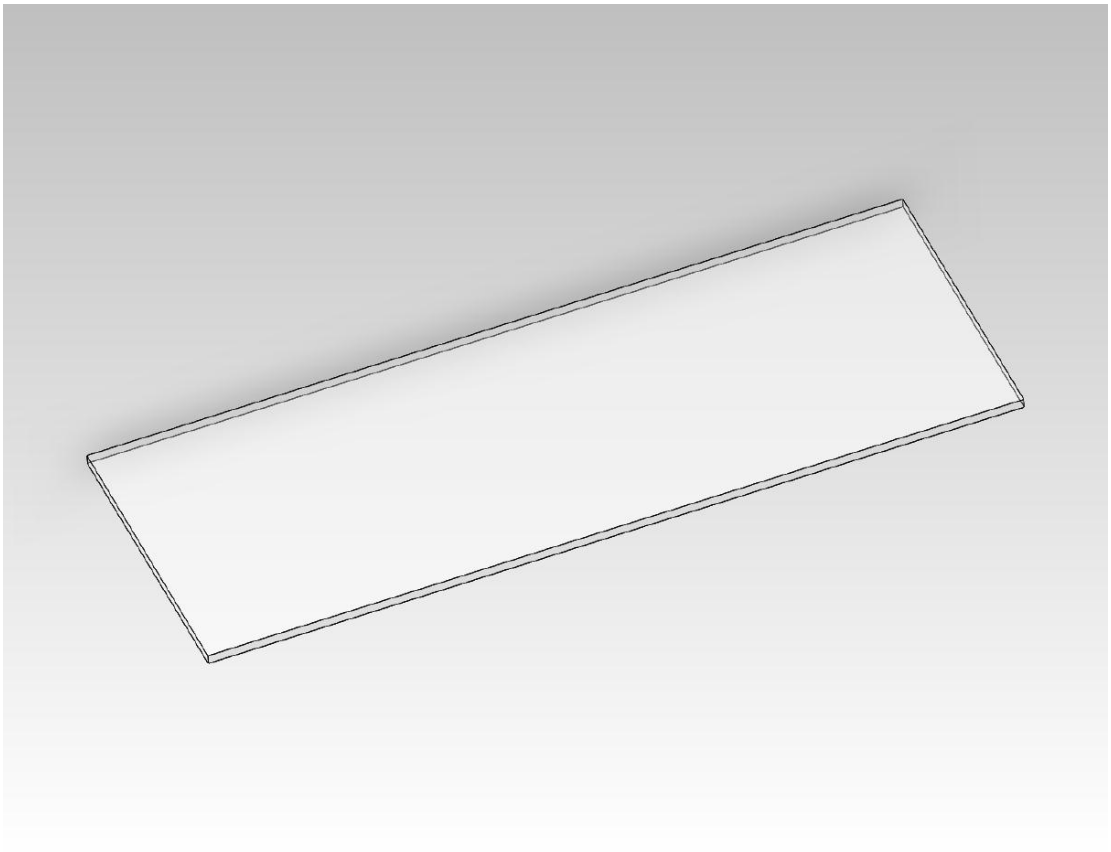

Drawing 3.4-9: The back cover plate with the corners cut at an angle to make it easier to manufacture.

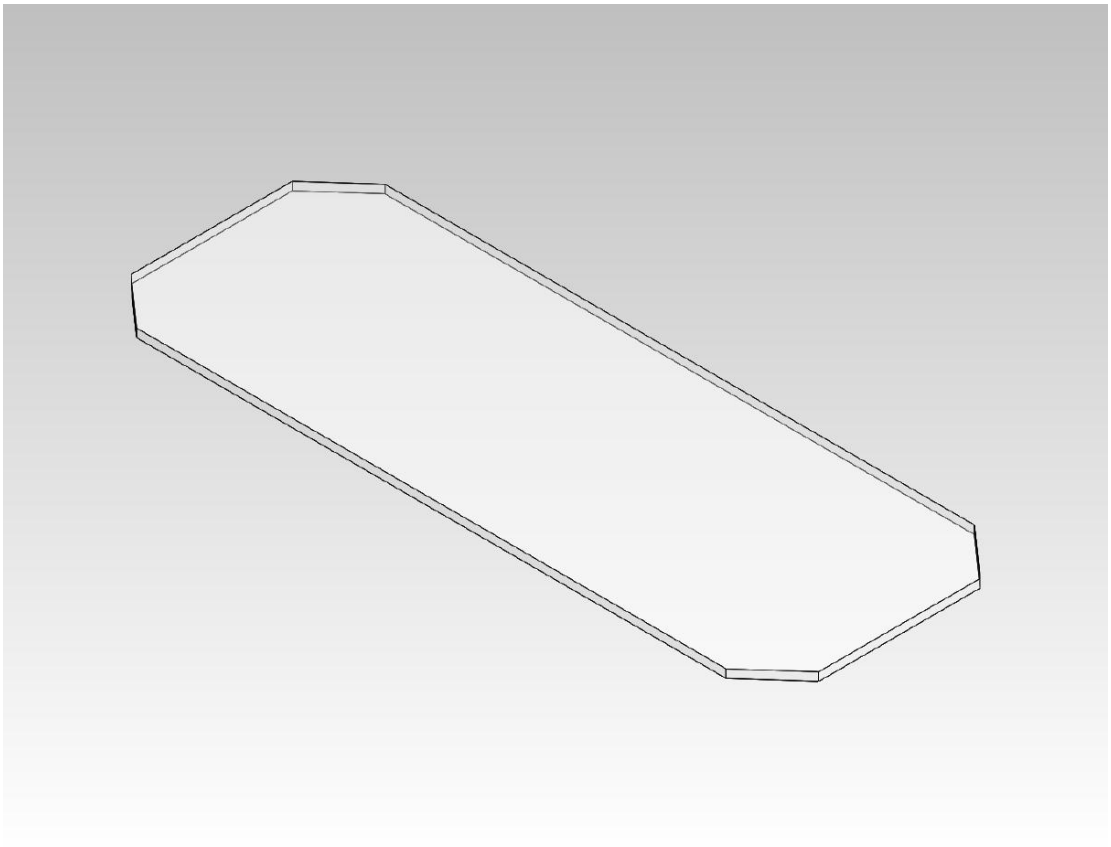

Drawing 3.4-10: The exact specifications used to manufacture the back cover plate.

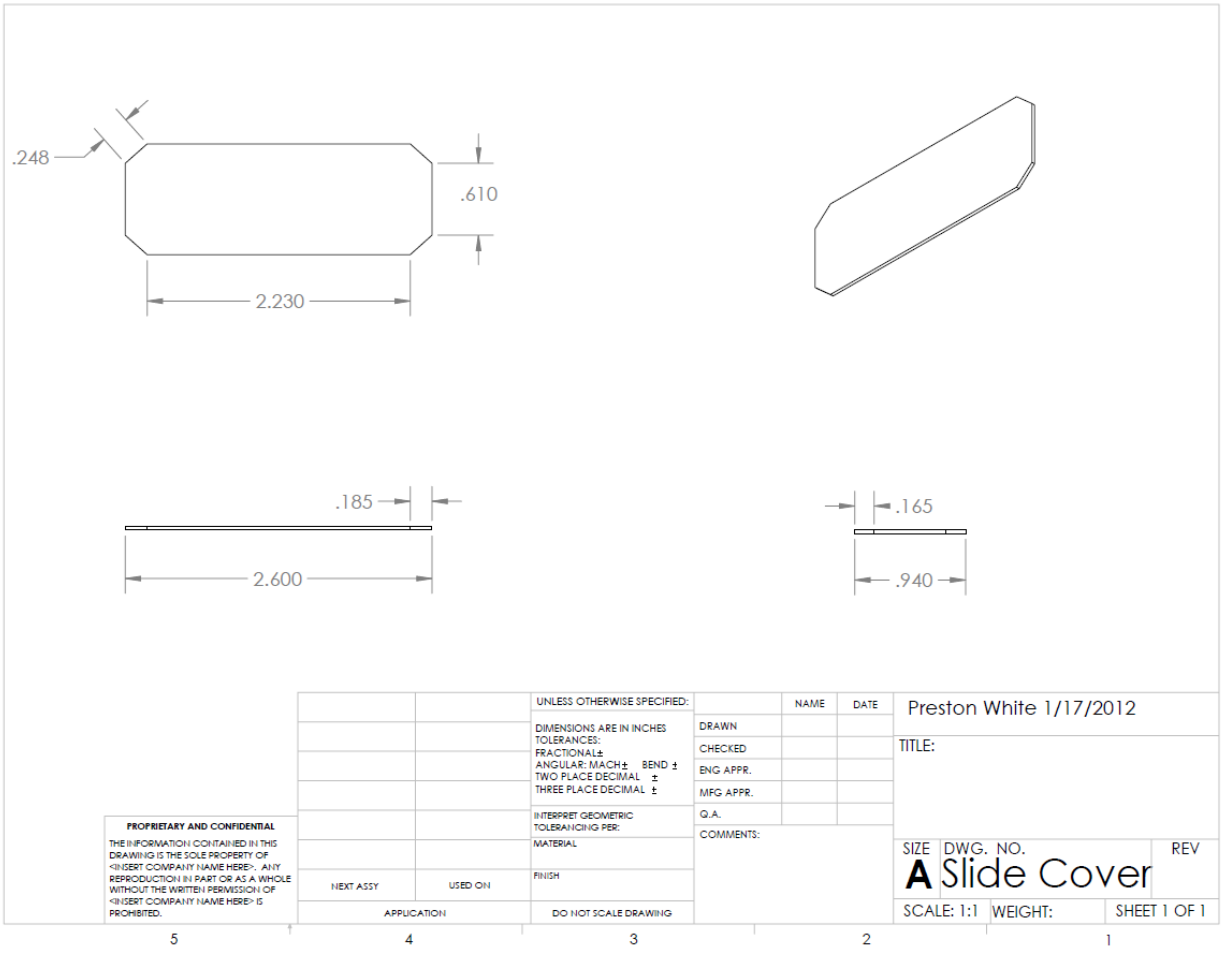

Drawing 3.4-11: Joint design recommendations made by Janet Devine for the shear joint and the tongue and groove joint.

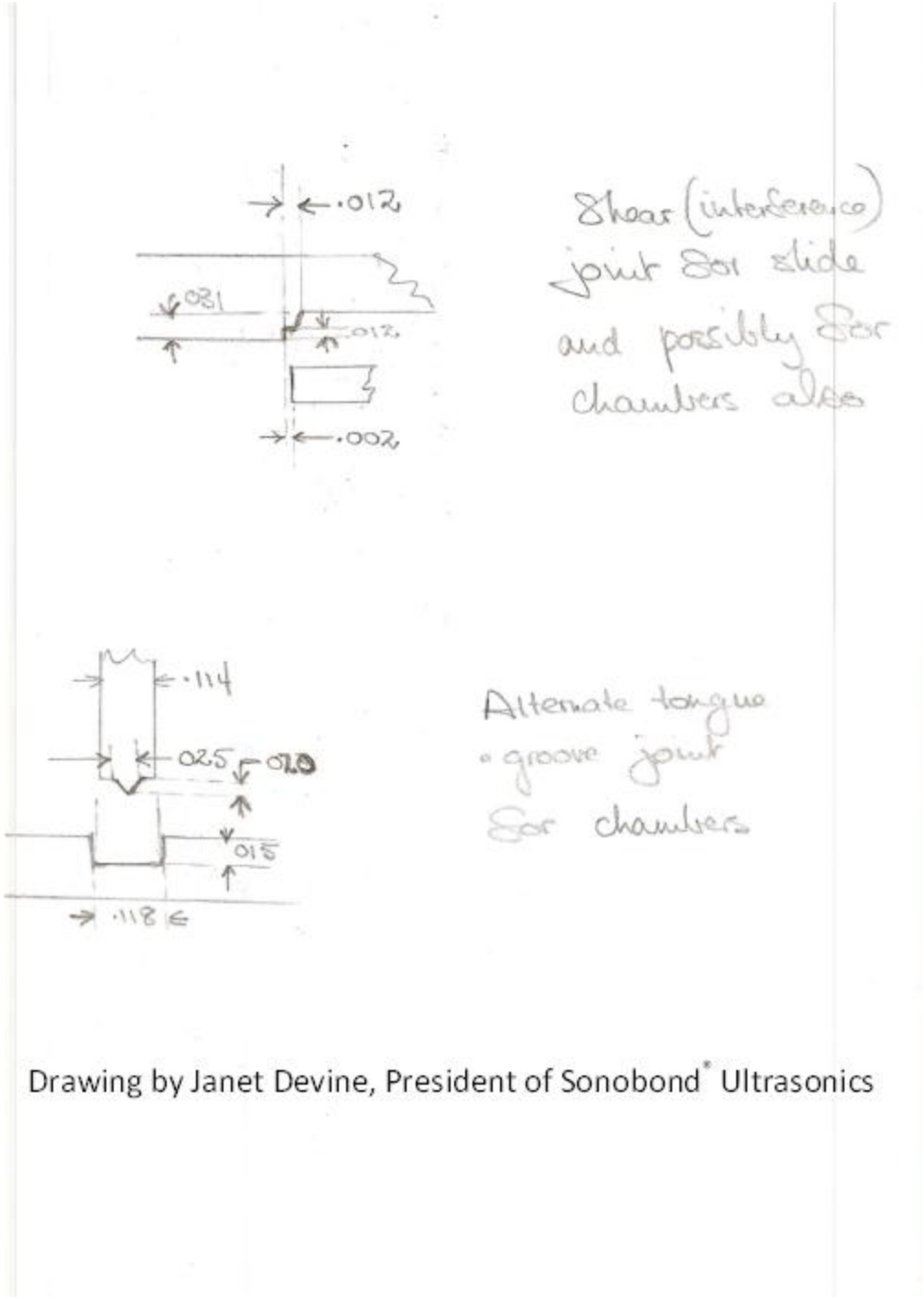

Drawing by Janet Devine, President of Sonobond® Ultrasonics